



U.S. Department
of Transportation

**National Highway
Traffic Safety
Administration**



DOT HS 812 789

February 2020

Stranded Energy Assessment Techniques and Tools

DISCLAIMER

This publication is distributed by the U.S. Department of Transportation, National Highway Traffic Safety Administration, in the interest of information exchange. The opinions, findings, and conclusions expressed in this publication are those of the authors and not necessarily those of the Department of Transportation or the National Highway Traffic Safety Administration. The United States Government assumes no liability for its contents or use thereof. If trade or manufacturers' names or products are mentioned, it is because they are considered essential to the object of the publication and should not be construed as an endorsement. The United States Government does not endorse products or manufacturers.

Suggested APA Format Citation:

Rask, E., Pavlich, C., Stutenberg, K., Duoba, M., & Keller, G. (2020, February). *Stranded energy assessment techniques and tools* (Report No. DOT HS 812 789). Washington, DC: National Highway Traffic Safety Administration.

| | | | | | |
|--|--|---|--|--|------------------|
| 1. Report No. DOT HS 812 789 | | 2. Government Accession No. | | 3. Recipient's Catalog No. | |
| 4. Title and Subtitle Stranded Energy Assessment Techniques and Tools | | | | 5. Report Date February 2020 | |
| | | | | 6. Performing Organization Code | |
| 7. Authors Eric Rask, Craig Pavlich, Kevin Stutenberg, Michael Duoba, Glenn Keller [Note: This report contains a sub-report written by Joshua Lamb, Christopher Orendorff, Leigh Anna Steele, Scott Spangler, and Jill Langendorf.] | | | | 8. Performing Organization Report No. | |
| 9. Performing Organization Name and Address Plaza Argonne National Laboratory 955 L'Enfant SW Washington, DC 20024. | | | | 10. Work Unit No. (TR AIS) | |
| | | | | 11. Contract or Grant No. | |
| 12. Sponsoring Agency Name and Address National Highway Traffic Safety Administration 1200 New Jersey Avenue SE Washington, DC 20590 | | | | 13. Type of Report and Period Covered Final Report | |
| | | | | 14. Sponsoring Agency Code | |
| 15. Supplementary Notes This report contains a sub-report written by By Joshua Lamb, Christopher Orendorff, Leigh Anna Steele, Scott Spangler, and Jill Langendorf. | | | | | |
| 16. Abstract The objective of this project is to research, develop, document, and demonstrate RESS assessment and discharge procedures with enabling technology and architecture requirements (if needed), including device concepts, which may be commonly integrated into RESS designs for the safe management, removal, and handling of stranded energy of an inoperative RESS. These methods and interfaces should be applicable to both damaged and fully functional RESS systems and should comprehend both the current state-of-the-art as well as probable future directions. Non-operational environments should include service repair, end of life disassembly, vehicle crash scene (minor damage), vehicle crash scene (major damage), fire damage (e.g., garage fire), vehicle towing, and vehicle storage. | | | | | |
| 17. Key Words Lithium-Ion Safety, First and Secondary Responders, Post-Crash Battery Assessment, Thermal Runaway, Stranded Energy, Battery Stability Assessment | | | | 18. Distribution Statement This document is available to the public through the National Technical Information Service, www.ntis.gov . | |
| 19. Security Classif. (of this report) Unclassified | | 20. Security Classif. (of this page) Unclassified | | 21. No. of Pages 98 | 22. Price |

Form DOT F 1700.7 (8-72)

Reproduction of completed page authorized

Table of Contents

| | |
|--|----|
| List of Figures | iv |
| Project Introduction | 1 |
| Battery System Architecture and Stranded Energy Background Research | 2 |
| Overview of Basic High-Voltage Battery System Architecture and Components | 2 |
| System Level Issues in Diagnosing Battery Stability and Removing Stranded Energy..... | 6 |
| Overview of Existing OEM Discharge Tools..... | 9 |
| Highlighted In-Field Battery Failures | 13 |
| Battery Failure and Thermal Runaway Background and Supporting Research | 18 |
| Stranded Energy Hazards..... | 18 |
| Thermal Runaway Overview | 18 |
| Highlighted Research: Battery Thermal Runaway Proclivity and Severity Versus State-of-Charge | 19 |
| Sandia LGCPI Battery Thermal Runaway Versus SOC Testing..... | 23 |
| Section Summary, Discussion, and Conclusions: Battery Failure and Thermal Runaway Background and Supporting Research..... | 36 |
| Battery Diagnostics and Stability Assessment Techniques..... | 38 |
| Introduction to In-Vehicle Battery Diagnostics..... | 38 |
| Overview of Additional Battery Sensing and Failure Mode Detection Techniques | 40 |
| Prototype Battery Stability and Safety Detection Strategy | 42 |
| Future Directions for Improved Battery Stability Assessment..... | 45 |
| Electrochemical Impedance Spectroscopy | 45 |
| Supplemental Sensor Development | 46 |
| Battery Communication Links | 46 |
| Evaluating the Robustness of In-Vehicle Communications..... | 49 |
| Estimating Battery State-of-Charge for Stranded Energy Purposes..... | 54 |
| Prototype Stranded Energy Tool-set Development | 56 |
| Stranded Energy Tool Design Discussion | 56 |
| Design Goals..... | 56 |
| General Interface Considerations and Recommended Design | 56 |
| Physical Versus Remote Sensing | 56 |
| Vehicle OBD-II Data Link Connector | 58 |
| Auxiliary Diagnostic Port:..... | 58 |

| | |
|--|----|
| High-Voltage Terminal Access..... | 60 |
| Dedicated High-Voltage Access Port..... | 62 |
| Generalized Tool Process Flow..... | 63 |
| Vehicle and RESS Identification | 64 |
| Visual Inspection and DLC Access | 64 |
| BMS Battery Assessment Through the DLC..... | 64 |
| Battery Assessment via Diagnostic Port..... | 64 |
| High-Voltage Terminal Connection..... | 64 |
| Prototype Stranded Energy Assessment and Discharge Tool Discussion | 67 |
| Handheld Diagnostic Unit and User interface:..... | 67 |
| Discharge Cart and Offline Diagnostics..... | 71 |
| Prototype Tool Deployment Highlights | 76 |
| Future Tool Improvements | 79 |
| Additional Prototype Tool Development..... | 80 |
| Low cost, handheld data monitoring..... | 80 |
| Simple Isolation Resistance Tracking and Notification (alarm)..... | 83 |
| Project Conclusions and Recommendations..... | 85 |
| References | 87 |

List of Figures

| | |
|---|----|
| Figure 1: Overview of basic high-voltage system and components | 2 |
| Figure 2: Example hybrid vehicle battery pack layout (Hyundai Sonata) [0]..... | 3 |
| Figure 3: Highlighted battery packs and modules break-down (left-Hyundai Sonata, right-Toyota Prius PHV) [0,2] | 4 |
| Figure 4: Example Battery Management System (BMS) components and layout [2]..... | 5 |
| Figure 5: Chevrolet Volt Battery Module and BMS sub-system..... | 6 |
| Figure 6: Battery system highlighted in overall HV system | 7 |
| Figure 7: Issue 1 - Loss of 12V power connection | 7 |
| Figure 8: Chevrolet Volt first responder instruction to cut 12V cable [3] | 8 |
| Figure 9: Issue 2 - Where to connect for discharge and evaluation..... | 8 |
| Figure 10: Chevrolet Volt battery terminal access in-laboratory (left) and under vehicle (right)... | 8 |
| Figure 11: Example Manual Service Disconnect Locations (clockwise from upper left: Hyundai Sonata, Chevrolet Volt, Toyota Prius PHV, Honda Accord HEV, BMW ActiveHybrid, Mitsubishi IMEV)..... | 9 |
| Figure 12: Midtronics GRX-5100 EV/HEV Battery Service Tool (connected to a vehicle and discharging on right) [4]..... | 10 |
| Figure 13: GRX-5100 example connectors and adaptors [4]..... | 11 |
| Figure 14: Toyota PHV damaged battery discharge tool [2] | 11 |
| Figure 15: Toyota Prius PHV discharge tool connections and display [2] | 12 |
| Figure 16: Example salt bath discharge method for severely damage batteries (Toyota Prius PHV) [2] | 13 |
| Figure 17: Mazda 2 i-ELOOP capacitor discharge port for discharge prior to disposal [5] | 13 |
| Figure 18: Highlighted battery arcing and VTSM (BMS) issues due to coolant leakage (Chevrolet Volt) [6] | 14 |
| Figure 19: Connector degradation with minimal damage (Chevrolet Volt) [6] | 15 |
| Figure 20: VTSM (BMS) lead overheating example (Chevrolet Volt) [6]..... | 15 |
| Figure 21: Water Intrusion of the entire pack..... | 16 |
| Figure 22: BMS damage and shorting | 16 |
| Figure 23: Module enclosure damage | 17 |
| Figure 24: Evidence of arcing/aggressive discharge..... | 17 |
| Figure 25: Evidence of actual individual cell damage..... | 17 |
| Figure 26: Nissan Leaf battery terminal voltage versus time (full depletion UDDS data)..... | 18 |
| Figure 27: Battery components and thermal runaway/degradation steps | 19 |
| Figure 28: FAA testing/presentation of Li-ion battery thermal propagation versus state-of-charge (SOC) [9]..... | 20 |
| Figure 29: Accelerating Rate Calorimetry derived heat rate versus temperature and SOC for Sony 18560 (LiCoO ₂) {Left} and Argonne Designed “Gen 1” Cell (LiNi _{0.85} Co _{0.15} O ₂) {Right} [8] | 22 |
| Figure 30: ARC derived heat rate versus temperature and SOC for Moli cells. Full response (left) and zoomed-in (right) to show initialization temperature trends [16] | 22 |
| Figure 31: ARC data of cell at 20 percent SOC | 25 |

| | |
|--|----|
| Figure 32 ARC data of cell at 40 percent SOC | 26 |
| Figure 33: ARC data of cell at 60 percent SOC | 27 |
| Figure 34: ARC data of cell at 80 percent SOC | 28 |
| Figure 35: ARC data of cell at 100 percent SOC | 29 |
| Figure 36: ARC exothermic rate data comparing 20 to 100 percent SOC..... | 30 |
| Figure 37: Exothermic rate data from Figure 6 showing the low rate exotherms present from 20 to 60 percent SOC..... | 30 |
| Figure 38: Enthalpy of the thermal runaway event (left) and peak heating rates (right) as a function of the SOC. | 31 |
| Figure 39: Thermal ramp test at 100 percent SOC showing a runaway reaction at ~210 C. | 32 |
| Figure 40: Thermal ramp test performed at 100 percent SOC showing a venting event, and some limited self-heating at 250 C, but no thermal runaway event..... | 33 |
| Figure 41: Thermal ramp test performed at 100 percent SOC, showing again a small self-heating event at 250 C, but no true thermal runaway..... | 33 |
| Figure 42: Thermal ramp test performed at 80 percent SOC | 34 |
| Figure 43: Thermal ramp test performed at 80 percent SOC..... | 34 |
| Figure 44: Thermal ramp test performed at 60 percent SOC..... | 35 |
| Figure 45: Highlighted operational and functional diagnostics and their usage (SOC estimation versus failure protection)..... | 40 |
| Figure 46: Chevrolet Volt Service Tool screenshot..... | 47 |
| Figure 47: Hyundai Sonata Hybrid individual cell voltage diagnostic request structure (in decimal notation) | 48 |
| Figure 48: Direct BMS communication access (Hyundai Sonata Hybrid) | 48 |
| Figure 49: Prototype evaluation tool screenshot..... | 49 |
| Figure 50: Distribution of failure modes across packs investigated | 50 |
| Figure 51: BMS functionality distribution of damaged packs in study | 51 |
| Figure 52: High-voltage loop functionality distribution of damaged packs in study | 52 |
| Figure 53: Distribution of HV loop and BMS functionality levels (color coded for severity) | 53 |
| Figure 54: Discharge and assessment capability for damages packs experiencing water intrusion | 53 |
| Figure 55: Terminal voltage versus reported SOC for two select BEVs | 55 |
| Figure 56: Prototype Battery Diagnostic Port Schematic | 58 |
| Figure 57: Diagnostic Port Location Suggestions Top left: within center console, top right: under rear seat (with metal cover), bottom: colocation with MSD..... | 60 |
| Figure 58: Volt high-voltage dc connector and Argonne adapted coupling adaptations..... | 61 |
| Figure 59: Developed prototype connector for high-voltage terminal access..... | 61 |
| Figure 60: Overview of basic high-voltage system including supplemental HV discharge port (area in red dashed box) | 62 |
| Figure 61: MSD, diagnostic port (red), and discharge port (blue rectangle) proposed collocation | 63 |
| Figure 62: The Handheld Diagnostic Tool and Control Unit..... | 70 |
| Figure 63: Discharge Cart Component Overview | 72 |
| Figure 64: Discharge Cart and Component Locations | 73 |

| | |
|--|----|
| Figure 65: Overview of Discharge and Assessment Tool Components | 74 |
| Figure 66: Load Bank On-board Control and Processing Boards (and isolation resistance sensing)..... | 75 |
| Figure 67: Screenshot - Vehicle Selection Screen..... | 76 |
| Figure 68: Screenshot – Connection instructions for DLC-based vehicle BMS assessment | 77 |
| Figure 69: Screenshot - CAN Communications assessment progress screen | 77 |
| Figure 70: Screenshot - Discharge Required, Discharge Cart Hookup Instructions | 78 |
| Figure 71: High-voltage and diagnostic interface port connections | 78 |
| Figure 72: Screenshot - Discharge Screen With BMS Provided Voltage Information | 79 |
| Figure 73: Screenshot - Discharge With No BMS Information | 79 |
| Figure 74: J1962 OBD-II connector | 81 |
| Figure 75: Example wireless diagnostic interface | 81 |
| Figure 76: Wireless diagnostic adapter integration with developed battery diagnostic port | 82 |
| Figure 77: Prototype wireless diagnostics using an off-the-shelf app and wireless connector (Chevrolet Volt data shown)..... | 82 |
| Figure 78: Offline isolation monitoring prototype tool..... | 83 |
| Figure 79: Tool installation in a BEV to evaluate isolation of half pack via removed MSD | 84 |

Project Introduction

A rechargeable energy storage system (RESS), commonly referred to as the vehicle battery, is an energy storage device consisting of the battery packs, and necessary ancillary subsystems for physical support, protection, enclosure, thermal management, and control.

In most electrically propelled vehicles, during an unintended or abnormal operation event such as a vehicle crash, vehicle safety systems referred to as high-voltage electrical contactor switches are designed to open the high-voltage circuit rendering the electrical propulsion system inoperative. In addition, these open circuit contactors deliver a means to electrically isolate the high-voltage battery from the rest of the vehicle providing safety from electrical shock as required for compliance to FMVSS No. 305. However, the opening of these safety devices prevents the remaining energy in the pack from being accessed or removed. In certain cases, if the battery is undamaged this energy will be contained in the undamaged battery without incident, and following proper diagnostics and handling by trained personnel, the battery may be returned to operation at the discretion of the OEMs repair procedure.

In other circumstances, when damage to the RESS has occurred, additional potential safety risks may have been introduced into the situation in the form of stranded energy. The damage to the RESS itself may elevate certain safety risks in terms of thermal stability, and since the electrical energy at the time of event is unlikely to be in a safety optimized condition, the safety risks increase in relation to the battery pack's state-of-charge (SOC). This combination of a damaged RESS and high state of charge can result in elevated potential safety risks to the people handling the vehicle and battery pack such as emergency responders, repair technicians, or battery recyclers. In addition, it is generally assumed that at the end of battery life, if by age or pre-mature damage, every battery will have to be discharged for safety handling purposes prior to secondary use or recycle.

The objective of this project is to research, develop, document, and demonstrate RESS assessment and discharge procedures with enabling technology and architecture requirements (if needed), including device concepts, which may be commonly integrated into RESS designs for the safe management, removal, and handling of stranded energy of an inoperative RESS. These methods and interfaces should be applicable to both damaged and fully functional RESS systems and should comprehend both the current state-of-the-art as well as probable future directions. Non-operational environments should include service repair, end of life disassembly, vehicle crash scene (minor damage), vehicle crash scene (major damage), fire damage (e.g., garage fire), vehicle towing, and vehicle storage.

Battery System Architecture and Stranded Energy Background Research

Overview of Basic High-Voltage Battery System Architecture and Components

When beginning a discussion regarding stranded energy, a high-level overview of a vehicle's high-voltage system is useful in providing context for the discussion to follow. As with many other vehicle systems, a vehicle's high-voltage distribution system contains many interconnected components that work together to provide functionality. Figure 1 highlights the main components contained in the vast majority of hybrid-electric and battery-electric vehicle battery systems.

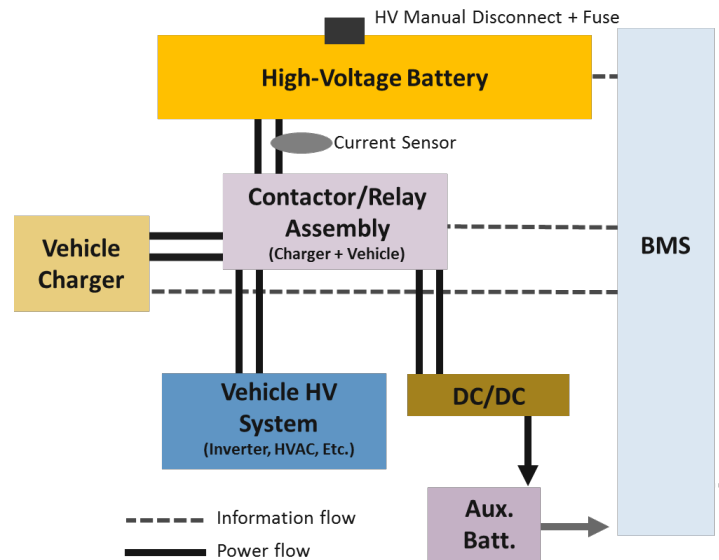


Figure 1: Overview of basic high-voltage system and components

Starting with the high-voltage battery and working outward, a variety of components as well as power and information flow pathways can be observed. The contactor/relay assembly acts as a gateway between the vehicle's high-voltage battery and other on-vehicle high-voltage componentry. The assembly is almost always powered by vehicle 12V power and the contactors close when power is applied. Contactors are open when the vehicle is in an "off" state or if the battery management system (BMS) detects a battery related issue that will also open the contactors, thus removing the battery from the rest of the high-voltage distribution system. The majority of vehicles have a contactor on both the positive and negative leads going to the vehicle system, there are also typically one or more additional contactors used to facilitate a discharge resistor and capacitor in order to reduce the voltage in-rush seen by other components as the contactors are activated. Vehicles with off-board charging capability (PHEVs and BEVs) will typically have an additional set of contactors (at least positive/negative) for usage of the vehicle charging system while retaining battery isolation to the rest of the high-voltage traction system.

The BMS is sometimes described as the brain of the high-voltage battery and this analogy is fairly fitting. The BMS and its related sensing components is used to assess a wide range of parameters and facets of battery operation such as battery state of charge, state of health, individual cell voltages, and module temperatures. Additionally, the BMS process and distributes this information across a vehicle's communications network so that battery state information as well as failure codes can be used by the higher

level control systems. For example, the BMS often provides failure information and battery state information to assist in the decision to close contactors at vehicle start or open them due to a critical battery system issue such as overheating or loss of isolation while driving. Although not always the practice, the BMS is also typically powered by vehicle 12V power to isolate the battery management system's functionality from the high-voltage battery it is supervising and evaluating. While its use is becoming slightly less widespread a manual service disconnect (MSD) is typically provided to add an additional safety layer on top of open contactors when repairing or evaluating a damaged vehicle. The MSD typically provides a means to physically split the battery into two separate pieces but removing a link in the battery's busing architecture, thus inhibiting any current flow across the terminals (although not inhibiting current from flowing out of ½ of a pack in certain damage scenarios).

Focusing on the battery itself, most modern battery packs are comprised of smaller modules and even sub-modules. Main modules are typically connected in series as shown in Figure 2 and Figure 3. Both figures show packs that are comprised of larger modules, which themselves are comprised of several cells. Although not highlighted in the following figures, sub-modules may also contain cells configured in a parallel configuration. This sub-module configuration allows for increased pack energy while retaining the desired operating voltage. For example, the Chevrolet Volt uses 96 sub-modules of 3 parallel cells each for its general pack configuration. For the Volt, the 96 sub-modules are then aggregated into three distinct main modules to facilitate packaging within the vehicle. Although a high degree of modularization within a battery pack may seem like a subtle issue, it has important implications for stranded energy assessment and discharge. It becomes difficult to determine by voltage measurements alone if a single cell within a parallel string has been damaged. For example if one cell of a set of 3 parallel connected cells becomes disconnected, the module will still provide the expected voltage, thus it becomes critical to determine additional methods to detect damaged cells, a topic of significant discussion later in this work.

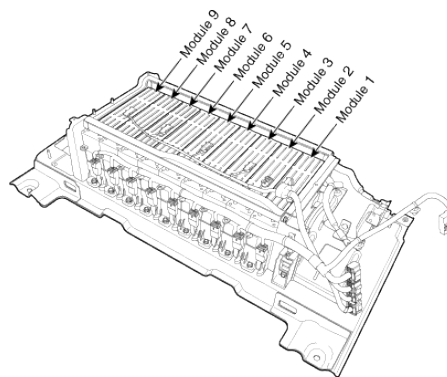


Figure 2: Example hybrid vehicle battery pack layout (Hyundai Sonata) [0]

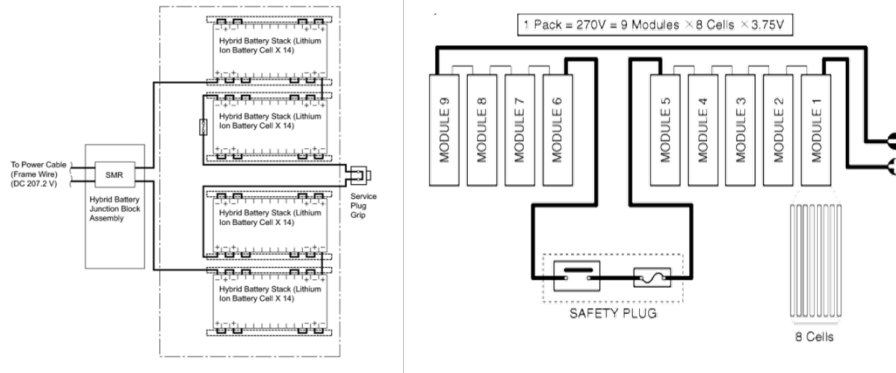


Figure 3: Highlighted battery packs and modules break-down (left-Hyundai Sonata, right-Toyota Prius PHV) [0,2]

Now that the basic pack architectures have been given a brief introduction, it is important to provide some additional discussion regarding the Battery Management System. While almost all battery packs have some form of management system, this work focuses mainly on Li-ion vehicle batteries and their associated management systems. Namely, since the vast majority of Li-ion batteries are sensitive to over/under charge, great care is taken to ensure that the cells stay within their chemistry specific operating voltage and temperature range. Thus a major function of a Li-ion BMS is monitoring individual cell or sub-module voltages in order to avoid over/under charge, aid in pack balancing, and monitor the pack for damaged or degraded cells. Sub-modules with parallel strings are typically assessed as one single “cell” since the parallel strings are inherently self-balancing. In addition to the sensing of individual cells or sub-modules, most BMSs typically evaluate the pack temperature at several locations, typically with at least one reading per main module. While individual cell temperatures are not necessarily needed, it is helpful to estimate approximate pack temperatures to identify any out-of-specification temperature excursions as well as provide information for state-of-charge (SOC) monitoring. While a full discussion regarding SOC monitoring parameters is outside the scope of this work, it is helpful to note that state-of-charge monitoring typically uses the cell/sub-module voltage information in conjunction with pack temperatures and current to estimate the SOC of the pack. In addition to voltage and temperature measurement, the BMS typically calculates pack isolation resistance, checking if the battery pack has somehow been connected to vehicle ground or another grounding source possibly allowing for unregulated battery current flow or high voltage to be exposed in an unexpected region. The BMS typically incorporates a battery current sensor to estimate the overall pack current flow at any particular time. The BMS also typically provides this information to other controllers within the vehicle allowing for the battery state (both function and safety related) to be incorporated into a vehicle’s overall control decisions. The BMS may also activate battery cooling such as the fan in an air-cooled pack. Figure 4 helps summarize the preceding discussion, showing a basic circuit diagram for an example BMS and battery system. Since it is so relevant to the stranded energy discussion, it is again mentioned here that most BMSs are powered using the vehicle 12V supply, such that removing vehicle 12V power will depower the both the BMS’s communications functionality as well as its sensing capabilities.

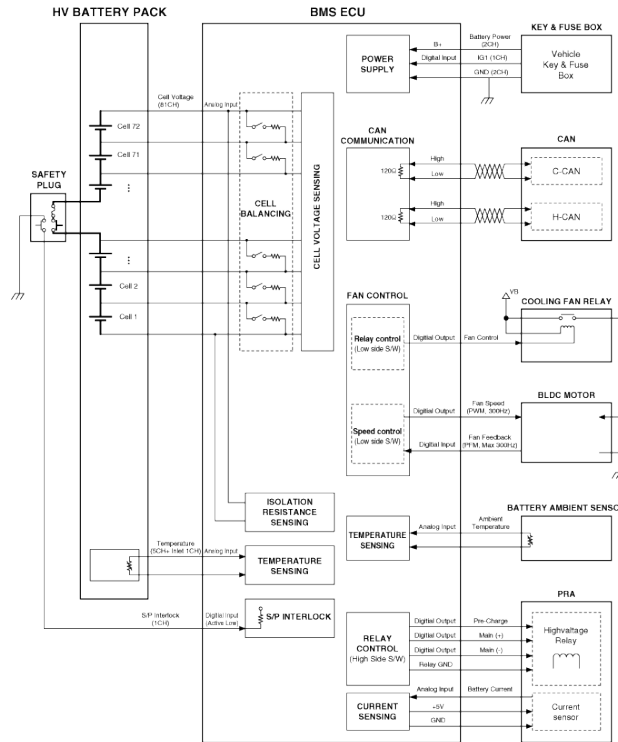


Figure 4: Example Battery Management System (BMS) components and layout [2]

As discussed in earlier paragraphs, many modern vehicle batteries and especially Li-ion batteries seen in recent battery electric vehicles (BEVs) and plug-in hybrid electric Vehicles (PHEVs) are often separated into several larger modules, themselves comprised of one or more sub-modules. With this modularity in mind, a clarification to the previous basic BMS diagram is needed. For many recent vehicles, individual cell voltages are not all fed to a single BMS controller, rather individual cells are read at a module level and then broadcast via an internal network to a main BMS controller that aggregates the module level information. While certain vehicles still provide all cell voltages to a single access/calculation point, this bridged communications architecture has become quite prevalent and is, in the mind of the authors, expected to continue. Since individual cell voltages are not readily available at a single physical access point, any system used to interrogate individual cells most likely will need to use the imbedded voltage measurement modules that are hardwired to the individual cells. To highlight this type of architecture, Figure 5 shows a single module (of three) for a Chevrolet Volt battery pack. On the top of the module, the red subsystem voltage/temperature communication boards as well as the actual connections to the individual cells can be seen.



Figure 5: Chevrolet Volt Battery Module and BMS sub-system

Relative to overall system operation and control, the fact that the BMS monitors and facilitates activation of the contactors is an important point to highlight. Moreover, the BMS and contactors are most often powered using the 12V battery system, therefore 12V power is critical for operation of the existing battery sensing and contactors (for discharge and assessment access). Similarly, since under normal circumstances, no battery power will flow when contactors are open, it is very important to realize that without 12V power (either on-board or off board) the existing battery contactors will not close, thus making battery depowering quite difficult. In the context of a PHEV and BEV, separate contactors allow for isolated vehicle charging or operation. Lastly, it is important to consider that the BMS usually calculates a wide range of battery related functional and fault information ranging from battery available power and energy level to isolation resistance and fault tracking. Without the aid of additional off-line analysis tools or the ability to use some low-level functionality, loss of BMS functionality makes assessing the stability and safety of a damaged battery very difficult.

System Level Issues in Diagnosing Battery Stability and Removing Stranded Energy

The goal of this subsection is to introduce the concept of stranded energy (SE) and help explain some of the technical challenges related to diagnosing and discharging a battery across a variety of situations. Broadly speaking, stranded energy describes any scenario in which energy remains in a battery without the means to remove the energy. More importantly, this work expands this term to also apply to a battery in which the stability and energy level is unknown due to a loss of communications functionality or damage. While other failure modes such as loss of isolation related to the traction drive system could also result in the loss of battery operation due to the BMS not allowing the contactors to close, this work looks to evaluate issues related to only battery pack and contactor functionality, as highlighted in red within the overall high-voltage system in Figure 6.

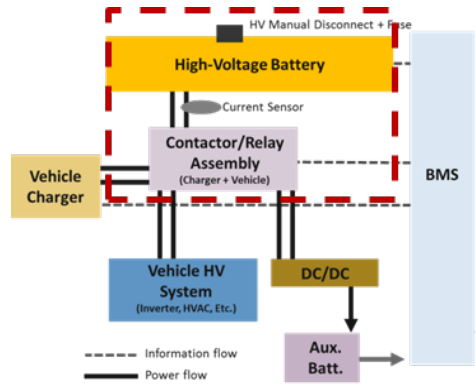


Figure 6: Battery system highlighted in overall HV system

Although the circumstances leading up to a stranded energy situation are fairly broad, several common issues emerge in SE scenarios:

(1) As introduced briefly in the previous section, the first problem encountered in many SE scenarios relates to the loss of 12V power. Since both the BMS and contactor assembly are typically powered with vehicle 12V power, the loss of this power is particularly troublesome in terms of both accessing the battery for depowering as well as providing BMS functionality (even in the case of a fully functional pack) to diagnose and monitor the stability of the pack.

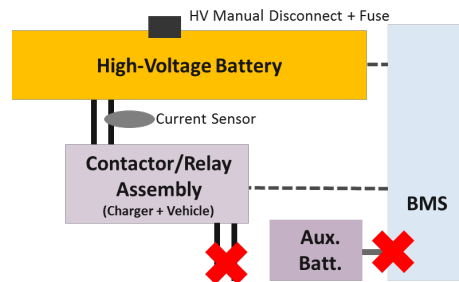


Figure 7: Issue 1 - Loss of 12V power connection

To further expand on this problem, many vehicle first-responder guides actually suggest cutting the 12V power supply cable to ensure that no 12V power is provided to the contactors (and airbag actuation system) to ensure a safe environment for emergency response personnel. Figure 8 provides an excerpt of the GM Volt first responder guide [3] showing the location and suggestion to cut the 12V cable in an emergency scenario. While the protocol of cutting 12V cables makes the stranded energy problem more difficult, it must be mentioned that removal of 12V power is a critical and successful part of reducing both high-voltage exposure as well as exposure to accidental air-bag firing. As the discharge and assessment tools and techniques were developed, the authors worked to retain the existing safety protocols as much as possible.

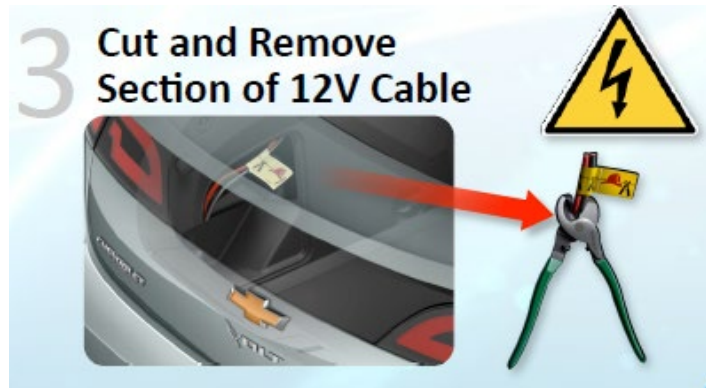


Figure 8: Chevrolet Volt first responder instruction to cut 12V cable [3]

(2) On the discharging side of the issue, one of the largest challenges of depowering a pack in-vehicle is lack of battery terminal access to facilitate the discharge. Most PHEV and BEV batteries are tightly integrated into the overall vehicle structure making terminal access very difficult compared to a pack in a laboratory situation. Interference from battery cooling hoses as well as a wide variety of other power/information cables further complicates accessing battery terminals in-field. To highlight this complexity versus an in-lab situation, Figure 10 shows the terminals for the Chevrolet Volt pack in-lab (very easy terminal access) and under-vehicle (very difficult and confusing access).

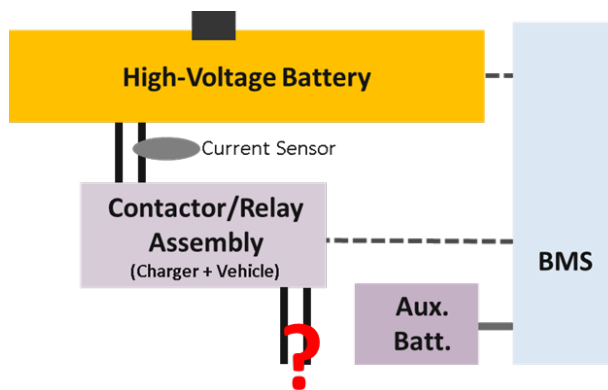


Figure 9: Issue 2 - Where to connect for discharge and evaluation

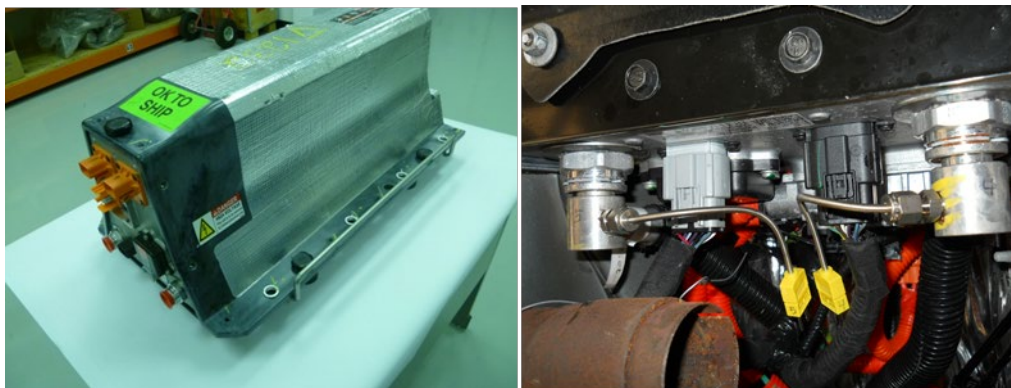


Figure 10: Chevrolet Volt battery terminal access in-laboratory (left) and under vehicle (right)

For vehicles with off-board charging capability, it is sometimes suggested that the charge port be used as a point of access for stranded energy removal. While this option appears tempting a first, two issues suggest that this may not be an optimal location for pack discharging. Firstly, the vast majority of current vehicles use AC wall power run through a converter in order to supply DC power to the battery. Moreover, this power flow is often unidirectional except in the case of a vehicle-to-grid (V2G) capability, which is expected to remain rare in the medium term. Secondly, the exterior vehicle charge port may be sub-optimal in terms of crash survivability given its prominent location on the exterior of the vehicle.

Discharge and battery assessment port accessibility is also of great concern from the perspective of developing a discharge and assessment tool. While most vehicles currently retain an MSD, the placement of these important safety items is very much non-standardized, with some manufacturers allowing easy access, whereas other manufacturers providing very difficult MSD access of placing the MSD in a location that is not particularly robust in a crash. To illustrate this point, Figure 11 shows a variety of MSDs for several vehicles. In fact, some vehicles are actually beginning to remove the MSD altogether, which removes the additional safety of a physical prohibition of current flowing as well as reducing access point to the battery.

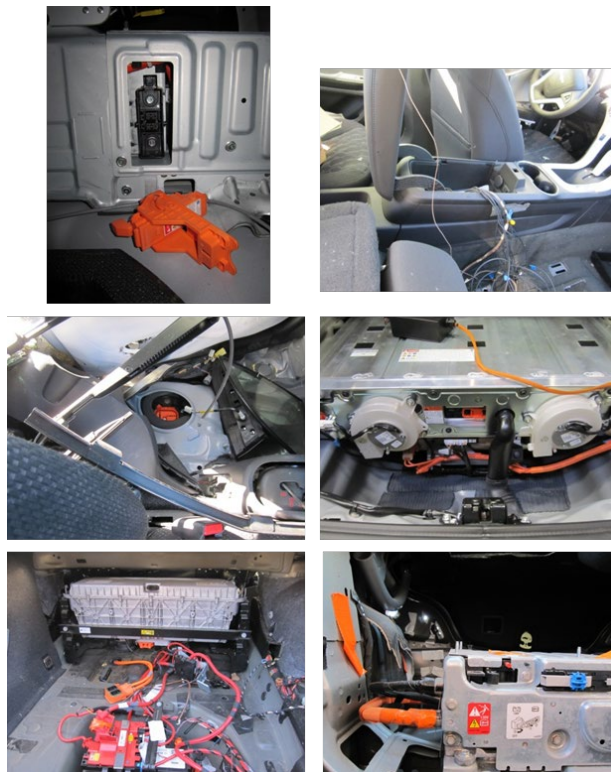


Figure 11: Example Manual Service Disconnect Locations (clockwise from upper left: Hyundai Sonata, Chevrolet Volt, Toyota Prius PHV, Honda Accord HEV, BMW ActiveHybrid, Mitsubishi IMEV)

Overview of Existing OEM Discharge Tools

An additional introductory task related to this work is to provide a brief overview regarding some of the existing OEM or aftermarket tools associated with discharging stranded energy and diagnosing the amount of damage in a pack.

The first tool of significant interest is the Midtronics GRX-5100 EV/HEV Battery Service Tool [4]. The GRX-5100 is used for the majority of GM products including PHEVs such as the Chevrolet Volt and Opel Ampera as well as some other hybrids such as the Buick Regal eAssist. Powered off AC 120V wall power, the service tool can provide up to roughly 3 kW of battery discharge capability and can also be used to charge or discharge individual pack modules if the proper connections are available (battery is removed from the vehicle in the case of the Volt). Figure 12 shows the main discharge/control box for the GRX-5100 (left) as well as the basic connections in use on a damaged vehicle (right). As can be seen on the right side of Figure 12, a typical battery-in-vehicle discharge connects the GRX-5100 to the battery using an adaptor that connects into the main DC cables that enters the vehicle's inverter/converter under hood. The GRX can also discharge a pack external to the vehicle, assumedly connecting to either the main battery terminals or module interconnections using custom adapters specific to a particular vehicle. During operation, the system tracks temperatures and individual cell voltages by interfacing with the vehicle's BMS and related connections.



Figure 12: Midtronics GRX-5100 EV/HEV Battery Service Tool (connected to a vehicle and discharging on right) [4]

In addition to the main under-hood high-voltage connector, the GRX also uses several different vehicle specific connectors to facilitate operation of the battery's other functionality (BMS, contactors, etc.). Although not entirely clear from the available documentation for the GRX-5100, it is hypothesized that the system emulates all BMS and vehicle inputs relative to a normally operating vehicle, such that the battery operates as if it were in a vehicle although it is actually controlled by the GRX system. If provided with sufficient information from an OEM, the GRX should be able to replicate and use all internal BMS and outside (i.e., other controller calculated) calculations related to items such as battery SOC, individual cell voltages, overall pack stability, and isolation.

Figure 13 highlights some of the specialized connectors used to interface the GRX-5100 to the Chevrolet Volt. The left side of the figure shows the connector for the main DC cables and the figure on the right shows the GRX-5100's custom connector adapter that connects the vehicle's battery communications/controls. As mentioned earlier, by providing a full adapter to the BMS and related battery inputs, the GRX can communicate and operate the battery as if it were in a vehicle. The GRX-5100 has seen a fair amount of successful in-field usage and highlights several points of interest for the more generalized development goals of this project. Most importantly, the GRX service tool provides a simplified front end that can be used with minimal training. Additionally, the tool highlights some of the high-and low voltage connection possibilities to facilitate battery discharge and diagnosis. In terms of working towards a more generalized tool, the GRX requires quite a few custom adapters to interface the tool with a particular vehicle. Some port and communications standardization would aid in this (or any other) tool work-

ing for a larger range of vehicles. Moreover, it appears that a fair amount of OEM level information regarding vehicle communications and calculations was provided to facilitate the GRX's communications with a vehicle. These issues highlight the value of working towards a more common diagnostic port and communication structure help to enable fewer custom adapters and reduce the exchange of specific vehicle information.



Figure 13: GRX-5100 example connectors and adaptors [4]

A second OEM tool of particular relevance to this work is Toyota's damaged battery discharge tool used for Toyota's PHEV Prius. Unlike most recent vehicles, all of the Prius PHEV's individual battery cell voltage monitoring connections route to a single monitoring location. This rather unique configuration allows for each cell to be individually discharge by placing a load connected between each of the sensor lines. To facilitate this type of discharge, the Toyota box is simply a set of connectors with some associated lights and fans to deplete the battery and indicate the status of each cell in the pack. Figure 14 shows the box and connector and Figure 15 shows a more detailed view of the connectors and the "display" used to indicated cell functionality. The Toyota tool is capable of discharging individual cells, but does so at an extremely low C rate ($\sim C/20$). When all of the lights on the display are out, the battery is in theory discharged (although the manual suggests letting the battery sit unconnected and then reattaching to check that it has actually been fully discharged).

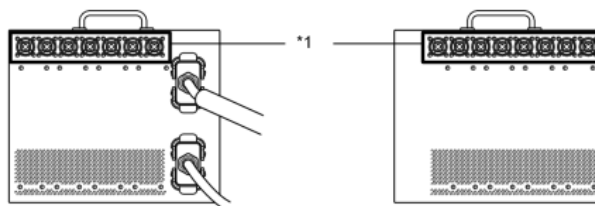


Figure 14: Toyota PHV damaged battery discharge tool [2]

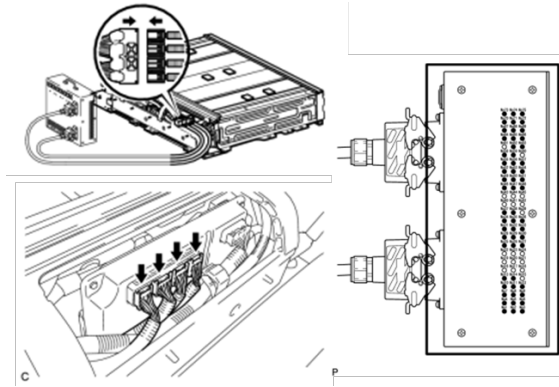


Figure 15: Toyota Prius PHV discharge tool connections and display [2]

The Toyota tool is particularly interesting in that no BMS or contactor system needs to be activated, thus allowing discharge capability across a wide range of damage scenarios. Additionally, the Toyota system uses essentially no battery diagnostic information to facilitate the discharge. Table 1 shows a paraphrasing of the Prius PHEV's battery inspection procedure that suggests a range of discharge possibilities depending on the damage scenario. While the BMS and voltage sensing structure of the PHV Prius is somewhat unique (in that all voltage sense leads connect into a single location versus using a module communication system with sub-module voltage relays) it does speak to a more general position that even in the case of a relatively damaged pack a very slow discharge appears feasible to remove the battery energy.

Table 1: Toyota Prius PHV Battery Inspection Procedure (paraphrased from [2])

| |
|--|
| <ol style="list-style-type: none"> 1. Inspect for electrolyte leakage <ul style="list-style-type: none"> • Pass - Proceed with evaluation • Fail – Discharge using salt-water bath 2. Check for battery related trouble codes using scan-tool <ul style="list-style-type: none"> • Nothing available - Proceed with evaluation • Battery high/low voltage or isolation errors – Discharge (method depends condition) • Other error code – Discharge if no physical damage is observed 3. Check if an pack temperature sensors have exceeded 50 C or if temps. are unavailable <ul style="list-style-type: none"> • Pass - Proceed with evaluation • Fail – Discharge (method depends condition) 4. Check pack voltage (between disconnect and ½ pack) < 114.8V <ul style="list-style-type: none"> • Pass - Proceed with evaluation • Fail – Discharge (method depends condition) 5. Check pack insulation resistance > 1 MOhm <ul style="list-style-type: none"> • Pass – If no physical damage, return battery using approved procedure • Fail – Discharge (method depends on condition) |
|--|

As with many other vehicles, a final suggested practice for removing the stranded energy remaining in a battery is to discharge it in a salt bath. Figure 16 highlights the suggested salt bath method from the Toyota PHV Prius manual. As with the other Toyota tool/procedure, this process discharges the battery very slowly and does not use and BMS or related functionality.

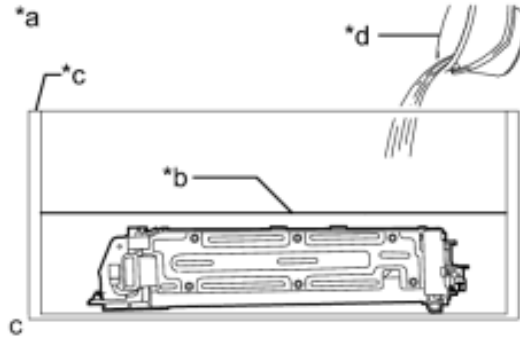


Figure 16: Example salt bath discharge method for severely damage batteries (Toyota Prius PHV) [2]

The last in-field discharge tool of interest is from the Mazda 3 i-ELOOP. This system uses a capacitor operating between 12 and 25 Volts to store energy during braking and supply this energy back to the vehicle during operation. When this vehicle or related parts are disposed of, the capacitor must be discharged to avoid the risk of fire or shock. To accomplish this goal, the i-ELOOP vehicle actually has an on-board discharge mechanism that can be activated by moving a connector to a special discharge plug. Figure 17, taken from the vehicle’s capacitor disposal manual, shows the how the capacitor can be discharged by moving a connector to an additional plug. Once connected, an indicator light will activate as the capacitor is discharged. Once the capacitor has fully discharged, the indicator light will turn off. The discharge process can take up to two hours once discharging has begun.

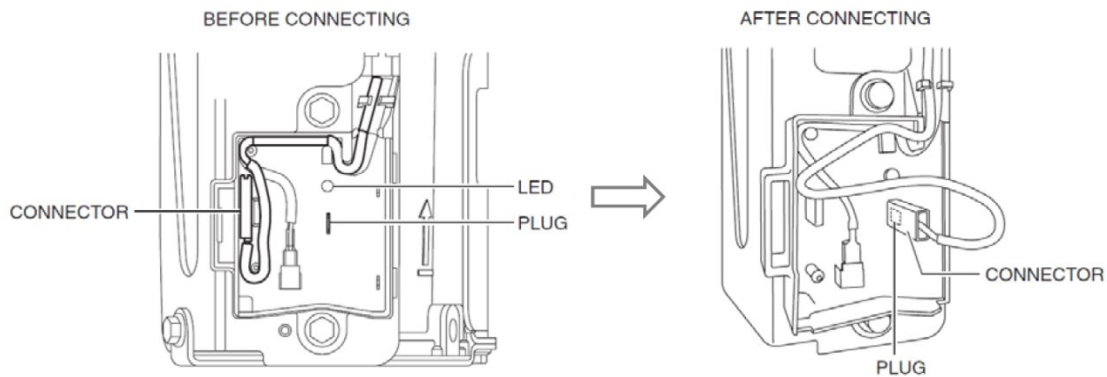


Figure 17: Mazda 2 i-ELOOP capacitor discharge port for discharge prior to disposal [5]

Although this system does not operate at high voltages and thus requires fewer protections to avoid high-voltage exposure, it does provide an interesting alternative to an offline tool designed to discharge a battery pack.

Highlighted In-Field Battery Failures

This section seeks to highlight some recent in-field failures related to stranded battery energy. These real-world scenarios are of particular interest since they point towards issues to be addressed in the field as well as some of the real world challenges associated with removing stranded battery energy. One of the most important points from both of these situations is the fact that these issues are cascading failures that ultimately lead to a thermal event. Furthermore, the initial failures that appear to start the cascade of reactions seem start in locations other than the battery cells themselves. This highlights

the need to assess not only the individual cells, but also the overall pack stability and isolation to avoid a possibly dangerous event. In contrast, recent issues with laptop batteries experiencing thermal runaway are more similar to a single event type situation where inclusions within the cells are often the initiation point of a thermal event.

Chevrolet Volt Post-Crash Incident Recreation

All discussion points and pictures shown in this section are from NHTSA funded work trying to recreate a delayed onset thermal incident that occurred following a vehicle crash test and subsequent rollover/leakage test. Over the course of these efforts, outcomes ranging from slight heating of connectors to full battery runaway and sparking were observed depending on test conditions and setup. Coolant leakage into the pack appears to be one of the major issue that starts these failures, evidenced by arcing/discharging to case and BMS modules. Figure 18 shows the overall battery and some highlighted components following a fairly significant thermal event in which the battery sparked and showed significant damage to the BMS units due to discharging. In the photos, it appears the initial fault happened in the Volt's voltage-temperature sub-module (VTSM) boards. The orange arrows in the bottom of the photograph highlights the likely spot of initial loss of isolation and are thus a likely location of discharge once isolation has been lost. In this scenario, isolation was lost due to leaking battery coolant coming in contact with the VTSM board.

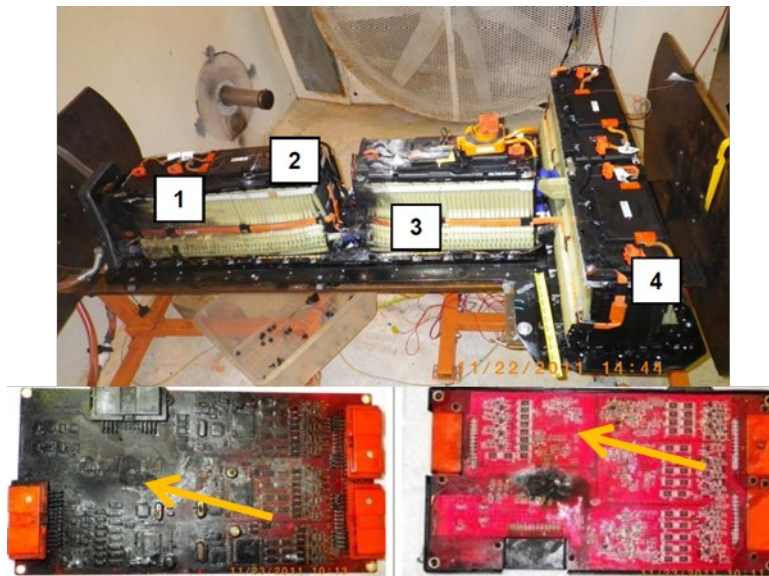


Figure 18: Highlighted battery arcing and VTSM (BMS) issues due to coolant leakage (Chevrolet Volt) [6]

Figure 19 shows another test where the battery only showed a small amount of heat degradation on the voltage sensing cables. Although this incident is much less severe, it again highlights an issue that appears to be led by faults on the sensing circuits as opposed to a battery cells themselves.

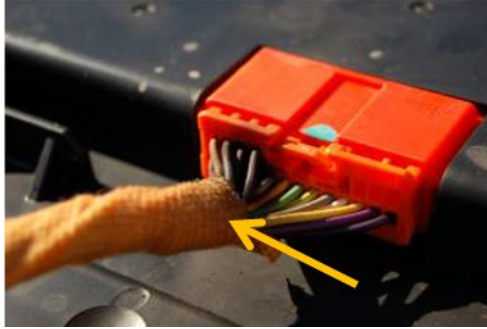


Figure 19: Connector degradation with minimal damage (Chevrolet Volt) [6]

Figure 20 shows yet another issue related to the interface between VSTM board and module level voltage measurement/balancing leads. In this example, the observed fire was extinguished prior to engulfing the entire pack, so it is uniquely helpful in identifying where the initial thermal event took place. As with the other examples the figure shows evidence of significant damage to the VSTM boards and connection circuitry, yet the cells themselves do not show any issues.

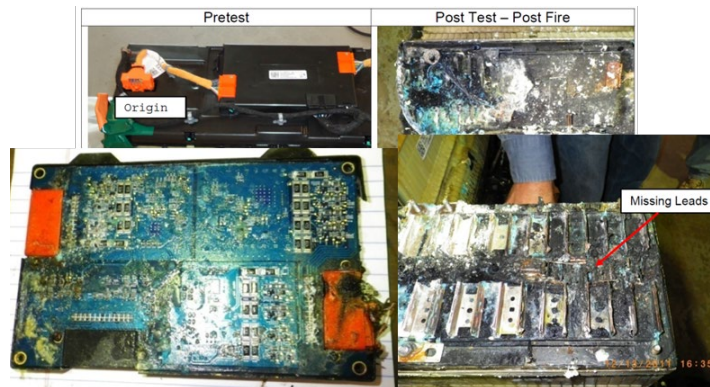


Figure 20: VSTM (BMS) lead overheating example (Chevrolet Volt) [6]

Another takeaway from this work is that issues related to coolant or water intrusion may respond fast or slow. In some cases, sparking was observed immediately once the battery was exposed to leaking coolant. In other cases, the reaction was delayed up to several weeks. Furthermore, loss of isolation that begins with a high-resistance pathway to vehicle ground may take a while to develop and may only be seen intermittently. This issue strongly suggests the value of tracking parameters as opposed to simply providing a go/no-go decision relative to a certain set of parameters. It is hypothesized that if isolation resistance was tracked for the delayed onset cases observed during this and other work, an early-warning indicator could have been provided relative to the overall battery system beginning to degrade.

Fisker Karma Issues Following Hurricane Sandy-Related Flooding

BMS related battery issues and failures also appear in many Fisker vehicles affected by flooding related to Hurricane Sandy. A wide range of issues ranging from cell damage to external enclosure damage (from heating) were observed. Anecdotally, batteries that had higher water levels actually had fewer and less severe damage (suggests more discharge in flood water likely reduced energy levels, thus reducing severity). Interestingly, many BMS modules on the higher row within the pack were actually still

somewhat operational as evidenced by flashing LEDs. Figure 21 through Figure 25 show the variety and degree of damage observed across many of these packs, varying from water intrusion to clear indicators of high-energy discharge. As with the Volt photos, many of the damaged packs show significant BMS board and connector degradation while showing no issues with the individual cells. This again suggests that many of these failures are related to system-level loss of isolation as opposed to cell-initiated failure.



Figure 21: Water Intrusion of the entire pack



Figure 22: BMS damage and shorting



Figure 23: Module enclosure damage



Figure 24: Evidence of arcing/aggressive discharge



Figure 25: Evidence of actual individual cell damage

Battery Failure and Thermal Runaway Background and Supporting Research

Stranded Energy Hazards

Given this project revolves around making batteries safer following damage or a vehicle incident, it is important to introduce the risks associated with stranded energy and damaged battery packs. Assuming that the pack is not already leaking electrolyte or sparking/on fire, the two largest risks associated with a damaged battery are high-voltage exposure and delayed onset thermal incident. As discussed previously, there are many in-place safety systems (contactors, hardware interlocks, etc.) to protect against high-voltage exposure. Moreover, aside from fully depleting a battery pack (and possibly causing irreparable damage), reducing the SOC level of a battery pack typically does not reduce overall pack voltage below a safe threshold. For example, Figure 26 shows the terminal voltage for a Nissan Leaf driven over a full battery depletion and the pack still has a relatively high-voltage level despite the pack being discharged to the point of inability to provide sufficient driving power.

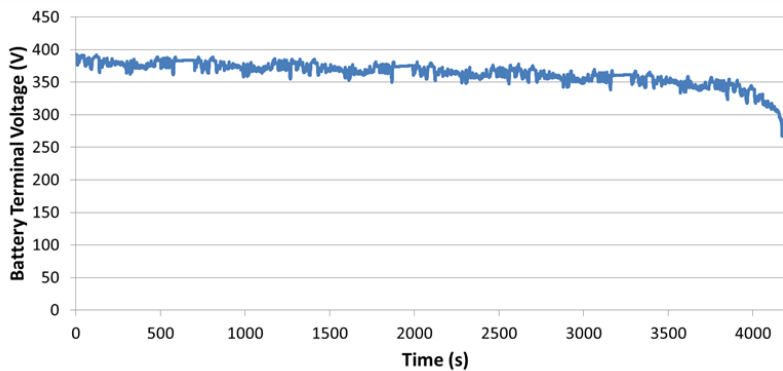


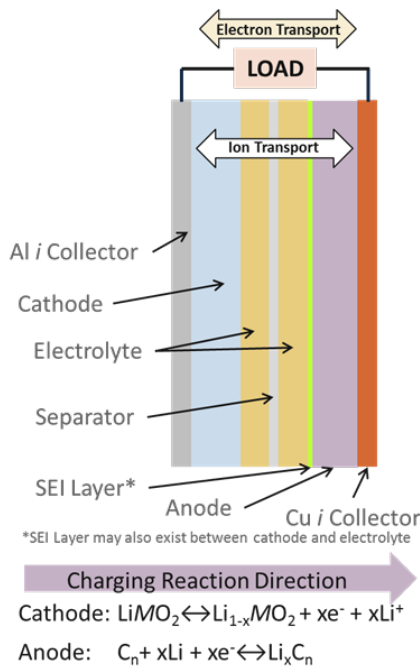
Figure 26: Nissan Leaf battery terminal voltage versus time (full depletion UDDS data)

Relative to a delayed onset thermal event, evidence suggests that lowering the SOC level of a battery pack will likely reduce the risk and severity of a thermal event. This is particularly important for towing/storage/repair/secondary responders since they will likely be at the greatest risk of delayed thermal event while a vehicle is in storage or being towed to a different location. Roughly speaking, reducing a damaged battery's SOC level is analogous to draining a fuel tank following an accident.

Thermal Runaway Overview

While this section does not seek to provide an exhaustive analysis of thermal runaway reactions and their causes, a basic understanding of the processes, stages, and battery components associated with runaway is helpful in providing context to the discussions contained in this work. Thermal runaway mechanisms are a topic of significant research and vary across parameters such as cell chemistry, cell design, and fault type. The reader is suggested to begin with Spotnitz and Franklin [7] and Doughty and Roth [9] for deeper insights into the mechanisms and phases of thermal runaway for Li-ion cells. Broadly speaking, thermal runaway is caused by a series of exothermic decompositions within a battery. If sufficient heat is not dissipated, these reactions drive additional reactions, compounding the overall heat release rate and furthering the decomposition to other battery components. As summarized in Figure 27, the initial onset phase of thermal runaway typically begins with partial decomposition of the solid-electrolyte interface (SEI) layer between a battery's anode and electrolyte. Once this passivation layer begins

to degrade, additional exothermic reactions between the electrolyte and anode can be observed. This continued degradation leads to the next phase of runaway: acceleration. In this phase, the anode and cathode begin to decompose, these reactions themselves contribute excess heat that then further pushes the decomposition of the battery's electrolyte. This multi-location exothermic decomposition begins to provide additional heating, which will typically push the battery into the third stage of the runaway process, namely the runaway itself. In this phase, multiple high rate decomposition reactions are taking place between the electrolyte and the anode/cathode as well as within the electrolyte itself. These intense reactions often lead to the rapid generation and expulsion of gasses, many of which are highly flammable. These gasses can also expel battery electrolyte that is typically also flammable. The combination of rapid gas and/or electrolyte expulsion alongside a physically degrading (and often sparking) battery pack often provides both the fuel and initiation point for an explosion or thermal event.



Stages of Battery Degradation

Note: These vary significantly with battery materials, additives, composition, etc.

Phase 1: Onset

SEI breakdown > Increased reactivity between electrolyte and anode > Some gas generation due to electrolyte decomposition >

Phase 2: Acceleration

Continued heating and gas generation > Exothermic anode and cathode decomposition > Continue electrolyte decomposition (depends significantly on electrolyte composition) >

Phase 3: Runaway

Multiple high-rate anode-electrolyte, cathode-electrolyte, and electrolyte decomposition reactions > Significant gas generation (some highly flammable) leads to possible electrolyte/gas expulsion and/or ignition

Figure 27: Battery components and thermal runaway/degradation steps

Understanding and avoiding, or at least reducing the severity of this type of runaway reaction is one of the desired goals of this project and the following sections discuss the sensitivity of thermal runaway relative to SOC level.

Highlighted Research: Battery Thermal Runaway Proclivity and Severity Versus State-of-Charge

While there is a vast and wide variety of battery thermal runaway research, this section focuses on highlighting some selected research that helps answer the question: "What is a reasonable SOC level to reduce the risks of catastrophic thermal runaway following an incident?"

While state-of-charge is widely known to be a major driver of cell/module/pack response in a thermal event or abusive scenario, there is not widespread research looking at response versus SOC for a variety of cell chemistries with a focus on finding "safe" SOC levels that sufficiently ameliorate both the intensity and onset of a thermal runaway event [9]. In fact, the vast majority of battery abuse testing as well

as material/cell evaluation [11, 12] is done at or above 100% SOC that is generally considered “worst case” for most test scenarios. Interestingly, the fact that the majority of battery abuse testing is done at 100 percent SOC or above is, in itself, a qualitative indicator that reducing SOC aids in reducing the severity of the response of a battery undergoing thermal runaway. As with most battery characteristics and responses, behavior varies depending on chemistry, previous use, and many situational factors, but this section seeks to highlight a range of research deemed specifically relevant to one of the primary goals of this project: understanding the thermal response of batteries relative to SOC as well as providing supplemental evidence that lowered energy states (and thus SOC) do contribute to reduced thermal runaway severity as well as elevated on-set temperatures required to initiate a runaway event.

Given their relatively earlier acceptance into commercial goods and the challenges associated with air-shipment of Li-ion batteries [10], regulations and research related to the air shipment of Li-ion batteries was selected as a possible avenue of research for information regarding the relationships between the severity of thermal events and battery SOC. As would be expected with such an important topic, the Federal Aviation Administration (FAA) has completed several research experiments regarding pack thermal response relative to SOC. More specifically, the work of Webster[13] provides some critical insight as well as data regarding both the cell level thermal response and pack propagation aspects of Li-ion batteries relative to SOC. The inclusion of pack propagation information is particularly insightful and relevant to this project since the majority of flammability and safety research focuses on individual cell response relative to SOC. In the pack propagation portion of these experiments, four 18650 format Li-ion cells were wired together to form a module and a 100W cartridge heater was placed next to the first cell in order to provide the heat for the runaway experiment. Tests were run at 100 percent, 50 percent, 40 percent, 30 percent, and 20 percent SOC and thermocouples were used to record individual cell temperatures for each of the four cells in the string as well as the cartridge heater. Figure 28, created with slides compiled from an FAA presentation [13], shows the experimental setup (left) and example results for this work (right).

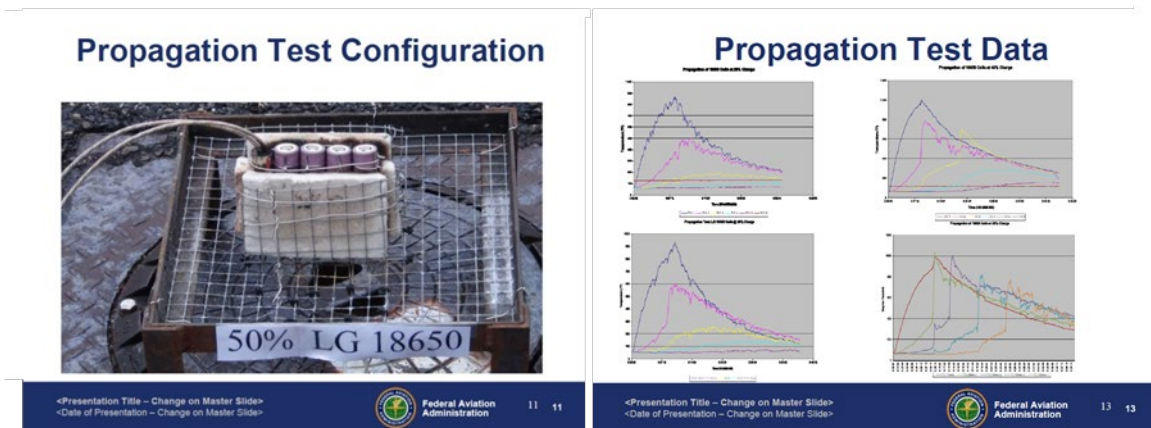


Figure 28: FAA testing/presentation of Li-ion battery thermal propagation versus state-of-charge (SOC) [9]

As discussed in the FAA presentation and summarized here, several behaviors were seen across the range of SOC's tested during the pack propagation study. As would be expected from the general trends of more aggressive thermal behavior at elevated SOC levels, the first cell in the 100 percent SOC case heated very rapidly and exploded with a peak observed temperature of 1030°F observed at Cell 1. Following the explosion, Cell 1 rapidly cooled and minimal heat was transferred to the other cells within the module, resulting in minimally elevated temperatures seen across Cells 2-4 (~200°F at Cell 2). For the 50

percent SOC test case, shown in the lower right sub-figure of Figure 28, all cells see elevated temperatures (Cell 1 max = 1044°F) and all cells are in fact consumed due to thermal propagation through the module. It is assumed that since the 50 percent SOC case did not exhibit the rapid cooling observed in the 100 percent SOC case following the explosion, more heat flowed to the remaining cells culminating in the consumption of the entire module. At 40 percent SOC Cells 1 and 2 are consumed due to thermal exposure (Cell 1) and propagation (Cell 2), while Cells 3 and 4 remain relatively stable. Testing at 30 percent and below shows minimal to no thermal runaway propagation. Although Cell 1 vented for both low SOC cases (30% and 20%), the peak observed Cell 1 temperature was roughly half compared to the 100 percent and 50 percent testing, again supporting the idea that, on an individual cell level, lowered SOC levels reduce the severity of a thermal event should one occur. More importantly, this work provides evidence that a SOC level below 50 percent, on the order of perhaps 30 percent or lower, may offer additional protections in terms of propagation of thermal runaway within a module and pack.

Further supporting the applicability of a maximum SOC threshold for reduced thermal response, another aviation group appears to be examining the possibility of including a maximum SOC threshold for Lithium-ion battery air shipment. According to meeting minutes, the Dangerous Goods Panel of the International Civil Aviation Organization has been evaluating a recommendation put forth from a meeting of the International Multidisciplinary Lithium Battery Transportation Coordination Working Group [14] that “all lithium-ion cells for shipment be limited to [an SOC] of no more than 30 percent as an interim means to reduce the probability of propagation of thermal runaway between cells.” While this statement is subject to adjustment for differing chemistries and form factors, as well as new research developments, it nevertheless highlights a case of reduced SOC levels being suggested for reduced battery thermal response.

As discussed previously, on the cell level, the majority of recent and on-going research focuses on thermal behavior at SOC levels at or above 100 percent, with minimal research relative to behavior across a range of SOC levels. While this worst-case analysis is obviously the most efficient way to develop new battery materials and safety systems, it somewhat limits the availability of data regarding SOC versus thermal response (severity and initiation). Fortunately, despite these challenges, there is still a useful body of research pertaining to battery thermal response versus state of charge within the larger battery research community. Sandia National Laboratory has done extensive work with several Li-ion cell chemistries across a range of SOC levels. Of particular relevance to this work, Sandia published a report [8] detailing the results of accelerating rate calorimetry testing for two different cell chemistries across a range of SOC levels. Figure 29, using figures pulled from the Sandia report, provides a summary chart for each cell chemistry evaluated from the report showing the heat release rates relative to temperature for the range of SOC values testing. Several interesting trends can be observed relative to SOC and thermal response. Both sub-figures show significantly reduced heat rates as SOC decreases, in fact, the “Gen 1” cells show little to no heating below roughly 50 percent SOC. Secondly, the onset of temperature of each cell’s runaway response is shown to increase as the SOC level is reduced, particularly in the case of the “Sony” cells. In addition to simply reducing the severity of a response given a thermal incident, this delayed onset result suggests that certain runaway propagating situations could be avoided at lower SOC levels due to the higher required onset temperature. Lastly, as discussed earlier, thermal response and onset temperature are dependent on cell chemistry, and while there are observable trends in both cases, there are very clear differences between the overall behavior of the cells and the relative impacts due to SOC.

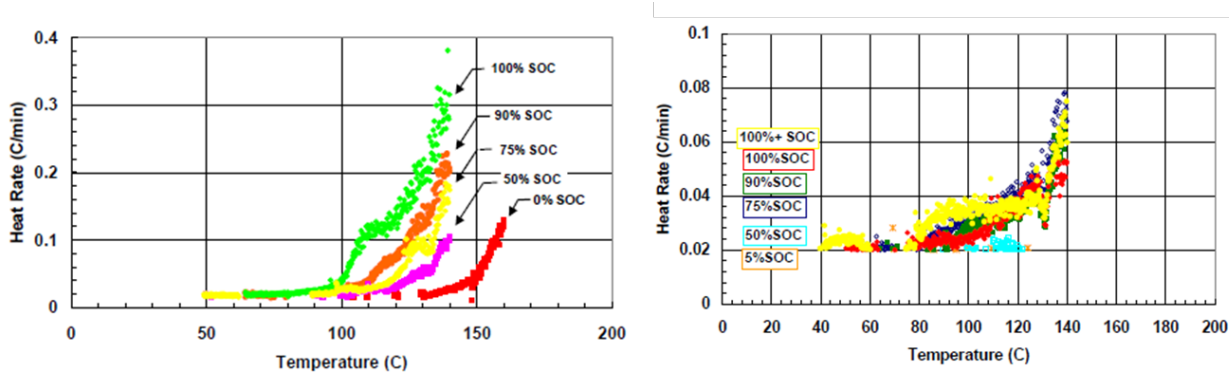


Figure 29: Accelerating Rate Calorimetry derived heat rate versus temperature and SOC for Sony 18560 (LiCoO₂) (Left) and Argonne Designed “Gen 1” Cell (LiNi_{0.85}Co_{0.15}O₂) (Right)[8]

Sandia has also tested some additional cell chemistries under similar test conditions. This work [16] includes ARC testing of “Moli” cells at range of voltage levels (and thus differing SOC) and shows similar trends to the previously discussed ARC testing. As can be seen in the left sub-plot of Figure 30, the maximum heating rate decreases with lower SOC levels, showing roughly a threefold decrease in maximum heating rate between the lowest and highest SOC levels tested. Additionally, the right sub-plot of Figure 30 shows increasing runaway initialization temperature as SOC level is decreased. As with the previous work, this highlighted research work again shows reduced thermal activity as SOC is decreased, similarly, initialization temperature of thermal runaway is also increased as SOC increases, which suggest a battery may have the ability to avoid entering runaway due to the higher initialization temperature.

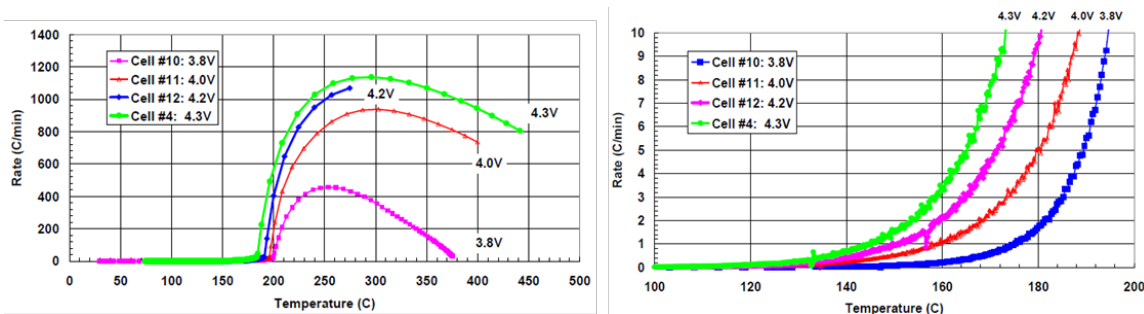


Figure 30: ARC derived heat rate versus temperature and SOC for Moli cells. Full response (left) and zoomed-in (right) to show initialization temperature trends [16]

Work by Wang [17] has also looked at the relationship between onset temperature, reaction heat, and peak temperature versus SOC for Li_xMn₂O₄ material alone as well as in a system with electrolyte. This work again comes to the conclusion that overall thermal stability increases as SOC decreases, which agrees with the other research provided in this section.

In summary, while there is limited work pertaining to evaluating thermal stability and runaway severity versus SOC, there are some valuable contributions to be found both in research literature as well as the regulatory environment. Despite differences related to factors such as cell chemistry, pack design, and cell form factor, there is a strong body of research that supports the conclusion that battery thermal stability and runaway severity is strongly affected by battery SOC. More specifically, as SOC increases, stability decreases and the severity of a possible thermal runaway event increases, often rather dramatically near 100 percent SOC. While some the previously discussed research seems to suggest that SOC levels 50 percent and below would generally allow for a relatively more stable battery, it seems prudent

that a level closer to 30 percent and below be recommended since it allows for some further stability and reduced severity as well as possibly helping to mitigate propagation as shown in the FAA analysis.

Sandia LGCPI Battery Thermal Runaway Versus SOC Testing

In order to include some more recent, large format cells into this assessment work, a study assessing the impact of state of charge on thermal runaway was funded through this project and performed at Sandia National Laboratory. The following section provides the report and analysis for this sub-project as completed by the authors listed below.

Final Summary Report of Studies on the Impact of State of Charge on Thermal Runaway for 16 AH LGCPI Cells

By Joshua Lamb, Christopher Orendorff, Leigh Anna Steele, Scott Spangler, and Jill Langendorf

Introduction

While the thermal runaway of lithium ion batteries is well studied, typical testing probes the response of cells in the worst-case scenario of cells at nominally full charge [20-23]. Cells at lower state-of-charge have long been assumed, and in some cases shown to be less likely to exhibit a self-propagating thermal runaway reaction when compared to higher states of charge. This is evident in DOT shipping regulations that require lithium ion batteries to be discharged to 50 percent SOC prior to transport. What is less well known is how batteries behave as a cell transitions from full charge to lower states of charge, and at what states of charge do batteries become less inclined to undergo thermal runaway.

Upon reaching sufficiently high temperatures a number of exothermic reactions can occur within a lithium ion battery. These can include break down of the anode and cathode, electrolyte reactions and self-discharge from internal short circuit events. A self-propagating thermal runaway occurs when the heat generated exceeds heat loss from the battery. This may first be observed as mild self-heating, but as the reactions progress their speed increases until a rapid runaway reaction begins. This is typically accompanied by rapid self-heating, voltage loss, and smoking and ejection of particulate matter. The electrolyte and vent gases are flammable as well, and in some cases the heat of thermal runaway is sufficient to ignite these materials leading to a fire [20,23-25]. At lower states of charge, it is likely that the heat loss from the battery exceeds any heat generated by thermal decomposition. If this is the case, while the battery may be irreparably damaged, it is unlikely to undergo an uncontrollable thermal runaway reaction.

This work examines the thermal runaway behavior of spinel-based cells at varying states of charge. The cells studied were tested using ARC as well as open-air thermal ramp tests. States of charge from 20 to 100 percent were tested. This will ultimately provide a better understanding of how thermal runaway is affected by state of charge, as well as provide detail for the cells tested on the threshold of runaway threat.

Experimental Methods

Sixteen-amp-hour LGCPI lithium-ion pouch cells were evaluated using ARC as well as thermal ramp to determine the impact of state of charge on thermal runaway. ARC testing was performed using a Thermal Hazard Technologies EV ARC calorimeter. The cells were constrained in ½-in. aluminum plates with cell temperature measurement made at the negative electrode. The cells were initially heated in 5-degree increments, with 45 minutes to allow for temperature stabilization after each heating step. A self-heating

threshold of 0.02 °C/min was used; if the cells exhibited self-heating above this threshold after the stabilization period the cell would be allowed to continue to exotherm without applying another heating step. If the rate of temperature change was below this threshold, the cells would undergo the next heat and stabilization step. The cells were tested up to a maximum temperature of 410 °C, or until thermal runaway had occurred. The heating rate is measured in °C/min by the calorimeter, and the heating rate in aatts is calculated using the calculated heat capacity of the cell holder (1,628 g measured Al mass, 1,460 jK specific heat) and an estimated average heat capacity of the cell (334 jK, based on measured average mass of cells and previously observed average heat capacity of similar cells).

Thermal ramp measurements were performed by heating the cells in brass heater block constraints at a constant rate of 5 °C/min up to 250 °C or until thermal runaway was observed. If thermal runaway did not occur by the time the cell temperature raised to 250 °C, the cell temperature was held for 30 minutes, after which the heat was removed if a runaway event had not occurred.

Cells were tested in 20 percent SOC increments, from 100 percent SOC down to 20 percent SOC. SOC was set by first charging the cells up to 4.2 V, followed by discharge to the desired state of discharge in amp hours based upon the rated capacity of the cells. Select cells were also subjected to capacity cycling at a C/5 rate to verify the rated capacity of the cells received.

Results

The data shown here details the adiabatic thermal runaway behaviors of 16-Ah spinel-based cells from 20 percent to 100 percent SOC. The heating rate curves collected during ARC testing can be seen in Figure 31 through Figure 35. An exothermic event is present at all SOC, however there are significant changes to the heating rates and total energy as the SOC increases. The collected data is compared in Table 2 as well as in Figure 36 and Figure 37.

Table 2: Tabulated ARC results, detailing onset of runaway, peak heating rates observed and enthalpy of runaway reaction.

| SOC | Onset of Runaway (C) | | Peak Heating Rate (C/min) | | Peak Heating Rate (W) | | Enthalpy of Runaway (kJ) | |
|-----|----------------------|-------|---------------------------|-------|-----------------------|-------|--------------------------|-------|
| | Run 1 | Run 2 | Run 1 | Run 2 | Run 1 | Run 2 | Run 1 | Run 2 |
| 20 | 216 | 216 | 0.126 | 0.091 | 3.77 | 2.72 | 40.5 | 38.7 |
| 40 | 190 | 192 | 0.131 | 0.142 | 3.92 | 4.25 | 79.7 | 116 |
| 60 | 185 | 189 | 0.74 | 0.814 | 22.1 | 24.3 | 127 | 117 |
| 80 | 188 | 193 | 3.1 | 2.6 | 88 | 73.3 | 140 | 154 |
| 100 | 194 | 199 | 20.3 | 13.7 | 607 | 409 | 164 | 183 |

Figure 31 below shows the exothermic heating rate of the thermal decomposition of cells at 20 percent SOC. This shows most of the energy of the event occurs within a single peak with an onset of 216 °C. Maximum peak heating rates of 2.7-3.8 W were observed, with total enthalpies of 38.7-40.5 kJ.

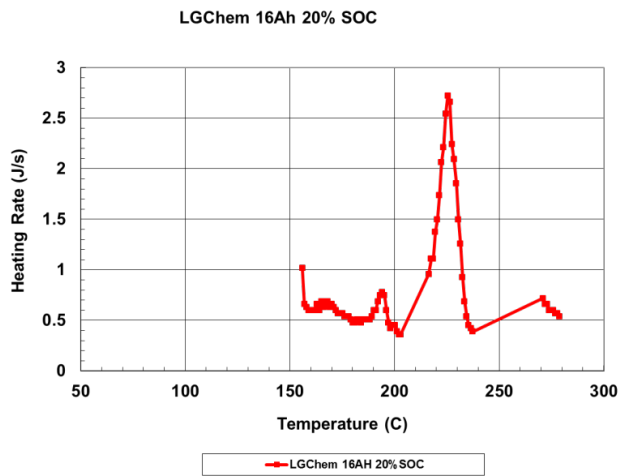
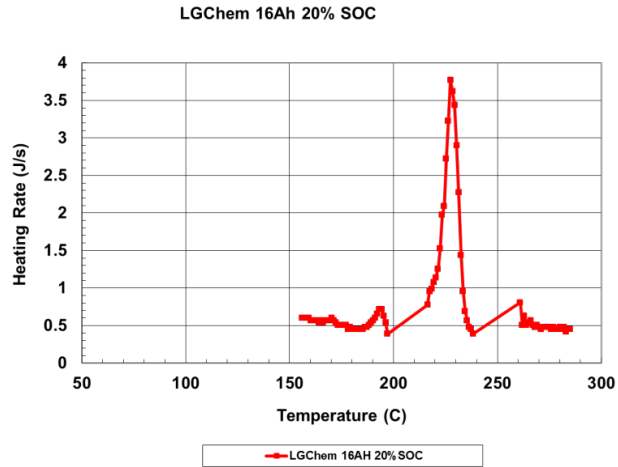


Figure 31: ARC data of cell at 20 percent SOC

Figure 32 shows the heating rate data collected at 40 percent SOC. The primary runaway shows an onset of 190 to 192 °C, with peak heating rates of 3.9 to 4.3 W. This also shows a second peak forming as part of the runaway reaction. This two peak runaway reaction is a common behavior for spinel-based chemistries. Enthalpies of 90 to 116 kJ were observed during the runaway reaction.

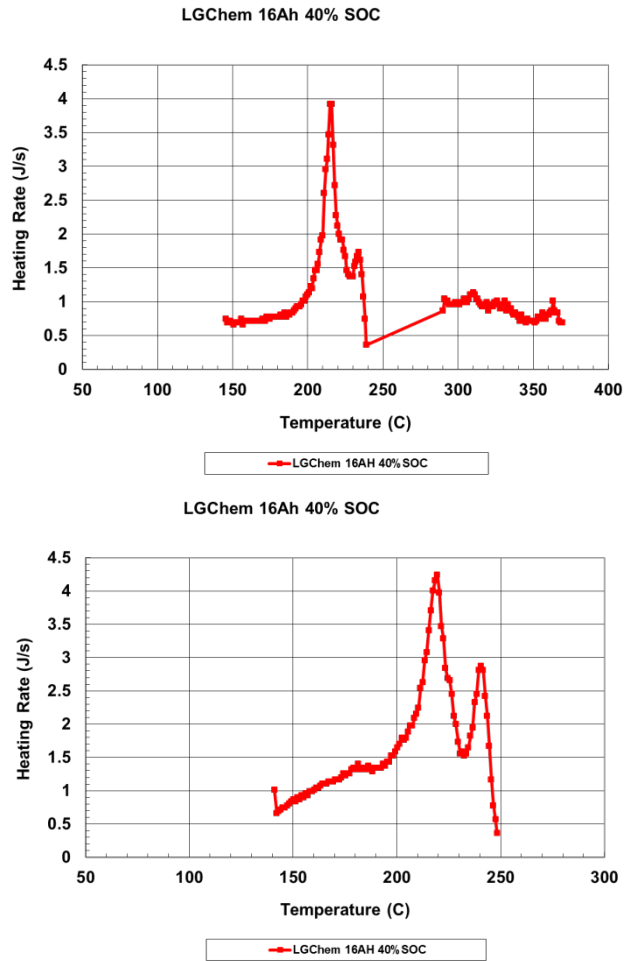


Figure 32 ARC data of cell at 40 percent SOC

Figure 33 below shows the heating rate data for cells at 60 percent SOC. An onset of 185 to 189 °C was observed with peak heating rates of 22 to 24 W. The two-peak feature is still present, however at this SOC the second peak has become the more predominant of the two. Total runaway enthalpies of 117 to 127 kJ were observed.

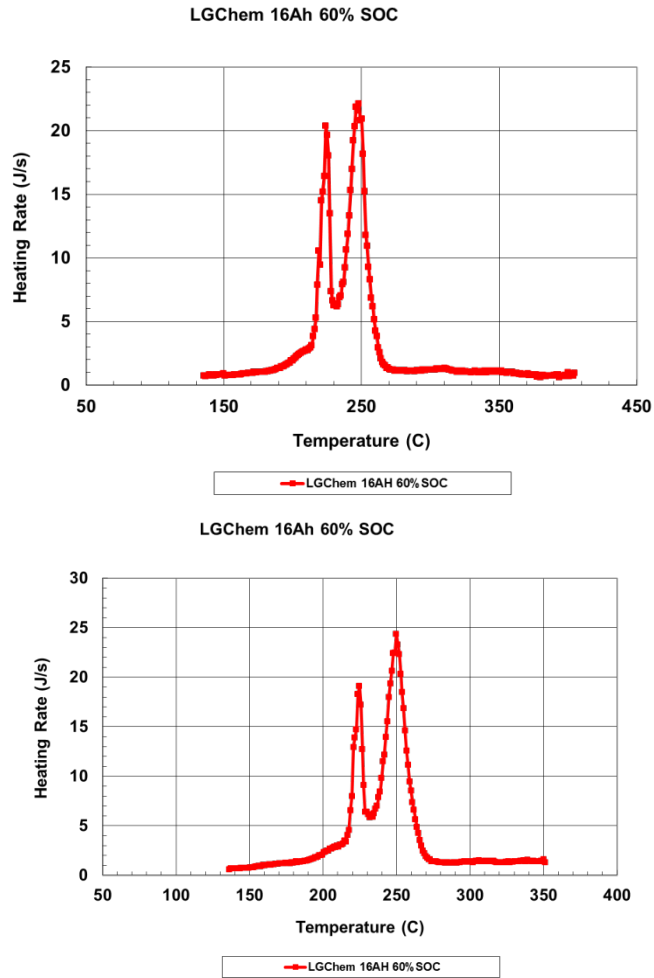


Figure 33: ARC data of cell at 60 percent SOC

Figure 34 below shows the heating rate data collected on cells at 80 percent SOC. An onset of 188 to 193 °C was observed, with peak heating rates of 73 to 88 W. This continues the trend of increasing prominence of the second peak, also the peak heating rates have begun to significantly increase at this SOC. Total runaway enthalpies of 140 to 154 kJ were observed.

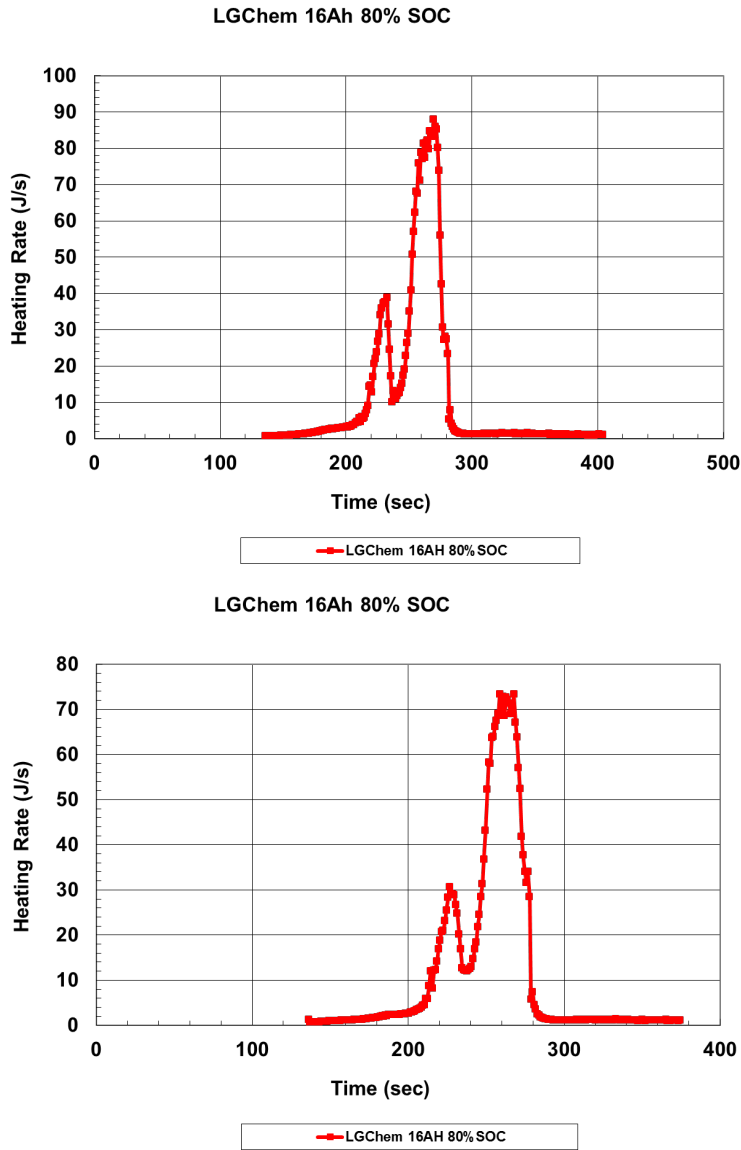


Figure 34: ARC data of cell at 80 percent SOC

Figure 35 below shows the heating rate data collected on cells at 100 percent SOC. An onset of 194 to 199 °C was observed with peak heating rates of 409 to 607 W. This shows a sizable jump in the peak heating rates with the increase to 100 percent SOC, showing the increased possibility for an uncontrollable thermal runaway at higher SOC. The total enthalpy, however, increases to 164 to 183 kJ. A definite increase is observed, but not an increase of several factors unlike the peak heating rates.

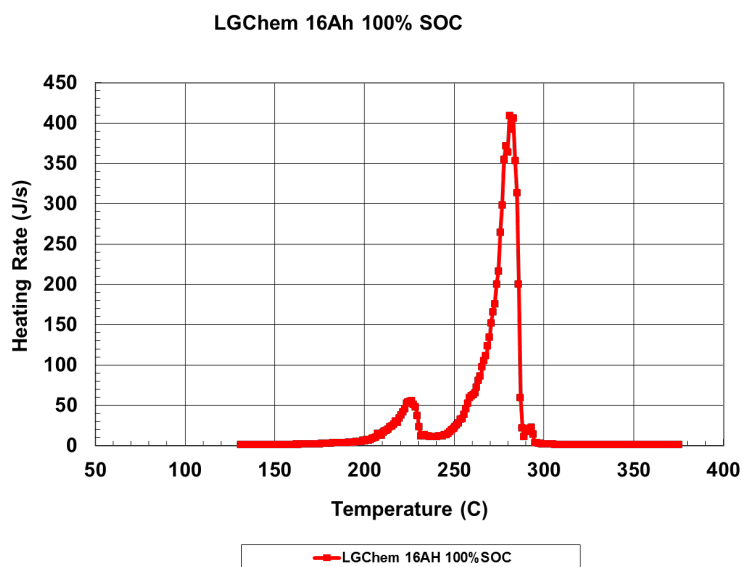
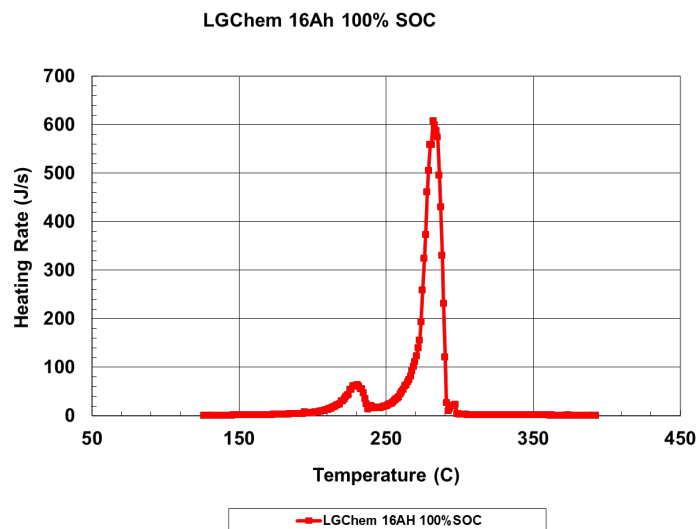


Figure 35: ARC data of cell at 100 percent SOC

The exothermic rate data from the ARC measurements are compared in Figure 36 and Figure 37. Figure 36 shows all runs collected together, and here it can be seen that the heating rates are very low at 20 – 40 percent SOC, but begins to increase at 60 percent SOC and ramps up very quickly from 80 to 100 percent SOC. Figure 6 shows the runaway events at 20 to 60 percent SOC expanded for greater detail. This shows the two peak feature of the runaway is still noticeable as low as 60 percent SOC, but begins to shift to one small peak at 20 to 40 percent SOC. The runaway from 20 to 40 percent SOC was measurable but ultimately a very low rate and would likely not self to perpetuate under non adiabatic conditions.

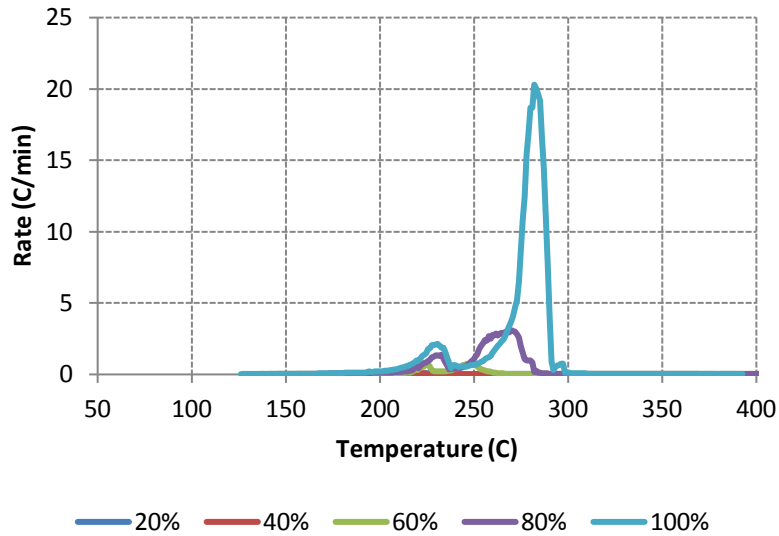


Figure 36: ARC exothermic rate data comparing 20 to 100 percent SOC.

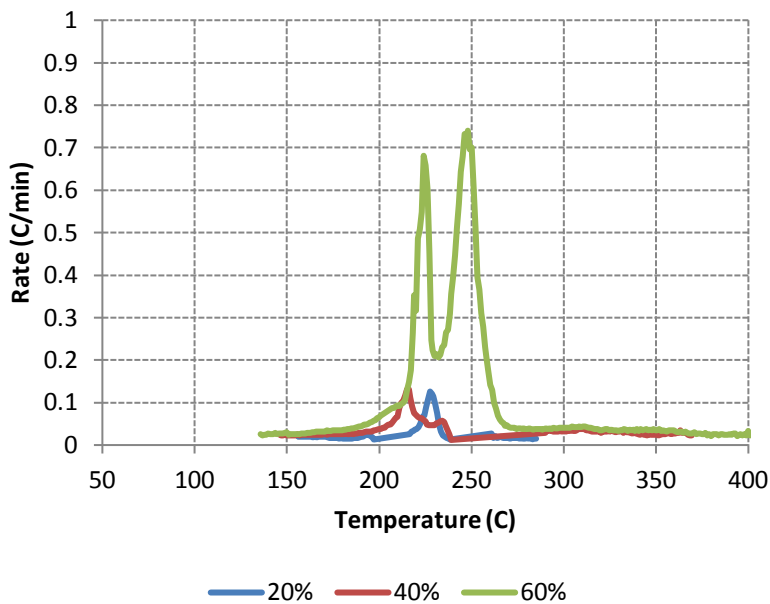


Figure 37: Exothermic rate data from Figure 6 showing the low rate exotherms present from 20 to 60 percent SOC.

Plots of enthalpy and peak heating rates of the runaway events are shown in Figure 38. This data shows that while the runaway enthalpy increases fairly linearly with state of charge, the peak heating rates begin low and rapidly increase with increasing state of charge, perhaps following an exponential path. This is significant in non-adiabatic systems, as if the heating rate remains below the rate of heat lost by the cell, no thermal runaway event will occur. Specifically the data here shows that a self to perpetuating thermal runaway would be very unlikely to occur at 40 percent SOC and below unless the system was very well insulated. This correlates well with data collected previously at Sandia on LiCoO₂ cells that observed a thermal runaway threshold of ~50 percent SOC [23,26]. This helps to reinforce the conventional wisdom calling for lithium ion cells being transported or under long term storage to be held at 50 percent SOC,

however it would be useful to examine this behavior with other cell chemistries, particularly as higher energy chemistries such as lithium rich materials and silicon anode materials are used more frequently in large format cells.

The battery system should also be considered when determining the threat of runaway. If the cells are well insulated they may be able to sustain a thermal runaway event even at lower states of charge. However, with the dependence on state of charge shown for the tested cells they would unlikely be able to sustain a thermal runaway below full charge if they are well cooled or even at ambient conditions. The propensity of cells under non-adiabatic conditions to undergo thermal runaway was further examined using a thermal ramp abuse test below.

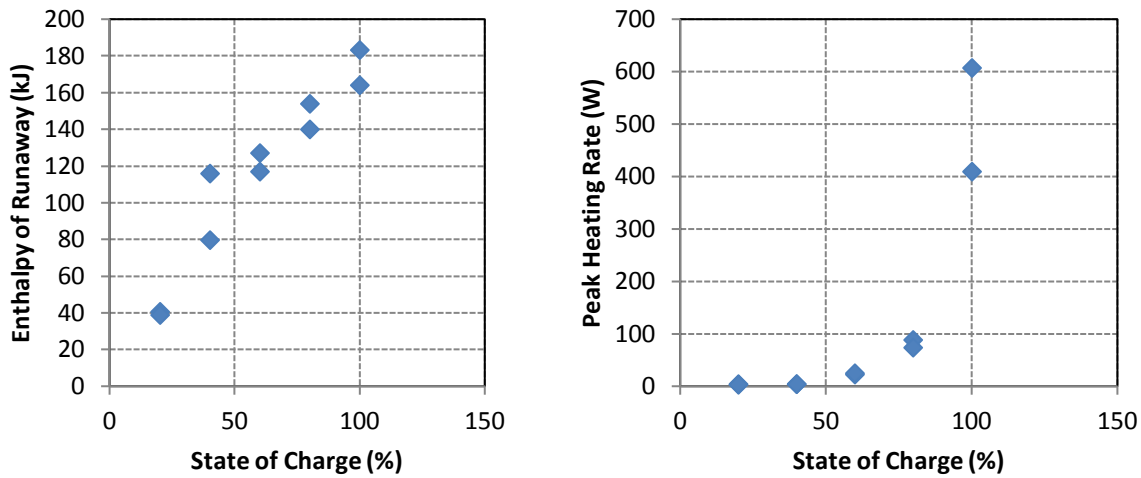


Figure 38: Enthalpy of the thermal runaway event (left) and peak heating rates (right) as a function of the SOC.

Figure 39 through Figure 44 show the results of thermal ramp abuse testing performed on cells at decreasing states of charge. Significant variability was observed at 100 percent SOC. Figure 39 shows a significant thermal runaway event with onset at 245 °C. This is accompanied by a sharp voltage drop down to 0 volts, as well as runaway up to a maximum observed temperature of 520 °C. Conversely, Figure 40 and Figure 41 show cells at 100 percent SOC that were able to sustain a temperature of 250 °C for 30 minutes without evidence of a sustainable thermal runaway event. Both Figure 40 and Figure 41 show signs of a more gradual self-discharge of the cell at high temperature. Where the voltage in Figure 39 shows a sharp drop accompanying the runaway, Figure 40 and Figure 41 show a more gradual decline. This may be evidence of a hard (low impedance) internal short circuit event that occurs in the first cell, while the second two experience either higher impedance internal shorting, or no internal shorting at all and the voltage loss and small temperature increase observed is attributable entirely to the decomposition of cell materials. While it is promising that the more severe event was the exception in these tests, prudent design would prepare for the most severe events and consider the possibility of the cells to undergo a significant thermal runaway at 100 percent SOC. This correlates well to the ARC data observed above, as cells at 100 percent show much higher peak heating rates than those at lower states of charge, creating a much more likely chance for thermal runaway at full charge.

Other features that are notable in the data include a drop in temperature at ~150 °C in each figure that corresponds to the venting of battery gases. Each figure also shows sudden drops and recoveries in the

voltage curve at temperatures of 180 to 200 °C, which may be due to the presence of a shutdown separator or other safety feature present within the cell.

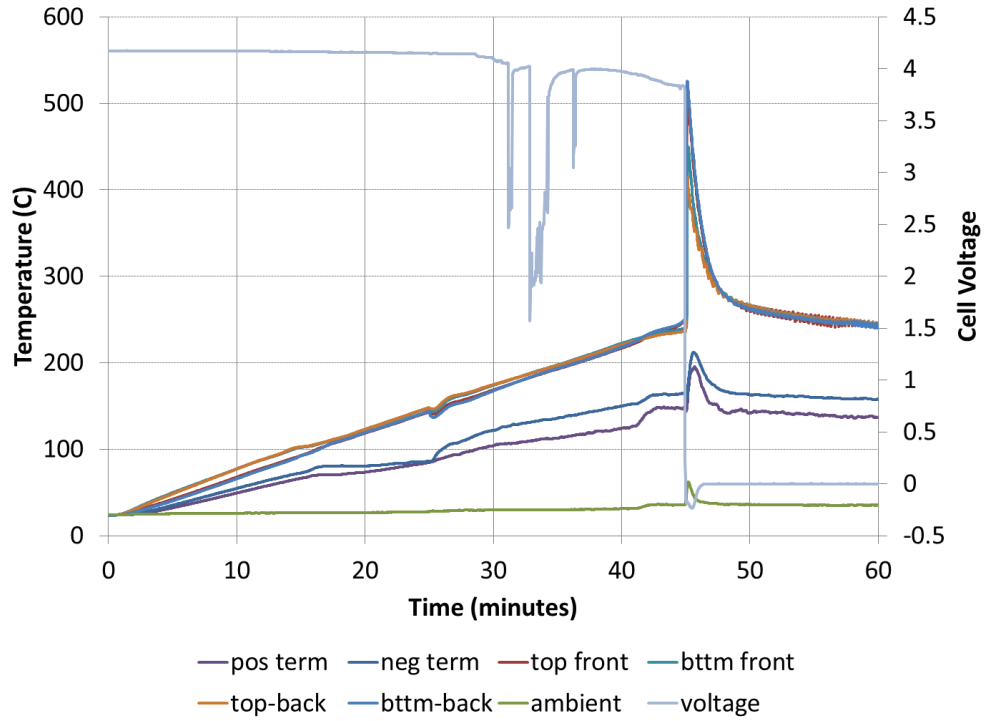


Figure 39: Thermal ramp test at 100 percent SOC showing a runaway reaction at ~210 C.

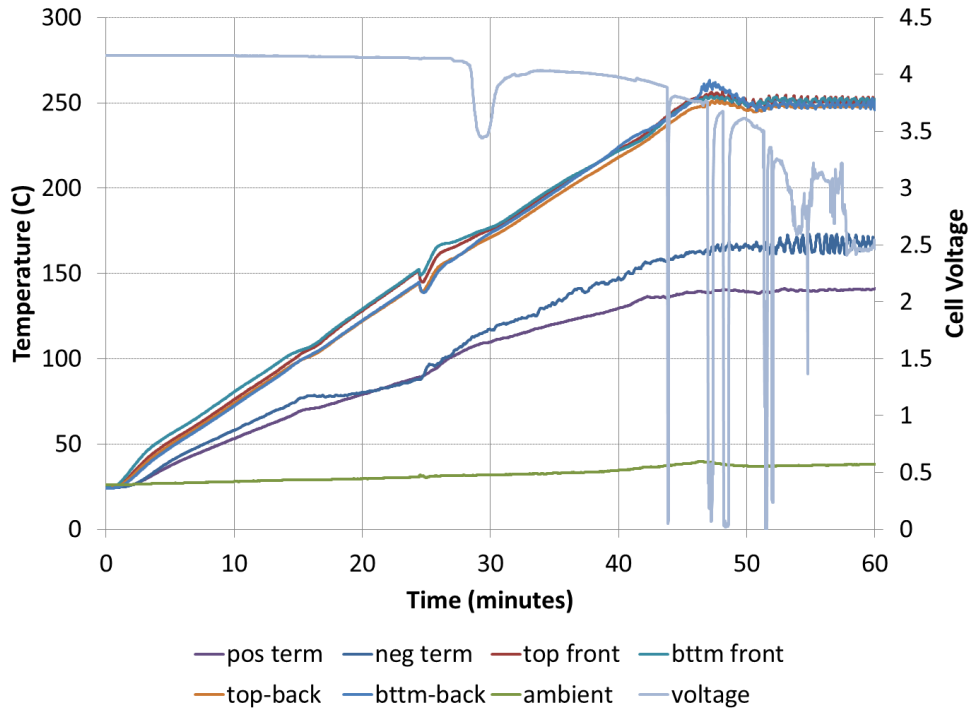


Figure 40: Thermal ramp test performed at 100 percent SOC showing a venting event, and some limited self-heating at 250 C, but no thermal runaway event.

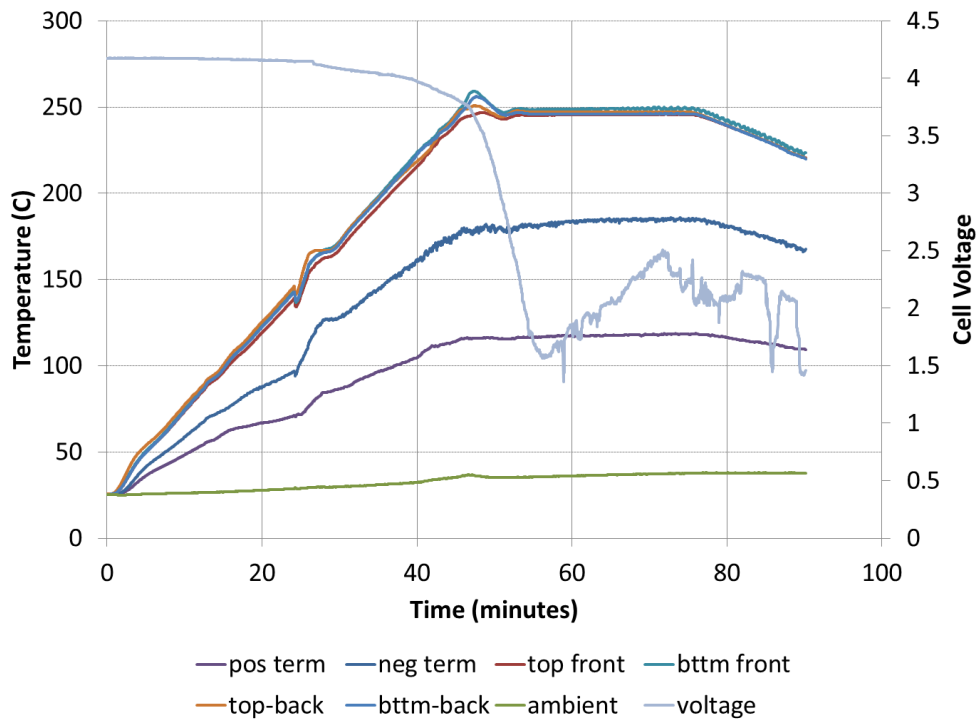


Figure 41: Thermal ramp test performed at 100 percent SOC, showing again a small self-heating event at 250 C, but no true thermal runaway.

Cells tested at 80 percent SOC showed a consistently mild response, with the results shown below in Figure 42 and Figure 43. A slight rise in temperature is observed at 250 °C, coupled with a gradual drop in voltage. Cells at this SOC were ultimately unable to sustain a thermal runaway.

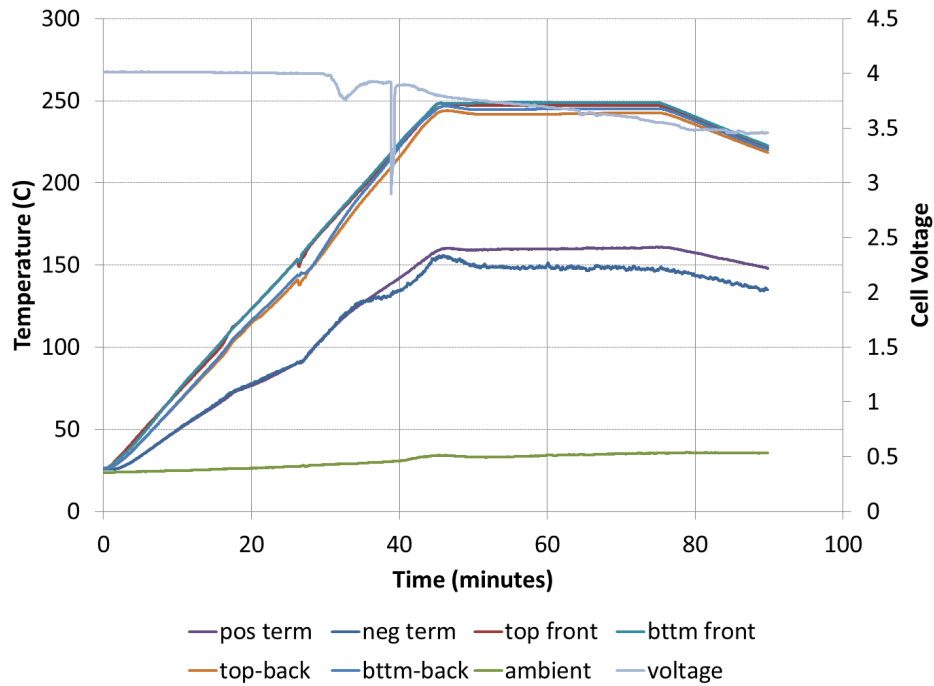


Figure 42: Thermal ramp test performed at 80 percent SOC

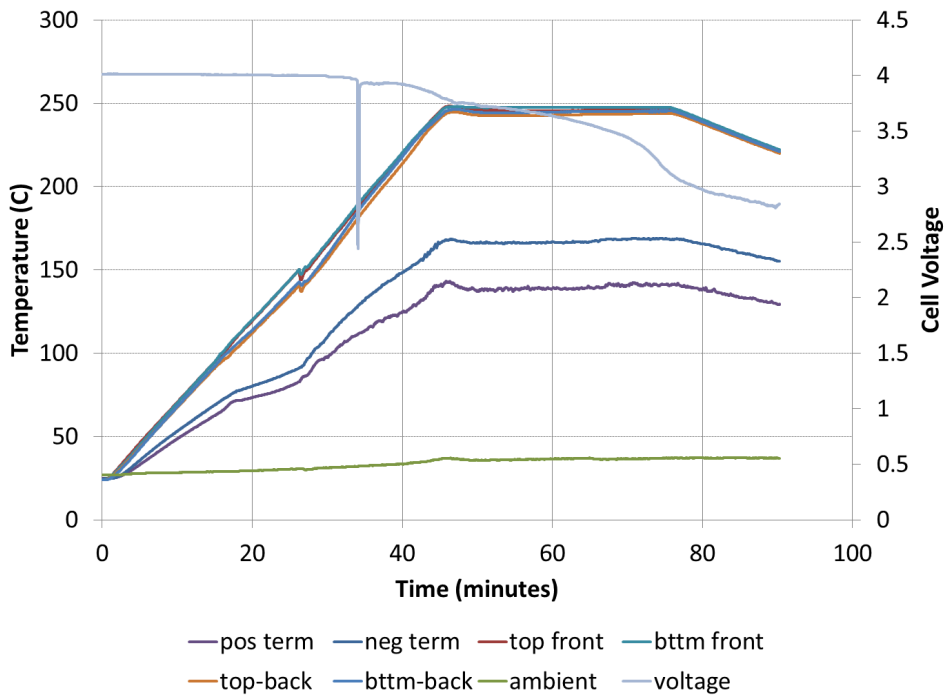


Figure 43: Thermal ramp test performed at 80 percent SOC.

Figure 44 shows a cell tested at 60 percent SOC. This shows no signs of thermal runaway and gives confirmation that self-heating at low states of charge is insufficient to initiate a thermal runaway in the cells tested. Lower states of charge were not tested at this point, as this data confirms that no thermal runaway would likely occur for the tested cells at 80 percent SOC and lower in open-air conditions.

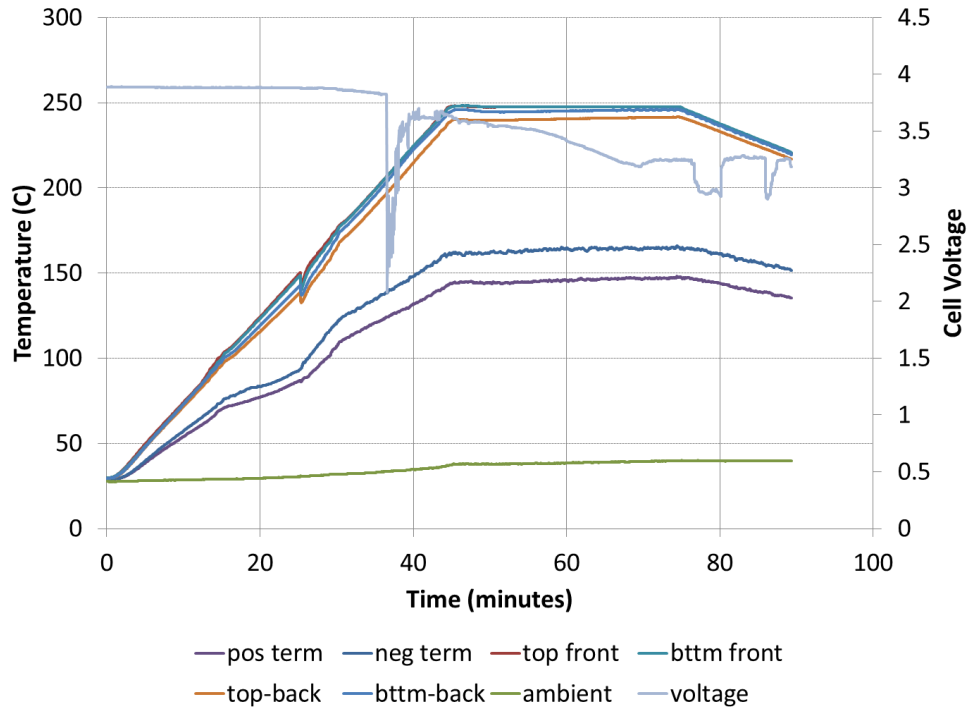


Figure 44: Thermal ramp test performed at 60 percent SOC.

Conclusions

This work demonstrates the effect of state of charge on the likelihood of undergoing thermal runaway at abusive temperatures on spinel-based LGCPI cells. The data shows that while the total exothermic energy of cell failure is linear with the state of charge of the cell, the peak heating rates are very low until 80-100 percent SOC. So, while the total energy available for a thermal runaway is directly related to the total charge of the battery, a self-propagating thermal runaway is unlikely to occur at 60 percent SOC or below. At these lower states of charge even a modest amount of heat loss from the cell would be sufficient to arrest a thermal runaway event. So while a thermal runaway may be possible in a very well insulated cell or under adiabatic conditions (such as within the ARC), under most conditions a thermal runaway at low states of charge would be very unlikely.

This data is primarily representative of the cell chemistries tested and a broader understanding requires testing multiple chemistries to observe their reaction, particularly for determining specific thresholds where thermal runaway is unlikely. Certain general behaviors can be inferred, however. While the threshold of the exact state of charge where a thermal runaway will occur will vary on specific chemistry as well as total heat loss in an individual setup, the rapid drop in self-heating rates as state of charge decreases is likely a typical phenomenon. This supports the conventional wisdom of conducting battery transport and storage at 50 percent SOC, as well as shows that running a battery at less than full charge may improve the safety performance. This should not be interpreted as covering all safety concerns, however. For while reducing the state of charge may reduce the likelihood of a thermal runaway caused by the battery itself,

electrolyte components remain flammable at any state of charge. While the batteries may be unlikely to initiate a fire or thermal runaway at low states of charge, they may be consumed by and contribute to a fire or other thermal event that they are exposed to. Abused lithium ion batteries may also produce battery vent gasses that are both toxic and flammable, even if a thermal runaway does not occur.

Section Summary, Discussion, and Conclusions: Battery Failure and Thermal Runaway Background and Supporting Research

As expected, the work done at Sandia does show a linkage between SOC and thermal runaway response and on-set temperature. As discussed in the previous section, the ARC portion of the work suggests that SOC values below 50 or 60 percent will likely lead to reduced thermal runaway risk. The thermal-ramp portion of this testing suggests that a threshold of 80 percent SOC or less may be sufficient to mitigate any self-propagating thermal runaway situation if sufficient “open air” conditions are met for adequate external cooling. Given the discussion in the introduction section of this work related to in-field failures showing several simultaneous or cascading issues, it is the belief of the authors that many situations in-field are more similar to the ARC conditions versus an “open air” situation that would enable sufficient cooling at even fairly high SOC levels. More specifically, following certain accidents there is often a cascading set of failures that contribute additional heat to the batteries (i.e., discharging through newly opened ground paths, module-to-module discharge, or other internal or external thermal events) ultimately leading to a thermal event. Strengthening this point, there is evidence of at least one field failure of a vehicle, utilizing a similar cell chemistry to those tested in the Sandia work, experiencing a thermal runaway event with a beginning state of charge on the order of roughly 58 percent SOC [6,18]. This thermal event occurred following a crash test that resulted in leaking coolant and eventually the full consumption of the entire pack and related electronic components. Later forensic analysis and investigative testing, also contained in [6], suggests that some degree of shorting and burning in the battery management boards may have contributed to the on-set of the larger thermal event.

The research highlighted in this section points towards the relationship between reduce thermal response with lowered battery state of charge across a range of different battery formulations. While reducing SOC does not ensure complete safety from a thermal event, it does appear to reduce the severity of thermal runaway as well as perhaps increasing the on-set temperature of a possible event. At the module and pack level, the FAA data and analysis suggests that reducing SOC below 50 percent is suggested in order to avoid propagation of a thermal event. Although it need not be measured or estimated with great precision, the authors suggest that an SOC target of 30 percent or lower be used as general guidance for a “safer” SOC level to be used in conjunction with the discharge and assessment tools provided in this report. Given the sensitivity of thermal response to a broad range of factors, if so desired, it is suggested that alternative levels can be considered with sufficient evidence for differing chemistries, cell form factors, and module designs, but, broadly speaking SOC of 30 percent and lower appear to mitigate many of the more undesired thermal responses following an accident or damage scenario

While the main focus of this section was on understanding the stability ramifications of elevated battery SOC, it is worth a few notes here relative to issues related to overdischarge. While there is a relatively small body of research regarding overdischarge as it relates to thermal runaway [28,29], most work has shown that while the cycle life and capability of the battery is affected by overdischarge, thermal stability and severity of response of an overdischarged battery is muted relative to higher SOC cases, consistent with the previous discussion. When dealing with a battery that has been deeply overdischarged (as might be the case if the stranded energy tool was used to fully deplete a battery pack), a significant stability and safety issue arises if the battery is later recharged following this deep discharge. Specifically, dissolution of copper from the current collectors may result in areas for dendrite growth [30].

These sites may later be the initiation point of a thermal event due to an internal short, the severity of which would be elevated at higher SOC levels. With this issue in mind, care must be used when assigning discharge “responsibility” to a particular party to ensure that packs that have been overdischarged to alleviate a stability/damage issue are not returned into the field and used.

Battery Diagnostics and Stability Assessment Techniques

Introduction to In-Vehicle Battery Diagnostics

As discussed in the introductory section, the vast majority of current hybrid and electric vehicles have some type of in-vehicle BMS. These systems are used for a wide variety of purposes [27, 28], but broadly speaking, the uses and components for these systems can be broken into several main functional categories: (1) individual cell/module and overall pack sensing, (2) battery operational state estimation, (3) functionality and safety evaluation, (4) communication of relevant information to/from the BMS. Although an all-encompassing discussion of battery management systems is outside the scope of this work, an introduction to BMS functionality with a focus towards components and techniques that may be useful in a stranded energy situation is a helpful reference point for this work.

Due to their sensitivity to over-charge [32], most Li-ion battery management systems monitor voltage at each individual cell or parallel cell module within a larger series configuration string or sub-module. This monitoring is primarily used to enable cell balancing within the pack and to assess the functionality and state of individual cells. Total pack voltage and current is also measured and used in conjunction with several additional signals and calculations in the state-of-charge/health calculations (SOC/SOH). Although typically not at an individual cell level, module temperatures are also collected and used within the SOC/SOH calculations as well as some of the safety evaluations in terms of looking for dangerously elevated or diverging temperature readings.

One of the most important and challenging functions of a BMS is that of SOC/SOH estimation. These estimates typically combine the cell and pack measurements into an aggregate state for the battery. Broadly speaking, SOC represents the amount of charge remaining in the battery, which, in conjunction with temperature, is often used to provide insight into a battery's current power limits as well as the energy remaining for useful propulsion work. Battery SOC estimation remains a topic of much research and development in both the automotive industry and battery industry as a whole. Battery SOH refers to an assessment of a battery's degradation over time. As with battery SOC estimation, battery SOH is a topic of much on-going research and development. Fortunately, in a stranded energy discharge scenario, a discharge tool will be commanding a very consistent and known discharge current that greatly reduces the complexity of the calculations required for SOC estimation. Moreover, as discussed in the previous section, the SOC required for "safer" handling during a stranded energy scenario need not be of great accuracy (<30% is the recommendation) that again eases the computational burden in contrast to the typical requirements of in-vehicle SOC, which is used to inform a wide variety of systems that require accurate battery state information (i.e., a range gauge or the motor/inverter controllers). For more background on BMS research and development, the reader is directed towards [33-37].

Although there is some overlap with the previous state estimation discussion, the functionality and safety evaluations done by the BMS are split into a different category as compared to SOC/SOH estimation. This is due to their difference in objective as well as their particular relevance to the task of estimating the stability and safety of a battery in a stranded energy situation. As opposed to the previous "state" discussion, these evaluations are used primarily to look for evidence of battery, cell, or high-voltage system failure. By comparing the individual cell/sub-module voltage measurements, faulty cells can be fairly rapidly identified. By comparing individual cell resistance estimates, or more specifically, the individual and relative cell voltages under load, faults related to degradation and internal bus issues can be assessed. Temperatures within the pack can be assessed to detect operation above the recom-

mended maximum operating temperature or possibly increased heating due to degradation as evidenced by unexpected differences in temperature across a pack. While sometimes computed elsewhere in a vehicle's control system, isolation resistance measurement is also included here as a BMS safety evaluation. Since a vehicle battery is a floating system, it is important to ensure that it is electrically isolated from the vehicle and surrounding environment at all times. When the battery contactors are closed, the isolation monitoring system checks to ensure that a suitably large system isolation resistance, typically at least 500 ohm/volt [38], is retained at all times. Since this test takes place when the contactors are closed, this means that the entire high-voltage system including the battery, cabling, electric machines, and power electronics are all evaluated for any degradation of isolation that could lead to a shock hazard. Given the introductory discussion regarding how many vehicle field failures appear to be at least partly initiated outside of the battery cells, system isolation measurement is particularly important for evaluating and tracking a battery following an accident or in a stranded energy type situation. For example, if one tracks isolation over time and sees a sharp decrease, this suggests that conditions have changed within the high-voltage system, thus pointing towards a possible discharge of stored battery energy, which in turn, could possibly lead to a thermal event. The concept of system-wide isolation monitoring is also important relative to evaluating the safety of a discharge tool connected to a battery. In this case, it is important to assess the isolation of the entire system, including the included discharge tool, in case there is a loss of isolation somewhere in the connection to the discharge tool itself.

Given the applicability of many current vehicle diagnostics relative to battery safety and stability, it is a reasonable goal to use the much of the existing vehicle sensing infrastructure for battery stability and safety assessment. Both from an intrusiveness perspective as well as a robustness perspective, leveraging the sensors installed for in-use battery management and functional evaluation is a reasonable direction. As discussed previously, certain differences exist between the fidelity of diagnostics required for safety and stability assessment versus the information required for in-use operational state and functionality/safety assessment. Fortunately, the majority of possible stranded energy and safety assessment opportunities are well within the objectives of a traditional vehicle BMS system. Moreover, the accuracy required for in-use SOC/SOH estimation is typically more demanding than the simple assessment of the rough state of the battery and its related stability needed in a stranded energy situation. Figure 45 seeks to summarize the preceding discussion and highlight some of the high-level operational and functionality/safety related diagnostics. The plot of battery usage (current) versus SOC is included to again stress the difficulties associated with in-use parameter estimation due to a wide range of battery usage. In contrast, a stranded energy discharge tool would likely use a known, controllable, and simple discharge profile that greatly simplifies some of the required state and safety calculations.

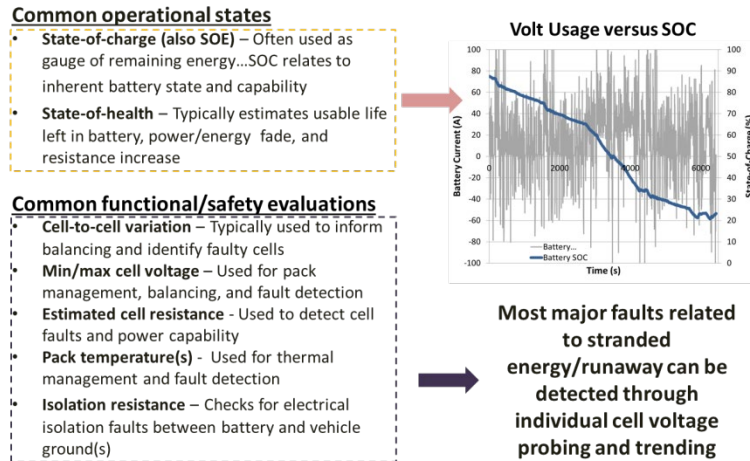


Figure 45: Highlighted operational and functional diagnostics and their usage (SOC estimation versus failure protection)

Despite the simplifications associated with stranded energy assessment, there is one challenge related to stranded energy assessment that is a bit more difficult versus the typical in-use cases. Namely, the lack of specific historical battery information and ability to compare specific parameters over the life of the battery. Most BMS systems compare parameters to a known set of data, both lab derived as well as recorded during vehicle usage. When leveraging an offline tool to assess battery stability and safety, minimal to zero information is available regarding historical trends, especially if the battery management system has been damaged and cannot communicate with the vehicle or the off-line assessment tool. This reduces the set of possible strategies available for diagnostics due to the need for more generalized metrics of stability and safety given the possible lack of comparison data availability in certain cases. Similarly, if a BMS is unable to communicate, any SOC information done internally will be unavailable, so a simplified metric for broadly estimating SOC must be developed as well. Fortunately, as discussed previously, SOC need not be estimated with a high degree of accuracy for a reduced thermal response.

In summary, by leveraging the existing in-vehicle individual cell/module voltage measurement infrastructure in conjunction with off-line total battery current and terminal voltage measurement, a very solid and fairly robust set of battery safety and stability assessment metrics can be assessed. Supplementing these battery assessment metrics, offline isolation resistance measurement between the assessment/discharge tool and the battery under assessment will identify any possible discharge paths between the battery and vehicle/other.

Overview of Additional Battery Sensing and Failure Mode Detection Techniques

Although the possible lack of historical data precludes several promising techniques developed for vehicle and industrial battery fault detection, there are some developed techniques that are useful to consider as a supplement to the vehicle-based diagnostics discussed in the previous section. This subsection seeks to highlight a few with specific focus on supplementing or expanding on the existing diagnostics used in the vehicle.

With a focus on detecting internal cell faults leading to thermal runaway, [39] contains some useful insights relative to “soft” shorts that often occur within cells due to dendrite growth or other internal inclusions that eventually lead to a cell failure. This type of short typically develops over time and often

induces noise into a charging or discharging profile due to a small or moderate short being created and then destroyed as some fault current runs through it. Ultimately this short is eventually large enough to induce a continuous fault current that may lead to thermal runaway, thus it is particularly useful to detect these initial shorts that induce terminal voltage noise prior to full cell failure. It is hypothesized that a medium or high-frequency filter applied to the voltage signal may be helpful as a detection trigger for single cell issues, but this technique is more challenging when tracking the entire battery's terminal voltage in the case of inaccessible individual cell voltages due to an overly damaged BMS. Additionally, since the frequency of the reported voltages provided by a BMS sensing systems is not necessarily known or consistent, certain high-frequency events may not be detected using current BMS and communication hardware. This work highlights the need for continuous monitoring to detect incipient faults before they grow into much larger ones, a concept that is particularly relevant to this work. As has been shown with several field failures, a thermal event may occur with a significant time delay from the original cause of the accident. Thus, continuous tracking becomes extremely important to identify faults and issues that may lead to thermal runaway as quickly as possible. Similarly, the identification of soft shorts that are often incipient to a large issue is useful not only in the individual cell context but also within the concept of vehicle isolation resistance and integrity. Given the delayed nature of many vehicle thermal events, it is likely that some soft short creation and destruction happened prior to an ultimate failure. Continuous monitoring of vehicle isolation would most likely aid in identifying developing issues as soon as possible.

While the evaluation period used in the study is outside of the timeframe of a stranded energy situation, a presentation discussing work done at NASA and NREL regarding battery internal short mitigation and screening techniques [40] highlights the importance of assessing individual cell open-circuit voltage (OCV) to detect incipient internal faults. This screening process assesses OCV following a 17 month holding period, looking for outliers with a lower OCV versus the others sampled during the screening process. While the lengthy rest period used in this study is too long for an in-field stranded energy assessment technique, these results again point toward assessing individual cells OCVs relative to the entire sample (a pack in this case) to detect any possibly failed cells indicated by an excessively low OCV and thus reduced SOC due to internal discharge (or possibly external discharge in the case of a vehicle pack).

Given the prevalence of battery backup power systems, regulations to “preclude, detect, and control thermal runaway” [41] for lithium metal polymer and VRLA-based battery have driven a range of companies to produce products providing monitoring and protection for battery backup systems [42-44,46]. The majority of these systems provide continuous or relatively frequently updated battery monitoring aggregated into a graphical display that allows for tracking as well as detection of issues if needed. These systems typically monitor parameters such as individual cell impedance, voltage, and/or conductance [45] alongside select cell temperatures and system current. These systems again highlight the importance of parameter tracking and trending for the detection of declining battery safety and stability. Interestingly, several of these manufacturers [44,46] discuss the difficulty associated with using temperature measurements as indicator of thermal runaway. More specifically, without significant efforts to model/estimate the thermal lag between measurement locations and the initiation point of a thermal event, temperature sensing may provide an indication of a serious issue too late for a proper mitigation response. This sentiment has also been expressed to the authors in discussions with several battery researchers and developers and suggests that while useful for a fuller picture of battery state, temperature monitoring may not be imperative for the assessment and tracking of a battery during a stranded energy situation.

Prototype Battery Stability and Safety Detection Strategy

Leveraging both the current in-vehicle sensor infrastructure, when available, as well as techniques from other industries, a set of post-incident prototype battery stability and safety assessment metrics have been developed. These metrics leverage existing vehicle sensing when possible, but supplement the sensing with offline calculations and sensing done in the prototype assessment tool. Including a baseline set of sensors in the tool itself is critically important since there are many possible scenarios in which the battery sensing or BMS communications functionality is not available. The tool itself is also helpful for tracking and illustrating parameter changes over time as well as providing a means to make safety and stability calculations outside of the vehicle's BMS. With a focus on battery stability estimation for stranded energy assessment and mitigation of a possible thermal event, the primary battery failure modes to detect included in this diagnostic discussion include the following.

- Battery short to ground
- Internal battery shorting
- Hard or intermittent shorting between battery and ground or BMS and ground
- Loss or reduction of buss bar contact between cells
- Degradation from external heating
- Cell separator shutdown or other safety mechanism activation
- Loss of cells in a parallel string

Related to these main failure categories, the following paragraphs seek to explain the selected metrics and techniques used for the prototype tool's safety and stability assessment capabilities. The metrics are categorized into two categories: passive and active detection. Passive detection is the initial evaluation step and requires minimal interaction with an unknown battery. During initial evaluation or long term monitoring of a very unstable battery, these metrics seek to assess the battery for any indicators of significant prior degradation or the increased likelihood of degradation later during storage. Following acceptable results from the passive evaluations, the assessment then moves into the "active" stage. This is done during discharge as well as during the monitoring of moderately damaged packs that slowly discharge the cell to get an assessment of additional safety and stability metrics. The mechanics of how this information is accessed, collected, and processed will be discussed later in the report.

Passive Fault Detection Metrics (Initial Assessment and Monitoring)

Individual static cell voltage (if BMS is functional) – If individual cell voltages are available from the BMS (via a query from the developed prototype tool), this is the first assessment metric to gauge battery stability. If the BMS sensing components are functional, reading individual voltages provides a quick gauge of overall battery damage with very little risk of exposure to unexpected high voltage due to the nature of the isolated voltage monitoring sensors. Unexpectedly low individual cell voltages typically indicate an issue related to cell damage as well as self or external discharge, which can be an indicator of larger isolation issues and circumstances that may lead to a thermal incident. While the issue may no longer be active (i.e., a temporary short that has since opened), lower than expected individual cell voltages nearly always indicate some form of damage. If multiple cells or an entire module shows a lower voltage, there is likely a loss of isolation issue allowing the cells to discharge to vehicle ground or an alternative discharge path. A significant number of low cells would indicate a large-scale battery damage issue and would necessitate a much lower power discharge if warranted or perhaps only monitoring and trending to assess stability prior to evaluating the next step in a course of action. Due to variations in chemistry

and cell design, the acceptable range for individual cell voltage would optimally be provided by the manufacturer for a specific vehicle, but some basic ranges can be specified by default if OEM information is lacking within the tool.

During the monitoring phase, individual cell voltage can be tracked over time, looking for decreasing voltage that again indicates self or external discharging. Additionally, soft shorts, both internal within individual cells or between the battery and vehicle ground, can typically be observed as noise on the otherwise stable cell voltages. For this work, variations in voltage above 5 percent during static assessment are considered a trigger for suspected cell/pack degradation.

Isolation resistance (all cases) – Although the most basic and important metric for vehicle safety and stability following an incident is isolation resistance, this is the second assessment (assuming the BMS sensing is functional) due to the need to close at least one contactor to assess the isolation between the battery and vehicle ground. Since only one contactor needs to be activated to assess isolation resistance, this is generally preferred as a next step (as opposed to closing both contactors). Although a vehicle's battery is typically isolated from vehicle ground as well as other grounding sources, an accident or similar damage to a vehicle's isolation can easily result in a dangerous voltage exposure situation and can indicate conditions conducive to the initiation of a possible thermal event due to rapid battery discharge. As with individual cell voltage, a manufacturer provided isolation resistance minimum target value would optimally be provided as an input to the discharge/assessment tool's interface screen, but reasonable default levels are included in the case of missing information.

The most powerful use of offline isolation resistance tracking is during the monitoring stage. While anything above the specified minimum isolation level for a particular vehicle would be acceptable, a decreasing trend in isolation resistance can be a very early indicator of reduced battery stability in the sense that the high-voltage system is edging closer to a loss of isolation event that could lead to cell discharge and a possible thermal issue. It is hypothesized that several of the delayed in-field battery thermal events could have been detected well in advance of any thermal runaway conditions if the isolation resistance was tracked and observed to be decreasing due to issues such as coolant leakage or intermittent grounding between the BMS and vehicle ground.

Overall static pack terminal voltage (BMS not functional) – While individual cell voltage information is preferred to overall terminal voltage, this is the only voltage information available if the BMS sensing is non-functional. If the isolation resistance has proven to be above the minimum desired level, the evaluation tool will close both contactors, enabling the measurement of pack voltage. Terminal voltage limits can give a rough estimate of stability only in the case that the battery has significantly discharged as evidenced by a particularly low terminal voltage, but this is typically not the case. As will be discussed later in this section, the pack terminal voltage will be used as a rough assessment of SOC when discharging the pack to below the desired SOC level (30%) for improved thermal stability and reduced severity of thermal response.

In a similar fashion to the individual cell monitoring assessment, noise on the typically static terminal voltage under no load is indicative of a possible issue due to intermittent shorting. At the terminal level, this would likely be due to a loss of isolation between the battery and ground since individual cell variations will be more difficult to assess using the aggregate terminal voltage as opposed to individual cell voltages. Voltage variations more than 5 percent during static assessment are again considered an indication of possible degradation and subject to greater scrutiny.

Active Fault Detection Metrics (Assessment and Monitoring)

While the battery is discharging, “active” measurements can be taken that provide additional insight into a battery’s stability and condition. Specifically, tracking terminal and individual cell voltages in conjunction with overall pack current during a discharge event can provide information to calculate a simplified model of battery resistance and provide a basic state of charge trajectory (over the course of the discharge) through monitoring voltages. While generally too basic for in-vehicle SOC estimation and operational usage, a simplified $V_{\text{cell_observed}}=V_o+iR_{\text{cell}}$ relationship can be used with available BMS-based cell voltage information to estimate and track individual cell resistances during a discharge. Additionally, by tracking and comparing individual cell voltages over time, damaged cells can often be identified by a divergent trend of voltage over time due to factors including the possible loss of a parallel cell in a series sub-module, degradation due to temperature exposure, or other physical damage. The following metrics obviously require both contactors to be closed and high-voltage power, however low, to be discharging through the system via the developed discharge tool.

Individual Cell Resistance Tracking (BMS Functional) – Provided with knowledge from the initial passive evaluation, information regarding whether all cells in a pack are starting with roughly similar SOC levels and thus Open Circuit Voltages (OCV) can be used to further evaluate the battery for resistance changes. Specifically, cell-to-cell variations in resistance can be identified via tracking the individual cell voltages under load. Cell and included interconnect resistance variations can be observed as a reduced/elevated individual cell voltage relative to the other cells under assessment due to the iR_{cell} contribution to observed cell voltage. While this the resistance could be tracked, shown, and used for targeting by the assessment tool, it is slightly more convenient to leave the comparison in the voltage space, since it removes one calculation and can reuse the initial unloaded assessment screen from the initial passive evaluation. When tracking individual resistances via voltage, it is suggested that a maximum cell-to-cell variation and a minimum cell target value be used to detect a developing (or current) issue with a cell or set of cells. While the minimum individual cell voltage under load would likely need to be specified by the manufacturer, a cell-to-cell voltage variation during loaded operation of roughly 3-5 percent appears to be a suitable point for identifying issues that may require additional attention.

Individual Cell Open Circuit Voltage Estimation and Tracking (BMS Functional) - While comparing individual cell voltages under load will typically identify a cell that has been damaged resulting in non-standard resistance, tracking the OCV over the course of a discharge may also provide additional insight relative to other possible cases of cell degradation. If a cell or sub-module’s overall capacity has degraded due to internal damage, heating, or other means of degradation, it will likely show a lower open-circuit voltage compared to the other cells following some amount of discharging. Although overall cell resistance may be similar to the other cells and not indicate an issue, the measured voltage of a cell with degraded capacity will eventually diverge from the other cells and indicate an issue. As with the single point tracking, although a manufacturer specific target range would be most useful, a 3 to 5 percent difference in cell-to-cell voltage would suggest some possible degradation.

Battery Total Resistance and Terminal Voltage Tracking (BMS Not Functional) – Analogous techniques for tracking both overall battery resistance and capacity fade are possible for the entire battery pack using terminal current and voltage measurement capabilities. While less sensitive than their individual cell counterparts, these methods still provide some basic direction whether degradation has taken place. Overall pack resistance is very difficult to generalize and thus a manufacturer specified range would be suggested for an overall resistance tracking and evaluation metric.

Table 3 seeks to summarize the highlighted metrics and provides some information relative to if an OEM provided target metric would be required or simply helpful given a suitable backup value. Additionally, while the proposed tracking metrics offer a range of insight into the stability, safety, and degradation of a pack under evaluation, some of the issues are more severe than others in terms of anticipated issues with thermal runaway or general safety and stability. To these ends, items highlighted in red are issues that have an elevated indication that there is a safety and stability risk. Both out of specification isolation resistance and high cell-to-cell variability have been highlighted in red given that these metrics suggest an elevated probability of later pack discharge (isolation) or provide evidence of a possible earlier uncontrolled discharge (passive cell-to-cell variability). In these cases, tracking is strongly recommended and reduction of SOC level to below threshold would likely be helpful in reducing the severity of an incident should it occur. While not necessarily suggesting a heightened risk of incident, items highlighted in yellow suggest a degree of battery degradation that will likely require removal and replacement of at least part of the pack, during which the battery may be taken to a lower SOC for long-term storage or shipping. Especially in the case of a non-operational BMS, these yellow highlighted metrics would suggest close scrutiny to the tracking information to see in the degradation has been consistent or the battery has worsened during the observation period.

Table 3: Basic Evaluation Capabilities

| Assessment Capabilities | | Check | OEM Metric | Baseline Metric |
|--|--|-----------------|--------------|-----------------|
| Passive Evaluation - Open Contactors | BMS (Sensing) Available | | | |
| | Individual Cell Voltages | Within Range | OEM Provided | - |
| | Cell-to-Cell Voltage Variability (unloaded) | Under Spec. | OEM Provided | 5% or more |
| | Individual Cell V Noise | Under Spec. | - | 5% or more |
| | Offline Calculations | | | |
| Passive Evaluation - TBD Contactors | Isolation Resistance | Above spec. | OEM Provided | FMVSS |
| Passive Evaluation - Closed Contactors | Terminal Voltage | Within Range | OEM Provided | - |
| | Terminal Voltage Noise | Under Spec. | - | 5% or more |
| | BMS (Sensing) Available | | | |
| Active Evaluation - Closed Contactors | Cell-to-Cell Voltage Variability - Single Point (loaded) | Under Spec. | OEM Provided | 5% or more |
| | Cell-to-Cell Voltage Variability - Tracking (loaded) | Under Spec. | OEM Provided | 5% or more |
| | Offline Calculations | | | |
| Active Evaluation - Closed Contactors | Terminal Voltage - Single Point | Within Range | OEM Provided | - |
| | Terminal Voltage Tracking | Expected change | - | Roll-off |

Future Directions for Improved Battery Stability Assessment

Although leveraging several of the common in-vehicle BMS sensors supplemented with some additional offline sensors and calculations provides significant insight into a battery’s stability and safety across a wide range functionality, there are several research and development areas in terms of specific sensors or techniques geared directly toward assessing the stability of a battery following an accident. While an in-depth discussion of these new techniques is outside the scope of this work, several promising directions have been highlighted for discussion.

Electrochemical Impedance Spectroscopy

While the basic resistance estimation and voltage tracking techniques discussed in the previous section often show general trends relative to battery stability, it is desired to have a technique that can focus on assessments pertinent to battery stability, more specifically evidence that a thermal event may be incipient or at least more probable in the future due to a certain level degradation being accumulated. Electrochemical impedance spectroscopy (EIS), a technique that has begun to see significant research and development for vehicle battery applications provides a direction toward this desired goal. Broadly speaking, EIS typically applies a small, single frequency sinusoidal input (voltage or current) to a

cell/module/pack under evaluation and measures the resulting response (current or voltage, respectively). Impedance is then calculated at this particular frequency by complex division of the voltage and current response and the process is repeated across a range of frequencies [47]. This frequency domain information is often used in the creation of a Nyquist plot, in which specific sections (or “semi-circles”) correspond to particular cell characteristics or behaviors [48,49].

Of particular interest within the improved insights provided by EIS is information related to the SEI layer as well as the ability to collect separate impedance information regarding both positive and negative electrodes. Simulation work done by Liu and Zhu [50] estimates the response due to SEI growth and equilibrium attainment during battery cycling. Work done in assessing failure mechanisms due to overcharging [51] also uses EIS to identify some of the basic mechanisms of degradation due to the overcharging. With a particular focus on identifying SEI layer degradation (an initial reaction in the thermal runaway process), EIS appears to provide an improved method of assessing and tracking a battery for stability and safety.

While EIS appears to be a promising direction for improved assessment and tracking of battery stability, there are some research and development challenges required for its ultimate inclusion in a battery management system. Much of the existing work in the area of EIS for battery stability assessment has used somewhat bulky, slow, and expensive specialized laboratory equipment that would not be easily integrated into an in-vehicle solution. Realizing this limitation, a significant portion of recent EIS work is working towards developing in-vehicle EIS systems to supplement current BMS sensing capabilities. For example, researchers have sought to leverage a vehicle’s on-board inverter to provide signals need to drive EIS responses [52]. Additional work has gone into developing streamlined, rapid impedance spectrum analysis hardware [53,54] and refining its calibration methodologies for generalized applicability across a range of in-vehicle battery evaluation use cases [55].

Supplemental Sensor Development

In addition to the discussed EIS techniques, a wide range of additional sensors have been proposed and developed for identification and detection of dangerous battery stability conditions. Given that several stages during a cell’s ultimate thermal runaway show off-gassing, gas detection sensors have been developed and evaluated as a means to provide an indication of an incipient thermal event [56,57]. While these sensors may not provide information regarding conditions that will eventually lead to a thermal event, they appear effective in detecting a severe thermal event prior to full thermal runaway. Other techniques such as spark detection [58] as well as strain and thickness measurements have also been proposed to identify a battery that is in the early stages of a thermal runaway event. While these supplemental sensors appear promising for identifying dangerous situations and raising awareness to both passengers and a vehicle’s ECUs, it would be preferable to identify conditions leading to a possible thermal event (i.e., loss of isolation) as opposed the beginning stages of what would likely be a full runaway event. Furthermore, as with the basic BMS quantities discussed earlier in this section, any supplemental sensing system would also require offline 12V power, thus requiring some sort of power and communications interface.

Battery Communication Links

Given the authors’ desire to leverage existing vehicle sensing and communication protocols, emphasis was put on adapting existing in-vehicle methods for accessing BMS information. Fortunately, the majority of vehicles on the market today provide BMS and other controller information retrieval and streaming via a specialized service tool. These tools connect via a vehicle’s DLC port and then send information

requests via a vehicle’s CAN network to the controller under assessment. Information is typically displayed on a laptop that shows the selected parameters of interest. For example, Figure 46 shows a screenshot of the Chevrolet Volt’s service tool query for individual module temperatures. Since a service tool is often used to evaluate a vehicle’s battery pack, individual cell voltages can typically be provided if the request structure is known. For all of the vehicles evaluated during this work, only one did not provide all individual cell voltages via the diagnostic tool; the vehicle in question providing only minimum and maximum cell information. While this min/max information is helpful and could be used as a diagnostic, it is the recommendation of the authors to provide all individual cell/series sub-module voltage information. Having all individual voltages available provides the user with a level of insight relative to the overall level of degradation in a pack. For example, it is useful to know that a high number of cells have dropped in voltage, which suggests a possible large scale issue whereas a single low voltage may simply suggest a dead cell or connection. Furthermore, since all cells are sensed via the BMS, providing this information to a diagnostic query requires very little additional effort in that the information simply needs to be indexed and relayed to the communication interface.

| Parameter Name | Control Module | Value | Unit |
|--|-------------------------------|-------|------|
| HybridEV Battery 1 | Battery Energy Control Module | 21 | °C |
| HybridEV Battery 2 | Battery Energy Control Module | 21 | °C |
| HybridEV Battery 3 | Battery Energy Control Module | 22 | °C |
| HybridEV Battery 4 | Battery Energy Control Module | 21 | °C |
| HybridEV Battery 5 | Battery Energy Control Module | 21 | °C |
| HybridEV Battery 6 | Battery Energy Control Module | 22 | °C |
| HybridEV Battery 7 | Battery Energy Control Module | 22 | °C |
| HybridEV Battery 8 | Battery Energy Control Module | 21 | °C |
| HybridEV Battery 9 | Battery Energy Control Module | 23 | °C |
| HybridEV Battery Pack Coolant Temperature Sensor 1 | Battery Energy Control Module | 22 | °C |
| HybridEV Battery Pack Coolant Temperature Sensor 2 | Battery Energy Control Module | 22 | °C |

Figure 46: Chevrolet Volt Service Tool screenshot

Although message addresses, scaling values, and message organization differ from vehicle-to-vehicle and manufacturer-to-manufacturer, the vast majority of diagnostic message requests and transmissions use a CAN-like structure in their messaging. ECU information is requested by the service tool followed by the ECU providing coordination and formatting information. The scantool typically sends an additional “ready” message and then the ECU will provide the requested information. In the annotated example shown below in Figure 47, the scantool (7e4) is requesting 3 separate banks of voltage information from the BMS (7ec). The BMS responds with individual cell voltage information regarding each cell that must then be scaled to find the actual cell voltage for each cell. If the values of roughly 185 are multiplied by 0.02, they equate to an expected individual cell voltage of 3.7 Volts. If the messaging structure, addressing, and scaling values are known for a particular vehicle, an outside tool can similarly communicate with a vehicle’s BMS to provide a range of desired information.

| Time | Signal | 7EX-0 | 7EX-1 | 7EX-2 | 7EX-3 | 7EX-4 | 7EX-5 | 7EX-6 | 7EX-7 |
|--------------|--------|-------|-------|-------|-------|-------|-------|-------|-------|
| 2.423469 7e4 | 2 | 62 | 0 | 0 | 0 | 0 | 0 | 0 | 0 |
| 2.4309 7ec | 2 | 126 | 0 | 0 | 0 | 0 | 0 | 0 | 0 |
| 4.476383 7e4 | 2 | 33 | 3 | 0 | 0 | 0 | 0 | 0 | 0 |
| 4.486381 7ec | 16 | 38 | 97 | 3 | 255 | 255 | 255 | 255 | 255 |
| 4.486674 7e4 | 48 | 8 | 2 | 0 | 0 | 0 | 0 | 0 | 0 |
| 4.486695 7ec | 33 | 185 | 185 | 185 | 185 | 185 | 185 | 186 | 186 |
| 4.506342 7ec | 34 | 185 | 182 | 182 | 181 | 182 | 182 | 182 | 182 |
| 4.516562 7ec | 35 | 182 | 182 | 185 | 185 | 185 | 185 | 185 | 185 |
| 4.526371 7ec | 36 | 185 | 185 | 185 | 185 | 185 | 185 | 185 | 185 |
| 4.536692 7ec | 37 | 185 | 185 | 185 | 185 | 185 | 0 | 0 | 0 |
| 4.539067 7e4 | 2 | 33 | 4 | 0 | 0 | 0 | 0 | 0 | 0 |
| 4.553409 7ec | 16 | 14 | 97 | 4 | 255 | 255 | 255 | 255 | 255 |
| 4.553729 7e4 | 48 | 8 | 2 | 0 | 0 | 0 | 0 | 0 | 0 |
| 4.561144 7ec | 33 | 185 | 185 | 185 | 185 | 185 | 185 | 185 | 186 |
| 4.571484 7ec | 34 | 185 | 0 | 0 | 0 | 0 | 0 | 0 | 0 |
| 4.585507 7e4 | 2 | 33 | 2 | 0 | 0 | 0 | 0 | 0 | 0 |
| 4.591301 7ec | 16 | 38 | 97 | 2 | 255 | 255 | 255 | 255 | 255 |
| 4.593282 7e4 | 48 | 8 | 2 | 0 | 0 | 0 | 0 | 0 | 0 |
| 4.60111 7ec | 33 | 182 | 182 | 182 | 182 | 182 | 182 | 182 | 182 |
| 4.611271 7ec | 34 | 182 | 185 | 185 | 185 | 185 | 185 | 185 | 185 |
| 4.621227 7ec | 35 | 185 | 185 | 185 | 185 | 185 | 185 | 185 | 185 |
| 4.631205 7ec | 36 | 185 | 185 | 185 | 185 | 185 | 185 | 185 | 186 |
| 4.641096 7ec | 37 | 185 | 186 | 186 | 185 | 0 | 0 | 0 | 0 |
| 4.643337 7e4 | 2 | 33 | 3 | 0 | 0 | 0 | 0 | 0 | 0 |

Figure 47: Hyundai Sonata Hybrid individual cell voltage diagnostic request structure (in decimal notation)

An additional advantage of using diagnostic messaging to access BMS information is that the information is carried over vehicle CAN lines and thus communication with an ECU can be set up in a variety of locations, namely anywhere there is an accessible CAN wire pair. In the proof-of-concept example shown below in Figure 48, direct access to the battery diagnostic messages (including individual cell voltage, isolation resistance, and module temperatures) is enabled by tapping the CAN wires directly prior to the battery pack. In fact, the battery pack in this demonstration was disconnected from the rest of the vehicle and was provided offline 12V power to show the capability of diagnostic messaging to access battery information without using the DLC port and without vehicle 12V power.



Figure 48: Direct BMS communication access (Hyundai Sonata Hybrid)

Once the diagnostic messaging structure is known for a particular vehicle, it is relatively straightforward to develop an enhanced assessment display tool. Using scantool diagnostic information developed for this project, the screenshots shown below in Figure 49 highlight some preliminary development screens displaying individual cell voltages, module temperatures and isolation resistances as well as an introductory screen that can read a vehicle's VIN and email a user if any of the measured quantities are outside of their specified boundaries.

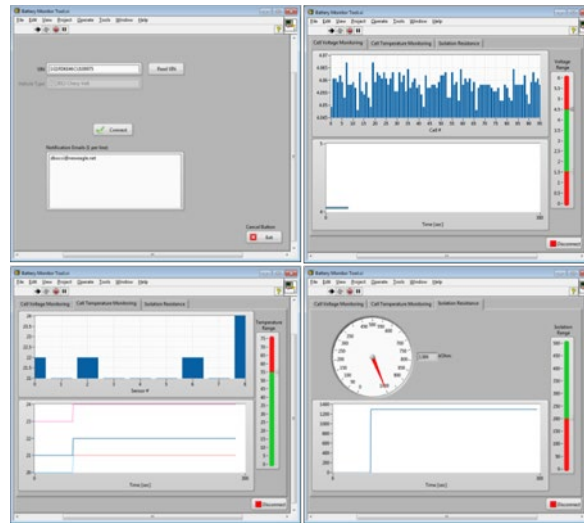


Figure 49: Prototype evaluation tool screenshot

In summary, leveraging a vehicle’s pre-existing diagnostic messaging structure and information lines is a relatively straight forward and effective tool to obtain BMS sensing information. This option is by far the lowest overhead choice in terms of requiring no additional wiring to provide information to an offline tool. Given these benefits, it is strongly recommended by the authors that vehicle diagnostic messaging is used to supply BMS related information to the offline discharge and assessment tool. Within this general recommendation, two more specific recommendations are suggested. First, providing information regarding every cell/sub-module in the series string (as opposed to min/max values) would greatly aid in determining the overall safety and stability of a battery given the importance of understanding the number of cells that appear damaged or unstable. Second, while it is not required, it would be extremely helpful to tool developers and users if at least a pack’s individual cell voltages were relayed using a consistent communication messaging protocol (message location and scaling). This could be similar to an OBDII information request that uses an agreed upon address and scaling factor across vehicles.

Evaluating the Robustness of In-Vehicle Communications

Since the proposed assessment techniques discussed in this section rely heavily on BMS sensed information, it is helpful to understand the functionality of these systems across a range of incident types. Additionally, the functional status of a battery’s high-voltage system, namely contactors and related components can provide critical insight for any stranded energy discharge scheme. In cases where the discharge protocol uses the existing high-voltage loop, this information can provide the feasibility of such a technique and in cases where an additional dedicated discharge port is included, the observed failures can provide insight into ways to possibly make the port more robust.

The result of collaboration and discussions with a variety of stakeholders along a battery’s value chain, this section seeks to provide some insight regarding how frequently a damaged battery’s BMS sensing systems will be operational and if the high-voltage system will be accessible and “discharge-able.” The majority of the discussion revolves around normalized and aggregated failure and estimated root cause data for 188 high-voltage battery packs that exhibited some degree of failure to the extent that they were removed from a vehicle. This analysis excludes cases of extreme damage and seeks to provide insight into more routine failure issues that would be much more likely to be experienced in-field and thus

would be major consideration points for a stranded energy assessment and discharge strategy. The energy storage systems described in this database are from on-road hybrid electric, plug-in electric and electric vehicles (xEVs).

Figure 50 shows the distribution of all failure modes observed during the study. Interestingly, the most common cause of failure was an issue related to a vehicle’s high-voltage loop. Looking at the root cause information for this failure mode, the majority of these failures (71%) was related to lose or degraded connections between cells or modules within the battery pack. The individual cells themselves in this scenario were generally not damaged. The second most frequent failure mode observed was that of out of balance cells. In this case, the root cause for the cell-to-cell discrepancies was generally unknown. Many of the observed State of Health related failures, the third most frequently observed failure mode, were due to issues related to elevated module or cell temperatures. These three failure modes account for slightly over 50 percent of the observed failures, with a wide mix of failures composing the remaining roughly 50 percent.

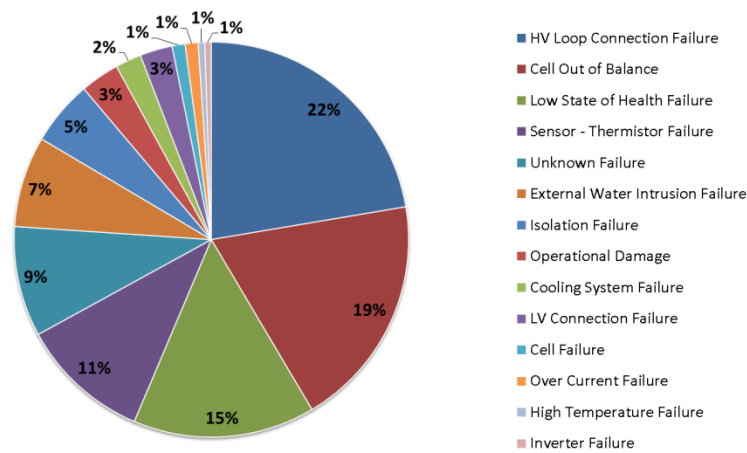


Figure 50: Distribution of failure modes across packs investigated

While these general failure trends are interesting, the more meaningful analysis in terms of stranded energy assessment and discharge is how these failures impact BMS and HV loop functionality. Since communicating with a vehicle’s BMS and reading the individual voltages of each series cell/sub-module is one of the main diagnostic strategies suggested in this work, understanding BMS functionality for these frequent failure cases is of great importance. With this issue in mind, the study investigated the BMS functionality of the damaged incoming packs. Functionality was broken into five categories, shown in the list below. From the battery assessment perspective, values of 100 percent and 75 percent functionality were determined to be “assessment-capable” in that all individual cells were reporting correctly. For the 75 percent functionality cases, data such as module temperatures was missing, but the cell voltages could still be read.

- 100 percent - Communication system is functioning correctly
- 75 percent - Loss of communication or function in peripheral sensors
- 50 percent - Loss of some cell or unit voltages or misreporting cell or unit voltages
- 10 percent - Loss of all digital communication
- 0 percent - No communication or control.

As can be seen in Figure 51, roughly 90 percent of the entire 188 packs evaluated for this work had “assessment-capable” BMS functionality. This provides some positive evidence that reading and communicating individual cell voltages via a pack’s existing BMS sensing infrastructure should be a viable method for a range of damaged and degraded battery packs. Although this is a positive, it should also be noted that a significant percentage (~7%) of the battery packs evaluated had no communications capabilities, reinforcing the need for a multi-tiered approach to battery in-field discharge and diagnostics.

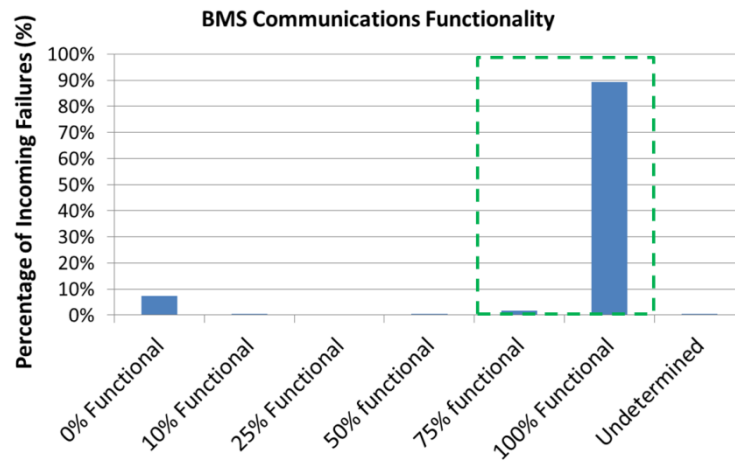


Figure 51: BMS functionality distribution of damaged packs in study

As with BMS functionality, operation of a battery’s high-voltage loop is of critical importance for assessment and especially discharge. In similar fashion to BMS functionality, the functionality of the high-voltage system (HV loop) was also broken into functionality bins for the packs assessed during this study. The list below discusses the levels of HV loop functionality used in this work. HV loop functionality levels 50 percent and above were considered optimal since batteries with this level of functionality could likely be discharged well within the specifications of a discharge tool, which would probably have a maximum power draw of roughly 2 to 4 kW (typically resulting in a relatively low C-rate during discharge).

- 100 percent - The HV loop is functioning correctly
- 75 percent - The maximum power of the pack must be de-rated due to some issue
- 50 percent - The maximum power must be significantly reduced to avoid damage to the pack
- 25 percent - Significant cell imbalances are observed or a noticeable voltage drop is observed at low discharge rates
- 10 percent - HV exposure is possible, however impedance is extremely high (i.e., failed module) or terminal functionality is extremely limited (i.e., failed main contactors, but operable pre-charge contactors)
- 0 percent - HV loop has been severed or no functionality at contactors

Figure 52 shows the distribution of HV loop functionality for the packs assessed in this study. A relatively high percentage of incoming packs (75%) have what would be considered optimal HV loop functionality, but the distribution of functionality is much more widely dispersed as compared to the BMS functionality cases. Roughly 16 percent of the packs evaluated showed no main contactor or HV loop functionality (0% and 10% levels) that would render a discharge tool unusable if designed to integrate with a battery’s existing terminal functionality.

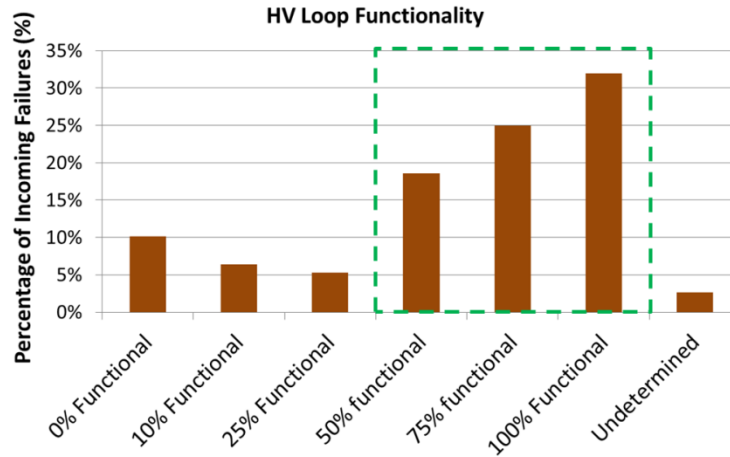


Figure 52: High-voltage loop functionality distribution of damaged packs in study

When analyzing the HV loop and BMS functionality levels and definitions, several broad categories of capability regarding stranded energy assessment and discharge emerge. In terms of discharge capability, “full” refers to the ability to discharge a pack around roughly 2 kW (a discharge level generally much lower than a pack’s normal usage profile). “Moderate” discharge capability implies the ability to discharge at lower power levels, roughly half of the “full” capability. “Limited” discharge capability suggests that the pack can likely be discharged very slowly at less than 500 W, but the discharge is partly to aid in assessing stability and safety of the battery. “No” discharge capability obviously implies the inability to discharge the pack at any level, predominantly due to lack of functional terminal access. In terms of assessment, the three basic capabilities are available. “Full” assessment capability implies that individual cell voltage sensing is operational and thus the individual cell diagnostic assessments discussed previously are feasible. “Limited” assessment capability suggests that the battery can be assessed for large-scale issues visible on the pack level via the terminals, but the fidelity provided by individual cell sensing is not available. Table 4 summarizes the capabilities associated with the combined level of both BMS and HV loop functionality. For example, if a battery’s HV loop is not functional, but the BMS is fully functional, that battery can be assessed, but not discharged.

Table 4: Discharge and assessment capability versus HV loop and BMS functionality

| Basic Functionality Level | Component Functionality | |
|--|-------------------------|---------------|
| | HV Loop | BMS |
| FULL Discharge, FULL Assessment | 50%+ | 75%+ |
| MODERATE Discharge, LIMITED Assessment | 50%+ | 0%-50% |
| LIMITED Discharge, FULL Assessment | 25% | 75%+ |
| LIMITED Discharge, LIMITED Assessment | 25% | 0%-50% |
| NO Discharge, FULL Assessment | 10% and below | 75%+ |
| NO Discharge, NO Assessment | 10% and below | 50% and below |

Clearly, the most desirable outcome for a discharge and assessment tool set would be full discharge and assessment capability, but there are subtleties between the other levels in terms of how severe an issue the combined functionalities are for stranded energy assessment and discharge. Figure 53 provides an approximate color coding relative to capability as well as the joint probability of occurrence for the two functionality criteria. Coded in green, full-discharge/full-assessment capability represents roughly 75 percent of all packs observed during this work. Roughly 6 percent of all packs observed fall within the red area due to their inability to be discharged or assessed due to complete lack of functionality, the worst-case from a stranded energy tool development perspective. Coded in yellow, cases with minimal

BMS functionality, but high levels of HV loop functionality imply that a moderate discharge would likely be possible although needing to be carefully tracked for deteriorating battery condition. Coded in pink, the no-discharge/FULL assessment packs can be observed and assessed, but not typically discharged if such a course of action is recommended. For the special case of 25 percent HV loop functionality, low levels of discharge would be possible, but great care must be taken during the slow discharge to track issues that suggest deteriorating battery stability.

| HV Loop Functionality | BMS Communications Functionality | | | | | | |
|-----------------------|----------------------------------|----------------|----------------|----------------|----------------|-----------------|-----------------|
| | 0% Functional | 10% Functional | 25% Functional | 50% functional | 75% functional | 100% Functional | Underdetermined |
| 0% Functional | 5.9% | | | | | 4.3% | |
| 10% Functional | 0.5% | | | | | 5.9% | |
| 25% Functional | | | | 0.5% | | 4.8% | |
| 50% functional | 0.5% | | | | | 18.1% | |
| 75% functional | | | | | 0.5% | 24.5% | |
| 100% Functional | 0.5% | | | | 1.1% | 30.3% | |
| Underdetermined | | 0.5% | | | | 1.6% | 0.5% |

Figure 53: Distribution of HV loop and BMS functionality levels (color coded for severity)

While the general trends regarding functionality of damaged packs is positive in that most packs can be assessed and many can be discharged at some functional level, the observation that roughly 6 percent of packs be neither discharged nor assessed suggests that a discharge tool will eventually meet some limitations regarding packs that need more intrusive and expert analysis and evaluation.

Specific to this point, several scenarios are highlighted from the data due to their more frequent occurrence in relation to a larger-scale thermal event. As discussed in the introductory section, many of the more noteworthy thermal events have taken place following vehicle flooding or some other type of water intrusion into the battery pack. Within the packs assessed for this study, 14 packs saw damage from water intrusion. Figure 54 highlights the capability distribution for these 14 packs. While a relatively small sample size, issues related to water intrusion appear to frequently lead to the inability to either discharge or assess the pack. This result is unfortunate for the water intrusion scenario since it has been shown to be the starting point for several of the more recently observed battery thermal events.

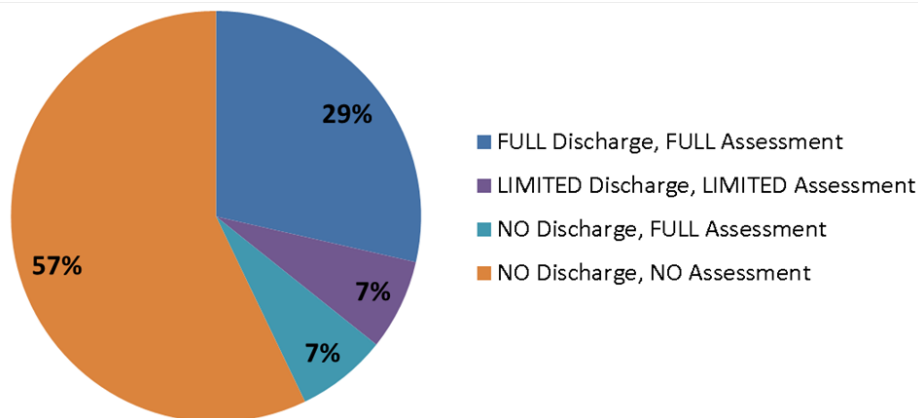


Figure 54: Discharge and assessment capability for damages packs experiencing water intrusion

Similar to packs that have experienced water intrusion, the following tables highlight results from two other areas that appear to increase the probability of a larger event: isolation failure and operational damage. Although the number of packs incoming and thus assessed in this study is limited, Table 5 shows the capability levels for several packs experiencing isolation related failure and Table 6 shows the

capability level for packs that have experienced operational damage. Fortunately, these cases suggest that the worst-case of both NO assessment and NO discharge capability is slightly more rare and at least full assessment capability is offered in several of the cases.

Table 5: Discharge and assessment capability for packs experiencing isolation failure

| Basic Functionality Level - Isolation Failure | |
|--|------|
| FULL Discharge, FULL Assessment | 8/10 |
| MODERATE Discharge, LIMITED Assessment | 1/10 |
| LIMITED Discharge, FULL Assessment | - |
| LIMITED Discharge, LIMITED Assessment | - |
| NO Discharge, FULL Assessment | 1/10 |
| NO Discharge, NO Assessment | - |

Table 6: Discharge and assessment capability for packs experiencing operational damage

| Basic Functionality Level - Operational Damage | |
|---|-----|
| FULL Discharge, FULL Assessment | 1/6 |
| MODERATE Discharge, LIMITED Assessment | - |
| LIMITED Discharge, FULL Assessment | - |
| LIMITED Discharge, LIMITED Assessment | - |
| NO Discharge, FULL Assessment | 4/6 |
| NO Discharge, NO Assessment | 1/6 |

While this study is by no means conclusive, it certainly contributes some information to the very limited data regarding the distribution of in-field battery failures and BMS/HV loop functionality following failure. On a positive note, these more typical failure cases seem to generally not cause severe BMS damage and the sensing information is available for use in an offline discharge and assessment tool. Second, a large portion of the batteries evaluated showed the capability for some level of discharge given main contactor functionality following the damage event. While BMS functionality was observed in many cases, inoperable BMSs were observed for a not insignificant portion of the incoming packs, highlighting the importance of some basic offline assessment capabilities as discussed in the previous diagnostics section. Last, issues related to HV loop functionality suggest that while main contactors are often usable in a post-failure scenario, this may not always be the case, especially as incident severity is increased. Overall, this work supports the direction of leveraging BMS-based sensors for the majority of assessment cases, while retaining some off-line assessment techniques in the case of no BMS functionality.

Estimating Battery State-of-Charge for Stranded Energy Purposes

While the primary focus of this section is on diagnostics related to battery stability, battery SOC level is also of importance given the SOC versus thermal stability and incident severity analysis earlier in this work. Accurate SOC estimation is of importance to typical vehicle operation, yet it requires quite a bit of sensed battery information as well as typically proprietary calculations that vary from manufactures to manufacturer. In contrast, the SOC level recommendation for increased stability and reduced severity of incident in a stranded energy type situation is a rough limit of 30 percent or less. Given this less restrictive SOC calculation requirement, open-circuit voltage (OCV) estimation and tracking is the recommended technique for estimating battery SOC for the purpose of developing a stranded energy prototype tool. Using OCV to estimate SOC is a widely used technique [59] and allows a wide range of failure and capability scenarios to be assessed since only unloaded battery terminal voltage or loaded battery terminal voltage and current are needed to estimate a pack’s overall SOC (given some a priori

knowledge relative to a battery's OCV versus SOC curves). Although some issues may arise due to failed or highly degraded cells within a candidate pack, the SOC threshold suggested for improved stability is wide enough to allow for only a moderately accurate estimate of SOC.

While an OEM provided target OCV value would be preferred for use in a discharge and assessment tool, the properties of OCV versus SOC do provide the ability to use a back-up method if OEM support is unavailable for a particular vehicle or battery configuration. Specifically, OCV begins to roll-off at reduced SOC levels and thus an evaluation mechanism could track when the OCV begins to drop off at a steeper than previous rate during a discharge. This roll-off typically begins at roughly 5 to 20 percent SOC, a level that would likely not promote any permanent degradation since many BEVs currently discharge well into his roll-off area. Figure 55 plots terminal voltage versus SOC for two BEVs and the roll-off can easily be observed for each vehicle, although the curves themselves are of different shapes. If individual cell voltage were provided, this information could be combined with the overall pack current to provide an OCV estimate on the individual cell level. This would allow a pack with degraded cells to monitor the depth of discharge for each cell and thus provide a better overall picture of aggregate SOC as well as avoid the overdischarging of individual cells if so desired.

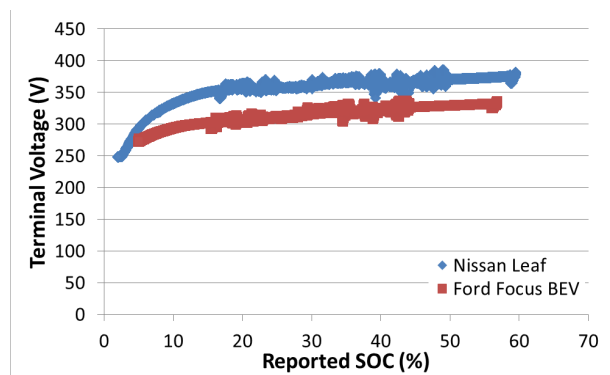


Figure 55: Terminal voltage versus reported SOC for two select BEVs

Combined with the previously discussed diagnostic metrics this simple, basic SOC estimate is the last piece of information required to assess and possibly discharge a battery post-incident. This basic SOC estimate would be used to stop discharging at or below the recommended SOC level that should reduce the severity in the rare case of a thermal event occurring.

Prototype Stranded Energy Tool-set Development

Stranded Energy Tool Design Discussion

Design Goals

The overall goal is a semi-portable tool that would enable field assessment and possible de-energization of a battery system following an accident or any other stranded energy situation where an assessment of pack stability would be needed. As such, the intended users of the tool are educated, but not necessarily expert, specifically, second responders such as tow truck drivers, salvage operators, or vehicle repair shops. While a production version of the tool will likely involve significant capital expenditure, it is our hope that the basic architecture of the tool, along with its operating principles, will allow significant flexibility in dealing with both present and upcoming vehicle technologies - thereby ensuring value through applicability and longevity for owners. Finally, great care in the design of the tool's interface to the vehicle was warranted. Although a range of options were considered, the selected prototype interface port sought to balance high-voltage terminal access and BMS information access against a strong desire not to introduce new failure modes or require unnecessarily complicated battery design and packaging.

General Interface Considerations and Recommended Design

A major objective of the diagnostics selected for incorporation into the prototype tool design was a general systems-level risk/benefit analysis. That is to say, that for any battery diagnostic information retrieved from the vehicle, its beneficial value was carefully weighed against its cost to implement. This assessment was in terms of hardware on each vehicle and the tool, and any failure modes or safety issues that new hardware might potentially introduce. A simple example might be additional wiring, which could augment the diagnostic method with added inputs, but which might also represent an added failure point or risk to users (either vehicle occupants or tool users. Though a complete FMEA or exhaustive reliability program is well beyond the scope of this work, we attempted to make a reasonably educated and objective first-pass assessment of the various options and suggestions available for offline diagnostic hardware access. In the interest of transparency, we have enumerated several examples of options considered to enlighten the logic behind our final prototype design and recommendations.

Physical Versus Remote Sensing

As discussed in the previous section regarding battery fault diagnostics, certain information must be gleaned from the battery to assess its safety and stability. For most diagnostic methodologies, several basic parameters must be measured directly, while supplemental parameters can be calculated from the basic data. The basic data selected for this tool development project and required for diagnosis is enumerated in the table below:

Table 7: - Battery Assessment Parameters

| Parameter | Criticality | Access Requirement |
|-----------------------------|---------------------------|-------------------------------------|
| Isolation Resistance | Safety & Mission Critical | Internal Pack or Terminal Access |
| Battery Current | Mission Critical | Terminal Access |
| Battery Terminal Voltage | Mission Critical | Terminal Access |
| Cell/Module Voltages | Preferred for diagnostics | Internal Pack Access (if available) |
| Cell or Module Temperatures | Helpful, but not required | Internal Pack |

FMVSS 305 requires isolation of the high-voltage DC bus from the chassis ground, also known as an un-earthed isolated system. Presently, when the vehicle is not in operation, or when an accident occurs, the general safety philosophy for most OEMs is to disconnect the energy storage systems from the bus via electro-mechanical contactor relays. In most cases, these contactors are located inside the battery enclosure as well. In this way, the high-voltage bus can quickly and conveniently be completely isolated within its associated enclosure.

Unfortunately, in a post-accident safety and stability assessment, this isolation denies easy access to some of the mission critical diagnostic data required above. Therefore, some scheme must be devised to acquire this data, from within the battery case enclosure, which may potentially be within a bent car.

Naturally, two obvious solution paths present themselves:

1. Direct access to the internal pack data via sensing wires that extend from within the battery enclosure to an accessible test point.
2. Remote access to the internal pack data employing sensing systems that are embedded within the pack, with a wired or wireless communication bus to an accessible data port.

As a recurring theme, each approach has corresponding advantages and disadvantages:

Direct Access – The clear advantage of this approach is robustness and reliability of consistent measurement and access. Because of the simplicity of sense wires as added equipment, the system is expected to be robust. Because the measurement would be carried out by an external device, no metrology quality control is necessary. On the other hand, this approach requires the installation and routing of sensing wires that are not present on the vehicle today. Such wires might add significant complexity and cost, but more critically, a poor design could introduce an additional failure points. For example, if individual cell or pack voltage sense wires were collocated to a single access point, this access point itself might represent an opportunity for water-intrusion resulting in a short and consequently, runaway. Moreover, since all individual cell/module voltage sensing would be routed to a single access terminal, this terminal would have a worst-case the possibility of exposing full pack voltage across the first and last terminals of the monitoring interface. Although this issue can be taken into consideration when designing the access port, the collocation of cell/module voltage sensing seems to introduce an undesirable, additional failure mode in certain cases.

Remote Access – The clear advantage of this process is ease of adoption. On most vehicles currently on the market, the onboard BMS) sometimes known as a battery energy control module (BECM) typically has all of the required sensing capabilities. In present practice, these sensing modules are located inside the battery enclosure and spread across larger sub-modules of the battery. These modules communicate their measurements and control parameters remotely via a CAN bus communication system (or similar). In this design, the communication bus is isolated from the high-voltage bus and sensing wires – thus addressing the chief disadvantage of the direct access design. The chief disadvantages of this design however, are the metrology and robustness aspects. In current implementations, the specifications of battery metrology vary in sensitivity, accuracy and calibration as defined by the manufacturer for each BMS. If desired, standard values for these performance parameters could be potentially be adopted to rectify this, but this is quite a bit on the restrictive side of the application and would likely hinder some new BMS designs and topologies. More critically, this scheme relies on the survivability of the embedded BMS sensors and communication infrastructure in order to assess the battery. That is, after an accident, the BMS system would need to remain functional and communicable in order for a safety and stability assessment to be made.

In the end, a hybrid approach is recommended. For the prototype, our approach employed the remote sensing capabilities of the BMS as the primary and preferred method for safety and stability assessment,

with a limited direct access port available as a backup means of assessment in case of BMS failure, and to assist in controlling battery discharging as the situation demands. This hybrid approach includes the following components:

Vehicle OBD-II Data Link Connector

In many frequent accident cases, the vehicle may be minimally damaged, including cases where the vehicle is un-drivable, but the powertrain and critical electrical systems are potentially unaffected. In such cases, it is still desirable to inspect the safety and stability status or check the battery RESS functionality, with minimal effort and intrusion. In such cases, our approach allows for quick assessment from the BMS through the DLC port. In short, provided that the vehicle's electrical systems (12V and HV) are intact and functional, and that a cursory inspection indicates that it may be safe to do so, the BMS may be queried through the DLC port. Should the vehicles condition permit it, the vehicle can be tested and recertified for driving (to manufacturers' specifications), or alternatively, the battery RESS can be monitored for towing and storage.

Auxiliary Diagnostic Port:

Should the vehicle be damaged beyond practical or safe BMS access through the DLC port, or should the initial DLC assessment indicate a discharge is required or basic communications functionality is not possible (loss of 12V), an auxiliary diagnostic and discharge port is recommended to facilitate connection and communication with the battery pack directly.

Functional Port Description:

In order to facilitate a range of operations from basic powering of the BMS to closing contactors and actually discharging the battery, the diagnostic and discharge port provides direct access to several critical interfaces for the discharge tool. As summarized in the list below and in Figure 56, the following access ports/connections are recommended and integrated into the prototype design.

- Direct 12V BMS Power
- BMS Communications (CAN) Access
- Direct Contactor Coil Control (+ & -)
- Common Contactor Ground

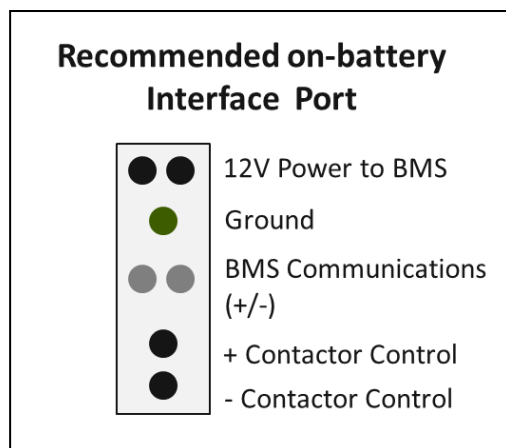


Figure 56: Prototype Battery Diagnostic Port Schematic

The following paragraphs summarize the individual ports in more detail relative to their need and functionality in the context of the prototype discharge tool.

Direct 12V BMS Power

In accordance with most existing first responder guides the onboard 12V bus will be physically disconnected (typically by cutting) in order to prevent unanticipated activation of the high-voltage systems (closing contactors) as well as deployment of the airbag safety restraint systems. Therefore after many accident scenarios and regardless of the overall battery condition, 12V power will likely need to be restored to the BMS in order to access the data available from it. Ideally, this would be done without incurring the aforementioned hazards present if the whole 12V bus were restored. To retain these existing and successful best-safety practices, we recommend that the port design facilitate activation of the BMS only, with unidirectional gates (i.e., diodes) or an isolated alternative power system of some kind, such that 12V power intended for the BMS applied via the port cannot back feed to power other 12V systems on the vehicle.

BMS Communications Access

Presuming that the BMS is powered and functional, it can typically provide the basic battery safety and stability assessment parameters discussed in Table 7. In normal operation, a typical BMS provides pack voltage, cell or module voltage, pack input/output current, pack or module temperatures, and HV system isolation monitoring to the greater vehicle via the CAN bus communication interface. For the prototype project, particular interest revolves around the BMS providing individual cell/module voltages since these are critical for the desired safety and stability assessment metrics. As will be discussed later in this section, the other parameters provided by the BMS (pack voltage, SOC, isolation) are useful but should not be solely relied upon given that this tool needs to be functional in situations where the BMS is inoperable and thus the critical parameters of isolation resistance and terminal voltage must be acquired on-tool as opposed to BMS only.

Direct Contactor Coil Control

First, in any case that the battery is ascertained to be damaged such that an energy reduction/discharge is recommended, a post-contactor terminal (or somehow otherwise isolated) connection would be useful in order to facilitate connecting the discharge cart without introducing the dangers associated with energized high-voltage hot-work. Such a configuration would therefore require contactor control in order to enable safe discharge. This contactor control could be provided by the BMS with access over the CAN bus, but given that the vehicle 12V bus will be disabled, and in some cases the BMS may be damaged, a simple wired interface to control the HV contactors is recommended. Further, should the BMS prove to be damaged, controlled access to the terminals will allow at least a partial safety and stability assessment of the battery to be made in support of discharging at reduced power levels, a critical requirement of this overall prototype development process.

Diagnostic Port Location and Design

The basic recommendation for the port location is that it must have high crash survivability and be easily accessible to first and second-responders in a post-accident scenario. Ideally, it would also be closely collocated with the BMS and battery enclosure as well as protected from normal wear and tear and weather. In general, a good location would be any crash-protected section of the passenger cabin – for example in the center console or floor for under-vehicle batteries, or behind the rear passenger seats or via the trunk for seat-back or trunk mounted battery designs. Near a battery's manual service disconnect (MSD), if included, is the suggested location both from a crash survivability and ease of collocation perspective.



Figure 57: Diagnostic Port Location Suggestions
 Top left: within center console, top right: under rear seat (with metal cover), bottom: colocation with MSD

Diagnostic Port Standardization

In order to achieve applicability for a stranded energy diagnostic and discharge tool across vehicle platforms and OEMs, a standardized interface would naturally be preferable. Non-proprietary standardization of the interface port/connector, available inputs/outputs, and metrology would ensure both the broad applicability of the tool as well as longevity, at reduced cost. Such standardization is particularly critical should the Remote Access sensing recommendation be followed, as a publicly available standard message format, unit system, and measurement accuracy would greatly simplify the tool design. Fortunately the automotive industry is already versed in the application of mandatory diagnostic standards for physical interfaces, specifically OBD-II. OBD-II, developed by the SAE and originally mandated by the EPA and CARB in 1996, specifies both the communication interface and the data link connector (DLC) port dimensions and pinout. Cars built after 2008 are required to incorporate CAN communications compliant with the SAE J-2284 standard. In the same way that OBD messages are specified and mandated for emissions systems maintenance, so too could messages relating to battery systems safety and stability Status be standardized. In fact, it is our recommendation that a standard set of CAN diagnostic messages relating to the basic battery safety and stability information (from Table 7) be devised and made available both via the OBD-II DLC port, and on the battery diagnostic port. It should be noted that this information is currently communicated using vehicle scantool diagnostic protocols, themselves a somewhat standardized method of relaying information. In the prototype process flow, we suggest the OBD-II DLC port be used to make a first pass assessment of the battery safety and stability, in case the 12V system has not been disconnected by first responders. If the battery is damaged, or the 12V system is no longer functional, then the Battery Diagnostic Port can be accessed.

High-Voltage Terminal Access

Adapter Based High-Voltage Terminal Access

Similar to the previously discussed Midtronics tool, the simplest and most straightforward location/method for high-voltage terminal access would be the adaptation of one of the vehicle's existing

connectors, such as the HV connection between the RESS and the motor inverter as shown on the GM Volt in the upper portion of Figure 58. Potentially a variety of adapters could be provided on a manufacturer specific basis. If applicable, such a connection would be the recommended first option, as it avoids dealing with the HV wiring, conduit, and shielding, as well as provides a relatively safely handled conductor access point.

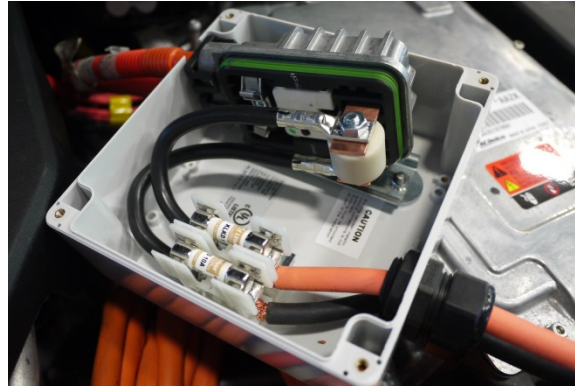


Figure 58: Volt high-voltage dc connector and Argonne adapted coupling adaptations

The actual prototype connector used for this work is shown below in Figure 59. Due to internal safety regulations regarding high-voltage connector design and battery discharging, the prototype connector needed a special enclosure and connector style, but an actual implementation would use a custom connector design for a particular vehicle's DC connection type. Although the Anderson style connector and adapter box is somewhat over-kill for this type of situation, any adapter/connector must provide adequate protection from high-voltage exposure across a range of usage profiles.



Figure 59: Developed prototype connector for high-voltage terminal access

Some complications arise against aligning around this adapter-based approach however. In some cases, the connector or the interconnecting HV cables could potentially be damaged or become inaccessible after an accident. Further, wiring between the RESS and the recommended access connector itself can become compromised, and the source of a post-contactor isolation fault, thereby preventing safe discharge. Finally, some vehicles without service disconnects or safely handled connectors may exist. In any of these cases, HV wiring may need to be accessed through a direct wire splice to the tool. In general, these cases will be difficult, and will require extreme caution in handling and treatment until HV wires

can be confirmed to be in a de-energized state. It is hoped that such cases will be rare, but certainly present, and is for this as well as the aforementioned hardware overhead reasons that a standardized HV connector was omitted lieu of a per-vehicle adapter-based design .

Dedicated High-Voltage Access Port

The second alternative considered as a possibility for terminal access is that of a dedicated high-voltage discharge and assessment port. In order to be truly safe, any high-voltage terminal pins included on the port would need to be de-energized in normal operation. This would require an additional set of HV contactors, just for the port pins. As shown in Figure 60, a standalone discharge port's contactors would need to be on the battery side of the main contactor assembly to ensure the rest of the vehicle remains isolated during a discharge.

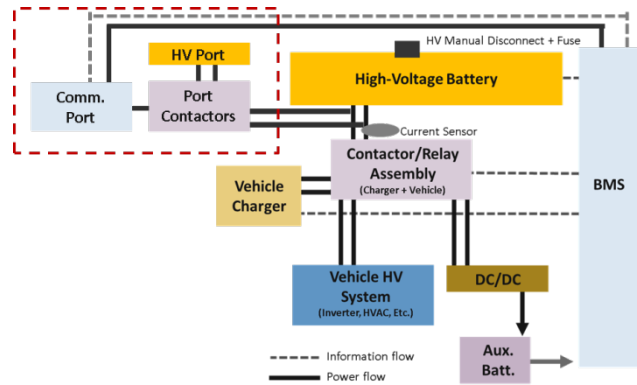


Figure 60: Overview of basic high-voltage system including supplemental HV discharge port (area in red dashed box)

In terms of the location for a supplemental discharge port, collocation near the MSD and recommended diagnostic port is strongly suggested. This enables the closest access to all discharge, safety and diagnostic functions, while additionally allowing for some synergy related to protecting the discharge and diagnostic ports from damage. As with the diagnostic port, the discharge port should be cabin accessible as well as robust to a variety of regular accident occurrences such as elevated temperatures, water intrusion, and physical vehicle deformation. Furthermore, great care must be used in designing the port since it will likely be collocated near the MSD and diagnostic communications port, which greatly increases the chances for a possible short between the MSD connectors and discharge port terminals. To summarize the suggested port location, Figure 61 shows an example MSD with locations identified for the diagnostic and discharge ports.

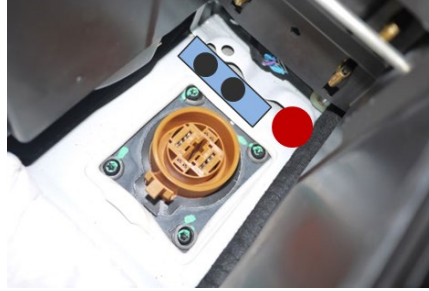


Figure 61: MSD, diagnostic port (red), and discharge port (blue rectangle) proposed collocation

While this supplemental discharge port is a viable option, this will likely require a significant amount engineering effort to integrate into a battery pack. Moreover, the added additional hardware, as well as wiring represents an additional failure point, and finally, no existing vehicles would support this configuration. Problems such as contactor failure and lack of 12V power would similarly impact such a port. Despite these negatives, a direct, cabin accessible battery discharge port provides the ability to assess and discharge a damaged battery pack across a wide range of scenarios. A standalone port would likely be somewhat safer in the sense that a responder would not need to remove high-voltage connections of unknown isolation just to hook up a discharge and assessment tool. The port would also allow for easier and more robust tool usage in scenarios that would normally damage an under-hood type connection solution. A standardized port would also help facilitate assessment and discharge in scenarios where the battery pack is outside of the vehicle. In this scenario, although the battery terminals are readily accessible, the terminal connectors themselves would likely differ across vehicles and would require a set of adapters. The contactors used for this supplemental port would also likely be designed to be more robust to scenarios such as water intrusion or anomalous battery behaviors and thus hopefully be more robust in terms of allowing direct battery access for assessment and discharge. Although it is not a direct match for the utility required in this case, the SAE J1772 standard, SAE Electric Vehicle Conductive Charge Coupler [60] provides a wealth of information relevant to the design of a proper port for discharging and connecting to the main battery lines for assessment and tracking.

Both the adapter-based and supplemental discharge port-based approaches have strong positives and negatives relative to intrusiveness, applicability, robustness, and practicality. The goal of this work however, is to provide workable options and a related discussion of both approaches. A final decision on port type, location, and design will need to be collaboratively discussed with a wide range of stakeholders including vehicle manufactures, battery manufactures, the first and second responder communities, and the current diagnostic and evaluation tool manufactures. From a prototype functional standpoint, the demonstration device can represent either option since the tool is just actuating a set of contactors and then running the operations.

Generalized Tool Process Flow

In order to avoid a full enumeration of all of the possible scenarios that might be presented, for both all existing vehicles as well as future vehicle cases in a post-crash assessment, only the core functionality is presented in the example.

Vehicle and RESS Identification

Identification of the vehicle is a critical facilitation in the automation of Safety and Stability Assessment. Fixed specifications such as battery chemistry, nominal battery voltage versus SOC, cell/module configuration, battery capacity, and nominal “healthy” isolation resistance need to be linked to the make/model of the vehicle under scrutiny. Further, operator instructions and reference material such as component location diagrams and wire-routing schematics, helpful in triaging a damaged EV in the field, could also be linked on a vehicle-by-vehicle basis. A discussion of a proposed Vehicle Specification Retrieval System is carried out in the Prototype Tool – Further Tool Recommendations section.

Visual Inspection and DLC Access

Once the vehicle has been identified, instructions will be presented to conduct a visual inspection of the vehicle and, if applicable, a diagnostic inspection of the battery system through the DLC port. The visual inspection should confirm that the vehicle is safe enough to access the passenger compartment and under-dash DLC connector. Of critical importance, active safety systems such as airbags or any other supplemental restraint systems must be deemed safe or deactivated. Signs of significant battery damage such as smoking, popping/cracking sounds near the battery, or spilled electrolyte indicate a very dangerous scenario that should be approached with the utmost care if at all. Finally, the 12V accessory power systems must be intact and operable, otherwise access through the DLC will not work.

BMS Battery Assessment Through the DLC

Should BMS access via the CAN bus be successful, all of the manufacturer’s battery assessment parameters would be available. Internal diagnostics such as isolation resistance, cell/module voltage, terminal voltage, and temperature, all typically deployed by OEMs as a component of their battery management strategies, should be sufficient to complete the safety and stability assessment. Naturally, some standardization of these metrics would be desirable. Typical OEM applications deploy an automatic assessment within the BMS as a diagnostic pre-condition for driving. In the interest of avoiding an overly-prescriptive approach, standardization could simply extend to a go/no-go output, shifting control and responsibility to manufacturer specified conditions. It should be noted that a battery can likely be discharged despite the vehicle BMS stating that the battery has failed. Since the discharge and assessment requirements are generally less strict as compared to the needs during typical driving, a much wider range of degradation can be considered acceptable from the perspective of allowing a low power discharge or simply tracking the pack metrics. For example, if a single cell in a pack was showing a 3 percent difference in voltage, a typical BMS would likely consider that pack failed and allow for no power to be drawn from the pack, whereas this scenario is typically within the realm of what is acceptable from a stranded energy discharging perspective. This issue is why the discharge tool provides its own decision making capabilities relative to data sensed from the battery and offline sensors.

Battery Assessment via Diagnostic Port

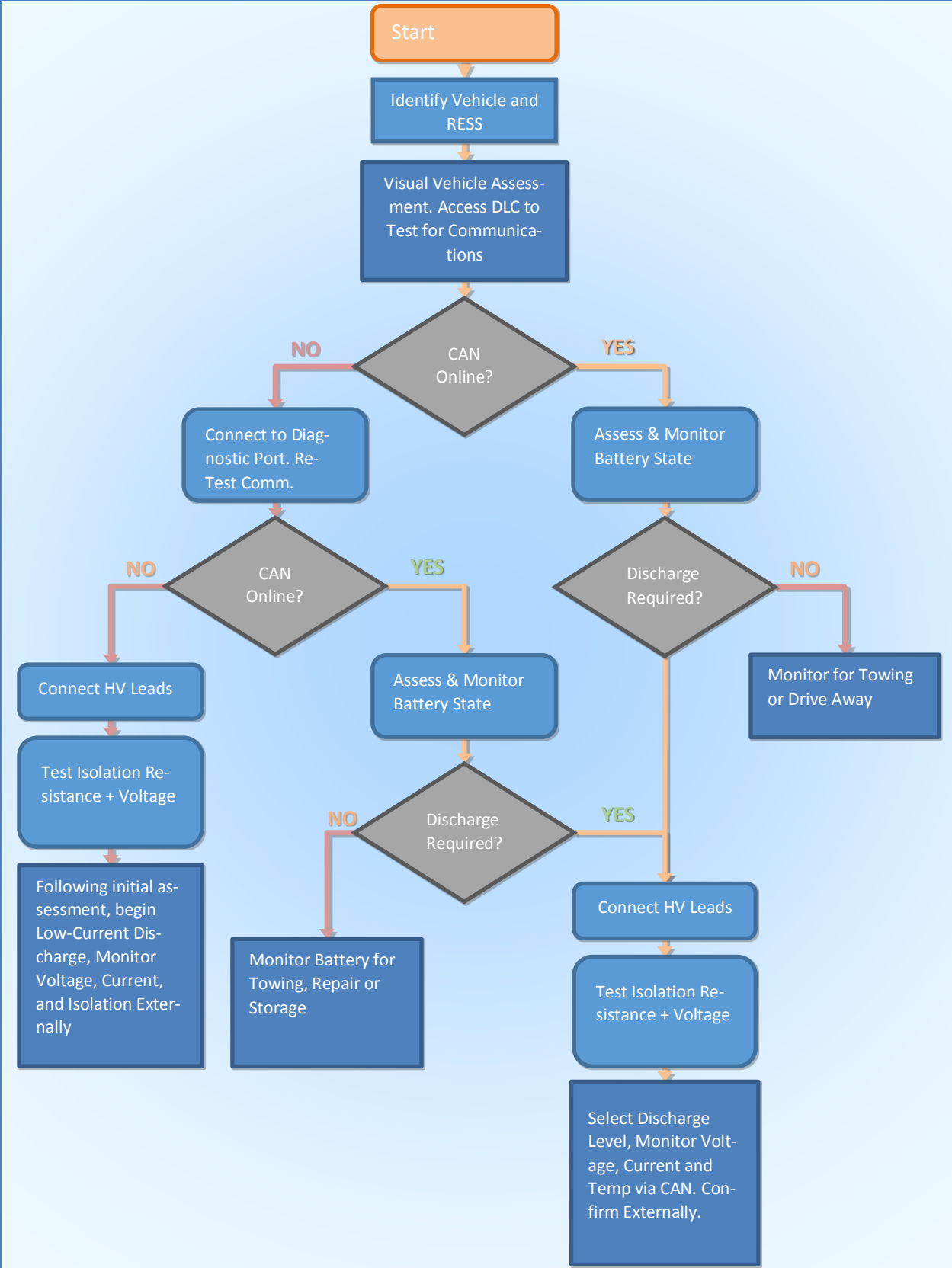
If a vehicle’s native, on-board BMS metrics are unavailable, the next step is to connect the recommended diagnostic port to the assessment and discharge tool. This will provide 12V power directly to the BMS, allowing for a check of the battery’s individual voltage sensing capability as well as providing a preliminary assessment of pack stability via comparing individual cell voltages.

High-Voltage Terminal Connection

To facilitate both stability assessment and as-needed discharge, a high-voltage connection must be made. The first step in the connection is to disconnect the vehicle 12V system. In this way, both the contactor control and supplementary restraint systems will be disabled. Contactor control and BMS access

can be restored through the auxiliary diagnostic and discharge port if not already completed. Next, remove the manual service disconnect (also known as the mid-pack service disconnect or MSD in some cases) if available. In doing so, the high-voltage bus can be made safe for handling, although normal HV work PPE procedures should be observed until the system is confirmed safe by the tool or other means. The process can then proceed to actually connecting to the high-voltage terminals.

After an initial HV connection is made and the auxiliary diagnostic port is connected (but before the MSD is reinstalled if applicable), the tool will make an isolation resistance check, to ensure that the isolation resistance between the tool and the RESS terminals post-contactors has not been compromised before or during the connection. Each leg of the HV connection will be tested before any contactor closure. The overall process flow of the developed prototype tool is summarized on the following page.



Prototype Stranded Energy Assessment and Discharge Tool Discussion

The general design goals enumerated above informed a myriad of basic design choices, which underlie the implementation executed for this study. As is ever the case, these choices are by no means mandatory, but instead are based on our best imagining of how the tool will be deployed in the field. With this in mind, we hope to justify our choices to the extent possible below.

Early in the development process, we realized that the diagnostic portion of the post-crash assessment might often be a stand-alone activity. That is, in many cases, if simple on-board diagnostic systems could verify the condition of the energy storage systems as stable and safe, then the engagement of the more complicated physical assessment and discharge tools might be unnecessary. For example, in case of a minor accident where the vehicle is disabled (damaged wheel or suspension) but the vehicle is largely intact, discharging the battery energy storage system might be overly invasive, and potentially damaging to a vehicle that would otherwise likely be repairable. In such cases, the system assessment and monitoring capabilities of the diagnostic tool would likely be enough to ensure safety without resorting to the more invasive and cumbersome discharge tools. For this reason we separated the tool into two major components: The diagnostic handheld unit and the discharge cart.

Handheld Diagnostic Unit and User interface:

In response to the expected users of the tool – that is individuals who are generally educated in automotive technologies, but not necessarily developers or experts from the manufacturer to which any given wrecked vehicle might belong, we wanted to ensure that the tool’s complexity was limited, and with it, the complexity of the knowledge required to operate it. As anyone who has deployed any technology accompanied by a 200-page technical manual would attest, the likelihood of oversight and misunderstandings is great, and the manual is likely to be skimmed or referenced at best. Certainly it would be unreasonable to anticipate that every second responder should study a course on EV specific tools given the relative rarity of such accidents.

For this reason, a guided graphical user interface (GUI) system was desired, by which the tool itself could act as a sort of “expert system” guiding the user through a scripted set of steps, based on the vehicle and situation at hand. Most anyone who is familiar with computers will be familiar with windowing software in which various configurable windows can appear or recede, based on prompts and user responses. The use of such a system allows reconfiguration of the user interface based on the instructions and controls required for each step. In this way, a process flow can be enforced, with minimum complexity presented to the user. In our design, the handheld diagnostic units handles all user instruction and interactions with the tool.

Obviously for a handheld unit, simple mobility was a core requirement, and fortunately recent years have witnessed a proliferation of platforms for this type of computing, extending from laptops to tablets (iPads, MS Surface, Chromebook), all the way to the ubiquitous smart phone. More recently, embedded computing platforms based on low cost hardware and software such as Raspberry-Pi (Linux) and similar ARM-Core devices (Linux and potentially Android) have become available. Each platform has unique benefits and drawbacks, each of which were considered within the scope of the project.

The first consideration for the selection of the GUI hardware platform was the difficulty of developing, implementing, and integrating the ancillary hardware that would be required to allow the device to interface with the vehicle and other tool components. Similarly, vestigial hardware, which would not be required for the tool’s operation, but which was included in the platform (at additional cost) was considered detrimental. A good example would be deployment on a laptop platform. Generally, a laptop

would need several add on devices (USB interfaces, etc.) in order to be a workable solution of a physical tool, but further, would also incorporate a myriad of features that would not be needed at all to complete the task at hand. These features would make a laptop-based solution a more costly, and possibly less reliable option in order to execute what is really a fairly simple application.

The second consideration was maintainability and reliability of the tool and its associated application software. Of particular interest in terms of the GUI application, was the operating system employed by each platform in order to present it. In any case where the operating system is maintained by a commercial entity, there will most certainly be operating system updates going forward. For any users familiar with Apple iOS devices, or with any Windows operating system, occasionally, these OS upgrades will impact application software functionality - necessitating upgrades to the application. Such updates might present a maintenance headache to a company or government entity engaged in maintaining the tool's application software, especially in the long run, after several generations of upgrades to the tool itself. So in short, all of this is to say that we considered each platform and its associated operating systems against the maintenance it might cost to the application itself.

One common solution to multi-platform operability is a web-based application, through which any device can access a common application via the internet. In essence, such a system offloads the GUI computing responsibility to a web-based server. This is an attractive solution because of its simplicity, and easy remote maintainability, though it does demand the maintenance of an active web site, potentially servers, and the application. More critically though, this option was rejected because it requires internet connectivity in order to function. While mobile internet connectivity is becoming more widely available, given some fairly remote U.S. roadways, it can by no means be assured.

While undesirably forced updates are something to be avoided, as new methodologies, tools and vehicles are developed, there may be some benefit to the ability to update on-board software remotely, or at minimum relatively simply. For example, as new cars come onto the market, the tool's process flow and instructions may need to be updated to accommodate them. Such updates can often cause problems on traditional embedded systems, particularly those without operational file systems. Because of this, the capability of occasional internet connectivity and an operating system that supports the deployment of updatable database files would be desirable.

A table outlining the pros and cons of the various platforms and approaches is listed on the next page.

Table 8: Comparison of Tool Platform Approach Possibilities

| Platform | Benefits | Challenges |
|--|--|--|
| Traditional Laptop Application | Infinitely flexible, relatively easy to program, many users have them. | Requires additional interface hardware, high maintenance overhead (security, updates). High difficulty ensuring compatibility across many brands available on the market. May pose a theft target, or be lost to other tasks. High cost. |
| Mobile Tablet Application | Relatively easy to program, many users already have them. | Requires additional interface hardware, high maintenance overhead (security, updates). May pose a theft target. High cost. May face application restrictions (Apple iPad apps). |
| Mobile Phone Application | Low cost, most users already have one. | Requires additional interface hardware, high maintenance overhead (security, updates). Very difficult to ensure compatibility and longevity across many rapidly evolving platforms. |
| Web Application | Universal compatibility, allowing users to use virtually any platform. Easy updates. | Very high maintenance costs for the tool developers in the form of website and servers. Very difficult to interface to vehicle hardware. Requires constant connectivity. |
| Single Board Computer With Embedded OS | Low cost, low maintenance overhead, very secure when not networked. Can interface directly with hardware. Relatively easy to update. | Somewhat difficult to program given rapidly evolving device market. |
| Embedded Computer (limited or no OS) | Very low cost, very secure. Can interface directly to hardware. | Nearly impossible to program complex windowing GUI interface. Difficult to update. |

Given the considerations listed above, in our quest for a graphical, guided-windowing application for the user interface, we settled on an application deployed on one of the many emerging single-board computers running embedded versions of the open-source Linux operating system. Although many suitable platforms exist for this work, we opted to use the BeagleBone platform. From the BeagleBone website: *“BeagleBone is an \$89 MSRP, credit-card-sized Linux computer that connects to the Internet and runs software such as Android 4.0 and Ubuntu. With plenty of I/O and processing power for real-time analysis provided by an AM335x 720MHz ARM processor, BeagleBone can be complemented with cape plug-in boards to augment functionality.”*

Processor: [AM335x 720MHz ARM Cortex-A8](#)

- 256MB DDR2 RAM
- 3D graphics accelerator
- ARM Cortex-M3 for power management
- 2x PRU 32-bit RISC CPUs

Connectivity

1. USB client: power, debug and device
2. USB host
3. Ethernet
4. 2x 46 pin headers

Software Compatibility

- 4GB microSD card w/ Angstrom Distribution
- Cloud9 IDE on Node.JS w/ BoneScript library



As can be seen from the specifications above, the BeagleBone met all of our desired design requirements. Specifically, it incorporates a fully functioning operating system, which can support guided graphical user-interfaces through the addition of a commercially available touch screen display. It supports direct hardware interfacing (including CAN networking) via a rich embedded peripheral set. It also has an Ethernet port enabling internet connectivity, which can be made Wifi compatible via a USB adapter.

Though many available Texas Instruments ARM-core boards have similar capabilities, an additional benefit to this project was the BeagleBone's simple snap-together physical architecture. Using the BeagleBone system, a 7" LCD touch display and CAN-network interfacing hardware could be incorporated with no soldering. In terms of prototype development, this was an attractive option. It should be noted that since the project's inception, a new, more powerful version called the BeagleBone Black has been launched, at an even lower price (\$55). Our BeagleBone is running an 11-2102 version of the Angstrom Linux embedded operating system, including QT C++ Libraries for GUI programming. All programming was carried out using C++ and C, on the QT Creator IDE, which was cross-compiled for deployment on the tool. Figure 62 below shows the board and enclosure for the prototype design.

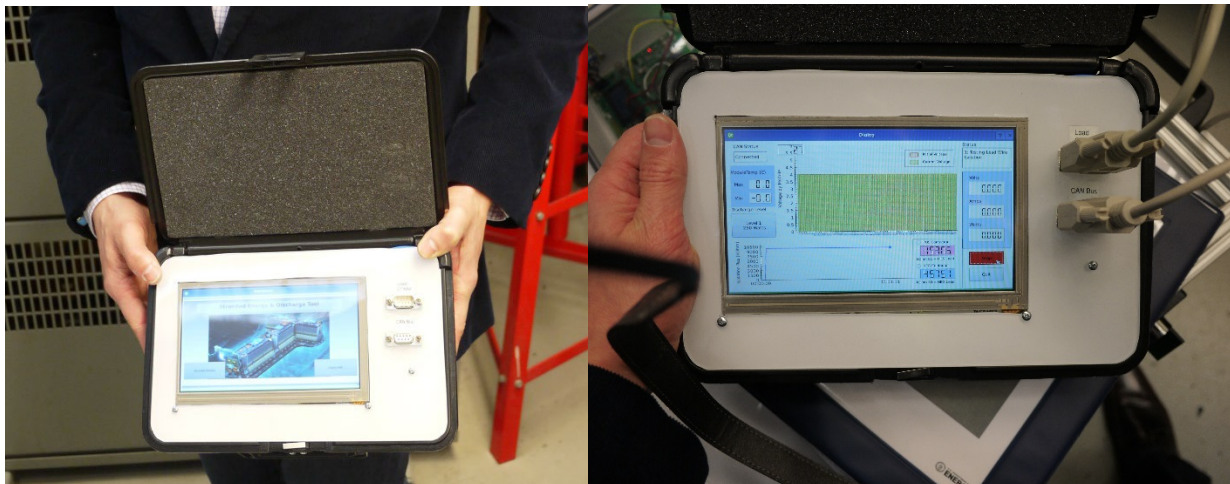


Figure 62: The Handheld Diagnostic Tool and Control Unit

During operation, the hand-held unit can be plugged into the standard OBD2 diagnostic link connector port. From there an initial assessment of the vehicles overall condition can begin. The diagnostic port on most modern cars and certainly on all electrified vehicles is operated using CAN networking protocols deploying diagnostic parameter IDs (PIDs). In addition to the standard OBD2 diagnostic message sets, most vehicles also employ this standard DLC port to conduct proprietary manufacturer defined enhanced diagnostics (ePIDs) using the same or similar protocols. Through these, in most cases, the energy storage system's internal diagnostics and sensor outputs (i.e., individual cell voltages) can be queried to assess the internal state of the battery. For prototype development, the ePID communication messages were simply reverse engineered. Although ePIDs do vary vehicle to vehicle, it should be mentioned that they are also provided (typically for a fee) to diagnostic tool manufacturers, thus highlighting that these value, while restricted, are not necessarily a competitive secret for a particular company. Moreover, if a more standardized protocol should be established for some of the basic battery information, tool applicability and ease of use would increase dramatically.

Querying the BMS diagnostics, through the DLC helps to establish several direct facts about the electrical condition of the car.

- The 12V system and CAN networks functional status
- The BMS/BECMs functional status.

If the 12V system is active, and the BMS can be reached via the network, several basic and important parameters can be obtained through the diagnostic ePIDs.

- HV system voltage and current
- Individual cell or module voltages
- Cell or pack temperatures
- Isolation resistance or status
- Contactor status (check)

If available, in many cases parsing and monitoring these messages can be sufficient to deem a battery system safe for storage or transport, precluding the necessity to connect the additional hardware from the discharge cart.

Discharge Cart and Offline Diagnostics

Should the initial diagnostics through the DLC port prove unsuccessful, the discharge cart should be deployed. Basic causes for the DLC/native BMS metrics to fail include:

1. Damaged 12V system,
2. Damaged CAN network, and
3. Damaged BMS/BECM.

The basic steps for continuing the battery energy storage system diagnostics are correspondingly:

1. Diagnose and if possible, externally restore 12V power to the BMS;
2. Avoid the vehicle's main CAN network, and plug directly into the diagnostic port; and
3. Deploy cart-mounted physical sensing systems (voltage, current, and isolation testing) in case the BMS itself is completely failed.

Finally, if the BMS is damaged such that diagnostic monitoring is impossible, then a discharge of the battery systems will likely be advised at relatively low power levels.

Based on this process flow, the design of the discharge cart was relatively straightforward. Figure 63 shows an overview of the recommended discharge and assessment tool's components and Figure 64 shows the prototype tool itself. In general the cart needed to include the following.

- Auxiliary 12V power supply (battery and charger)
- Current and voltage sensing systems
- Isolation testing systems
- Ability to interface to the LV bus systems and BMS/BECM directly
- Ability to interface with HV bus systems and control contactors
- A HV capable energy dissipation system aka "DC Load Bank"
- Some means of control and user interface

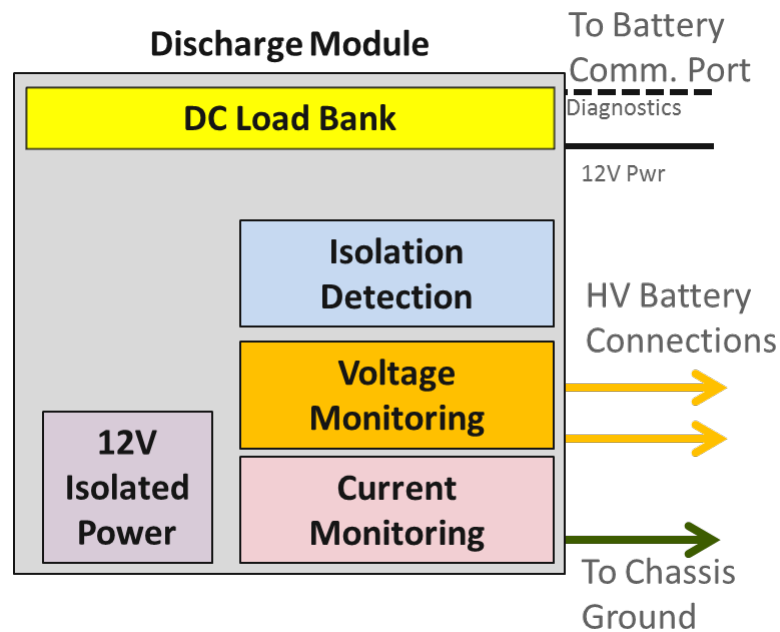


Figure 63: Discharge Cart Component Overview



Figure 64: Discharge Cart and Component Locations

It should be noted that all control of the discharge cart and its diagnostic control systems are carried out through the handheld unit, and its aforementioned touch screen menu system. When the discharge cart is deployed, the handheld unit is plugged into it, making control and further diagnosis possible.

In order that the cart be field-mobile, a 12V battery system was necessary. A basic 12V lead-acid vehicle battery is deployed as both an auxiliary supply in case of vehicle 12V bus failure, and to power the cart and all of its included electronic systems in the field. Included with the 12V system is an AC charger and inverter module. This allows our battery to be charged easily from 120V AC outlet, as well as the cart to use line power when in the shop, for indefinite monitoring and easy maintenance. When using the diagnostic port, the BMS/BECM can be powered directly from the cart, and the remainder of the CAN network is circumnavigated, thus allowing direct access to the battery system alone. In this way, even a battery system that has been liberated from its vehicle can be queried. Should attempts to query the BMS/BECM fail, or should the diagnostics or vehicle condition warrant a discharge, the high-voltage bus of the vehicle can be connected to the discharge cart's load bank. When both the HV and interface port are connected to the cart, the cart has full control over the battery system output, and is capable of monitoring the batteries functional state either alongside, or in lieu of the diagnostic systems status display. A connection diagram is shown below in Figure 65.

- Handheld diagnostic unit → CAN diagnostic pass through and cart control cable.
- LV mandatory port connection including BECM power, contactor control commands, and CAN wiring.
- HV connection including high and Low contactor outputs, integrated sensing systems
- Chassis ground clamp? (Could connect this through BECM ground?)

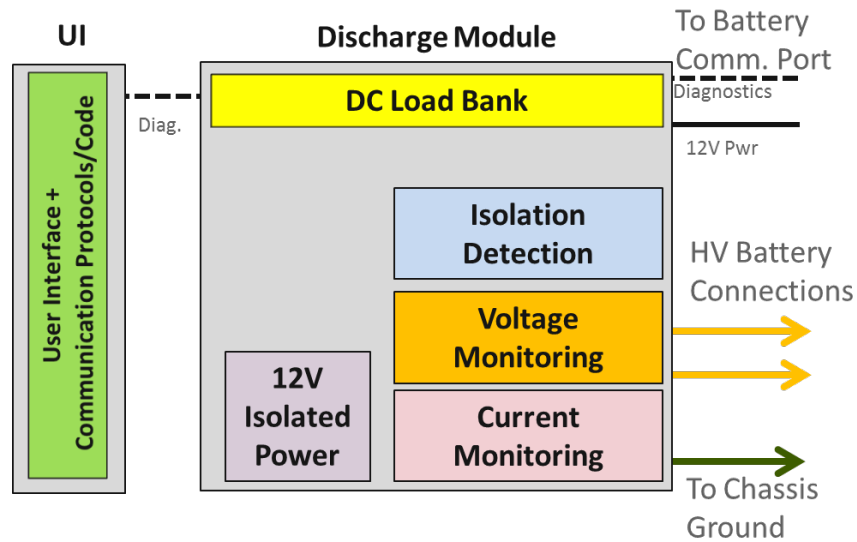


Figure 65: Overview of Discharge and Assessment Tool Components

The following paragraphs seek to expand on the various tool sub-components in greater detail.

Isolation Detection System:

The isolation resistance detection system consists of two Bender IR155 isometer Insulation monitoring devices, originally intended to be embedded as a component of an electrified vehicles battery management system. In general, the operating principle for these systems is relatively complex owing to their designed intent to continuously monitor isolation resistance in an EV system while the vehicle is operational. Vehicle operation introduces large transients on both the battery system output current, complicating simpler isolation measurement methods. While simple high-voltage isolation resistance measurement systems are available (mega-ohm-meters), care may need to be taken when choosing an isolation resistance measurement technique to avoid damaging battery connected components (BMS boards) by using a high-voltage pulse to detect isolation resistance.

Specific to the case of post-crash battery isolation assessment, this work sought a solution that would allow isolation measurement both within the energy storage system (pre-contactor) and downstream of it (post contactor) independently. Further, the developed tool sought to conduct isolation tests with minimal possibility of introducing HV potential at any point until isolation was fully assured. In order to do this in a straightforward fashion, two Bender IR155 boards were deployed, one for each leg of the HV system. The independent testing of individual legs is also helpful from the perspective of diagnosis where a isolation failure has occurred. The test leads are connected to the HV system when the discharge cart is connected. HV system isolation is thereby monitored continuously during the entire discharge process, independent of the BMS/BECM diagnostics.

Load Bank:

The load bank deployed is a BK Precision 8522 (a rebranded Itech IT8516B), selected primarily for its mix of relatively low cost and power/voltage capabilities. We initially considered designing and implementing our own simplified and more portable load system, but quickly realized that the design time and effort required for a prototype system would quickly outrun the cost of simply purchasing one of the many

commercially available systems. This choice also simplified our cart mounted sensing systems for terminal voltage and current, as the BK Precision load can be both controlled and queried through its included RS232 serial port. Specifications and photos of the equipment can be found on the BK Precision website [89]. From the website:

“The affordable, laboratory grade model 8522 Programmable DC Electronic Load is well suited for testing and evaluating a wide variety of DC power sources. This DC electronic load can operate in CC, CV, CR or CP mode while voltage/current or resistance/power values are measured and displayed in real time and is fully programmable via RS232 or USB interface. Over temperature, over power, over voltage, over current and reverse polarity protection will help protect your valuable prototype and circuits. Its flexible operating modes and excellent measurement accuracy make this DC electronic load a great choice for characterizing DC Power supplies, DC-DC Converters, batteries, fuel cells and solar cells.”

Maximum power capability for the selected load bank is 2.4kW that allows for reasonably fast discharging, while remaining well within a safe limit for discharging packs with an inactive cooling system. Additionally, this power capability is similar to other devices on the market. Higher power levels and thus faster discharge times could easily be implemented with this current prototype, but as the discharge power increases, the amount and fidelity of the information required to track battery safety and stability increases dramatically. All data from the load system is relayed through the connected handheld control unit, as well as on the front panel display.

Ancillary Hardware and Connections:

Finally, some ancillary hardware including: Power electronics, emergency stop buttons and an additional onboard processor are employed to integrate the systems. Of note, onboard processing was employed to simplify the control of the discharge cart from the handheld unit. Figure 66 on the following page, shows the assessment and discharge tool’s control and processing boards as well as the isolation boards.

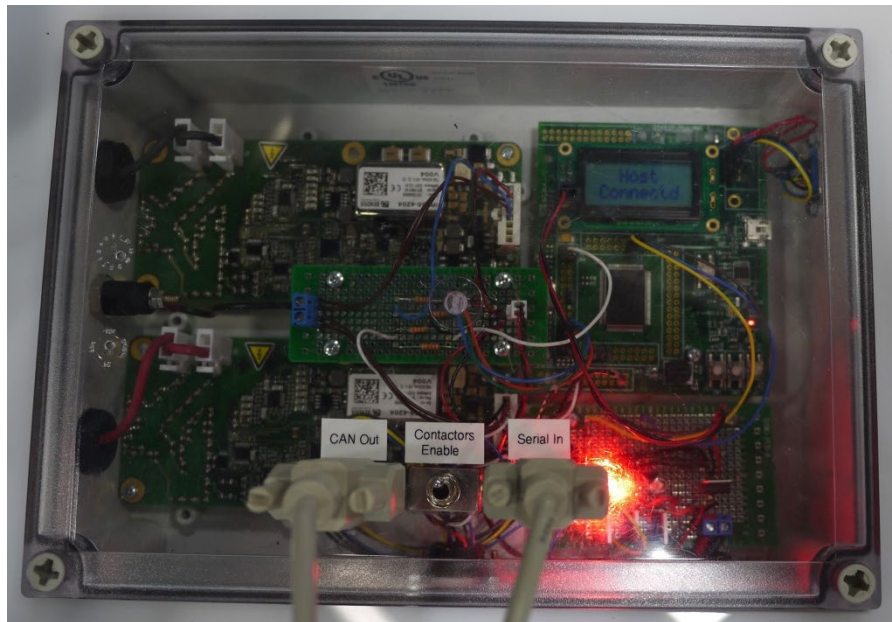


Figure 66: Load Bank On-board Control and Processing Boards (and isolation resistance sensing)

Prototype Tool Deployment Highlights

This section seeks to highlight some actual screen-shots from the tool during use on a (non-failed) Chevrolet Volt. While actual screen shots are used, it should be noted that this battery is within specifications and thus the screens look fairly commonplace.

Once the tool has booted, the vehicle selection screen, shown below in Figure 67, appears. While the prototype development focused on only two vehicles, a much more thorough menu or vehicle-lookup system could be implemented to identify the vehicle type.

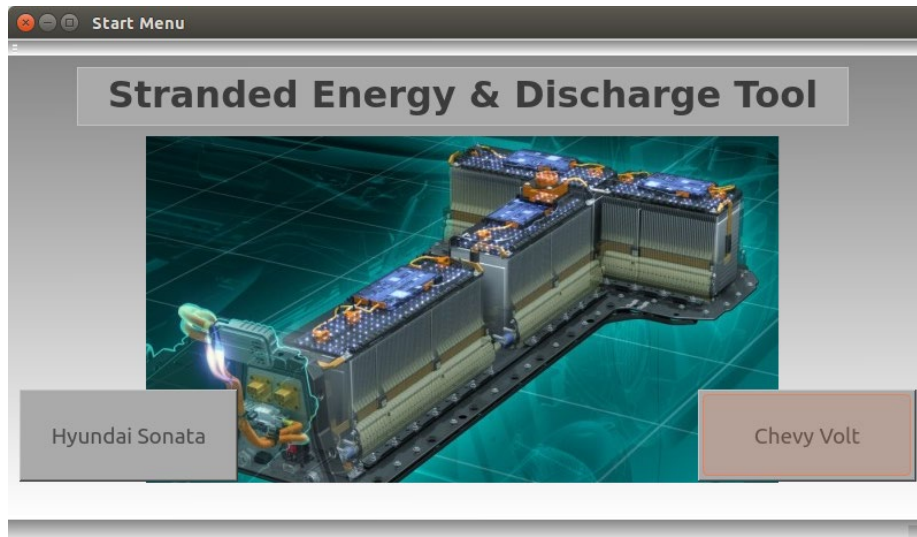


Figure 67: Screenshot - Vehicle Selection Screen

Pressing the appropriate button on the touch-screen (in this case the Volt), the tool then provides clear instructions how to hook up the tool to the vehicle DLC port to assess if vehicle CAN functionality and 12V power is available. As can be seen in Figure 68, one of the main benefits of this style of hand-held tool is the ability to provide detailed information to the user. Pressing "ok" will begin the process of checking for vehicle CAN functionality. Status bars were frequently employed throughout the tool's user interface in order to provide the user an indication of what was going on at all times during the assessment process.



Figure 68: Screenshot – Connection instructions for DLC-based vehicle BMS assessment

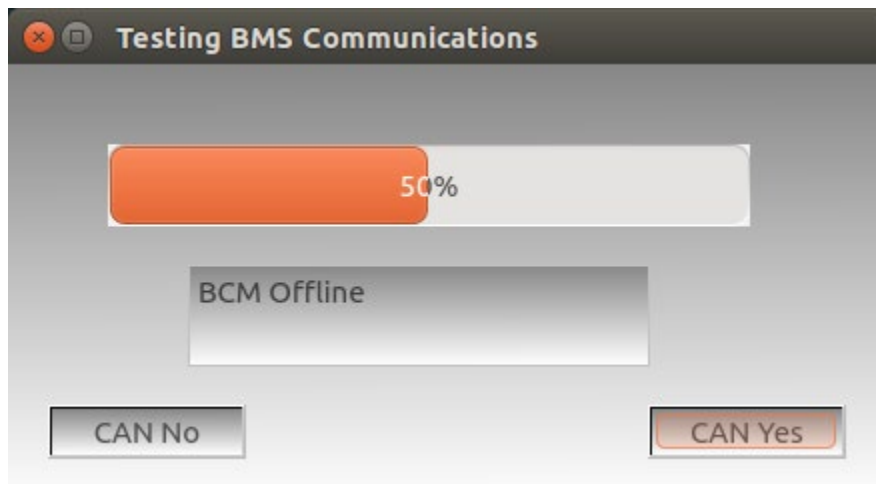


Figure 69: Screenshot - CAN Communications assessment progress screen

In this scenario, the vehicle 12V power was unavailable, so the actual BMS was not yet available for evaluation. Given a result of “CAN no” the next step is to connect the handheld unit to the discharge cart and then connect the cart’s diagnostic port and high-voltage discharge connections to the vehicle. Figure 70 again shows the advantages of the tool’s touch screen to provide concise directions and locations for setting up the discharge and assessment tool.

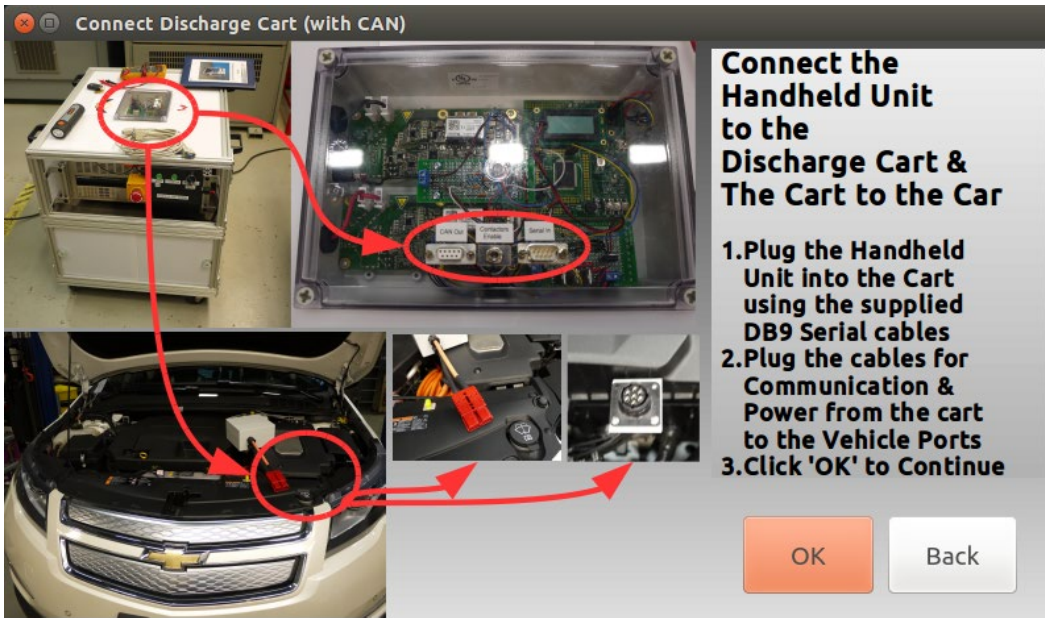


Figure 70: Screenshot - Discharge Required, Discharge Cart Hookup Instructions



Figure 71: High-voltage and diagnostic interface port connections

Once the vehicle connections have been made, the tool can now start to be used in diagnostic and discharge mode. Figure 72 highlights the discharge screen if individual battery voltage sensing is available via the previously discussed diagnostic protocols and Figure 73 highlights the screen for a discharge when the BMS sensed information is not available. In both cases, terminal voltage, current, and power are displayed prominently to aid the user in understanding the current operating mode. Isolation resistance is also displayed, tracked and plotted in both screens, providing users the ability to identify changes in isolation over time.

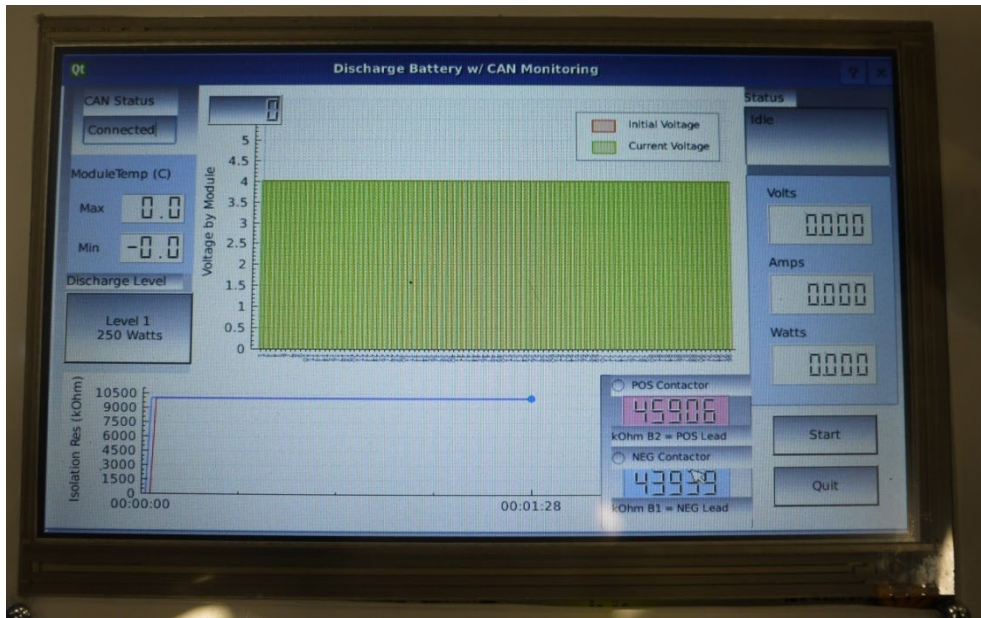


Figure 72: Screenshot - Discharge Screen With BMS Provided Voltage Information

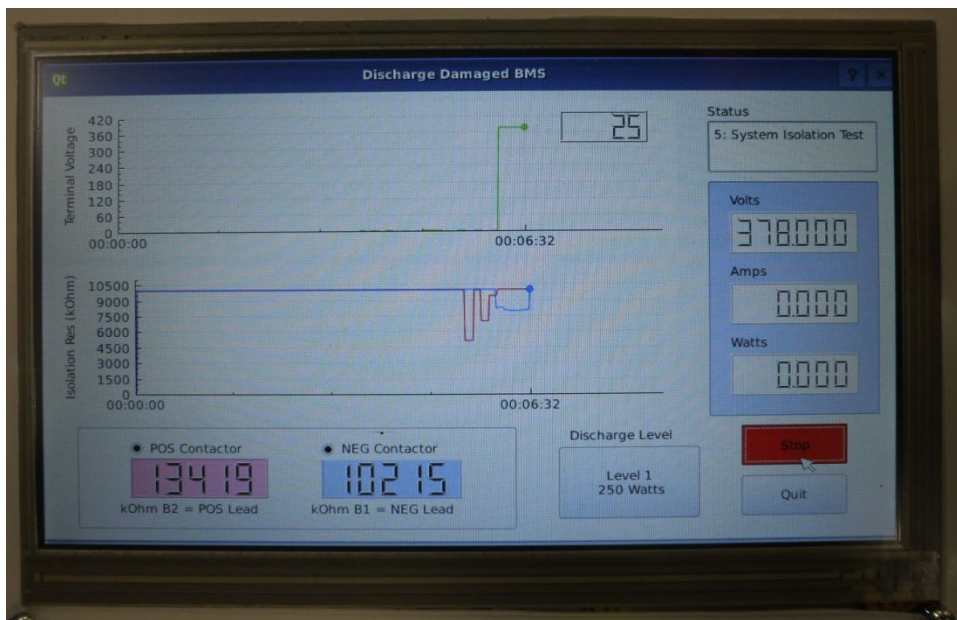


Figure 73: Screenshot - Discharge With No BMS Information

Future Tool Improvements

As is typical through the design process, some lessons learned and potential improvements to the tool were identified, which were not able to be reasonably implemented by the project deadline. Nonetheless, it is valuable to capture these suggestions, for a developer wishing to produce a similar tool or a researcher seeking to push the tool's applicability further.

1. Wireless Handheld Unit – we had actually started implementing a wireless link between the discharge cart and the handheld unit for the purpose of controlling the cart, but soon realized that the handheld unit would still need to be plugged into the DLC/CAN bus in the likely case that the BMS was available. In a future version, we would implement the tool such that both the CAN link and tool

cart control link could be conducted wirelessly. In practice, this would require an additional piece of hardware, a dongle that would still need to be physically plugged into the CAN bus, but it would facilitate remote monitoring of the vehicle's status (assuming it could be powered). For example this would allow remote monitoring from inside a tow-truck cab, or from a salvage/repair yards office. For this task we planned to use the ZigBee wireless protocol operating on IEEE 802.15.4 physical layer standard. Using the Xbee hardware (Xbee pro 60mW) we had specified, outdoor ranges of up to one mile are feasible.

2. Vehicle Specification Retrieval System – Ideally, a database of the relevant specification of any given vehicles energy storage system would be maintained within the tool, leveraging a-priori knowledge of the vehicles operating fundamentals to more quickly and accurately identify the batteries' safety disposition. Fixed specifications such as: battery chemistry, nominal battery voltage, cell/module configuration, battery capacity, nominal "healthy" isolation resistance, as well as component location diagrams and wire-routing schematics could all be helpful in triaging a damaged EV in the field. Currently, the application relies on the user to correctly identify the vehicle or system in question (similar to most first-responder situations), in order to retrieve the appropriate corresponding information. In future iterations, the tool could be enhanced by the use of a bar-code or QR code reader that would be linked to the corresponding vehicle's data. Ideally, such identification would reside on the battery system itself (i.e., on the case, or near the interface port), in case the battery were extracted from the vehicle. In this way, the energy system would always be absolutely identifiable. VIN coding or multiple ID locations could also be added for easier access.
3. Software Update Application – Given the deployment of a vehicle specification database from 2, naturally the database system would require regular updates as new vehicles come to market. In order to handle this inevitability, a software update application should be incorporated into the handheld unit's software, allowing the unit to download updated database definition files when connected to the internet. Such a program could be quite simple, directing the tool to updated files on a static FTP site, or something equivalent.

Additional Prototype Tool Development

Over the course of developing the final battery assessment and discharge tool-set, several other prototypes were created as a proof of concept or design exploration of a particular aspect related to battery assessment. This section seeks to discuss two of these prototypes in greater detail as something that could be used as a supplement to the developed prototype tool or as a simple tool for basic stability assessment and tracking.

Low cost, handheld data monitoring

As has been discussed in other sections, considerable data is accessible from a vehicle's diagnostic communications. Following this inception of a standardized hardware interface, the female 16-pin J1962 connector standardized with OBD-II, shown in Figure 74, a market has developed for devices with the ability to communicate to modules throughout a vehicles communication network.

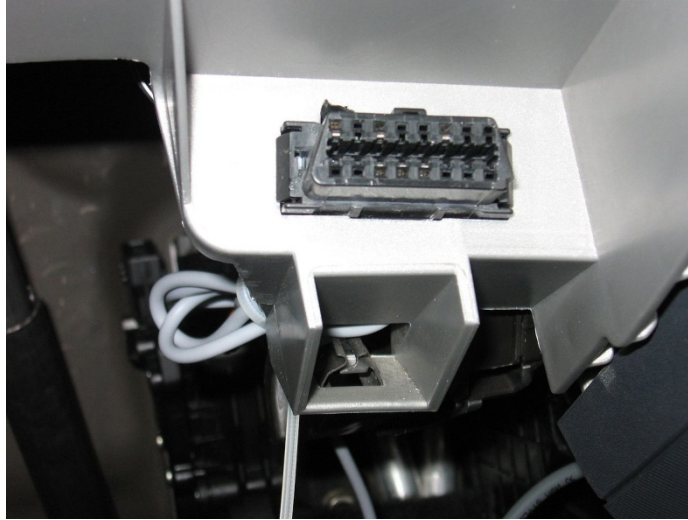


Figure 74: J1962 OBD-II connector

Of particular interest to this project, is a wireless diagnostic communication tool that allows a separate interface, such as a mobile smartphone, tablet, or laptop to communicate with the wireless adapter. Many of these devices are available, and can be purchased for a moderate cost (\$10 to \$200). Figure 75 shows the connector used for this work, with a quarter provided for context into how small and un-instructive these types of connectors can be.

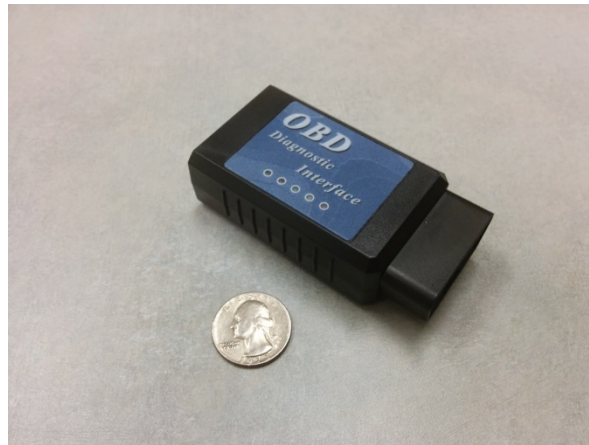


Figure 75: Example wireless diagnostic interface

These wireless diagnostic connectors then allow for a software device to communicate with vehicle's ECU modules, commonly by requesting diagnostic codes. As these systems have decreased in costs, and smartphones have become increasingly popular, several developers have created software interfaces (apps) with the ability to connect to an OBD-II adapter, and capture not only diagnostic data, but also standardized data parameter identifies (PIDs), which contain data from an ECU. A series of PIDs is required for emissions monitoring that make available data available pertaining to vehicle emissions systems, and overall operation. These include things such as vehicle speed, engine speed, mass air flow rate, and calculated catalyst temperatures. Additionally, manufacturers incorporate their own specific PIDs that are not required to be in a standard naming format. These PIDs can be sent in using the same communication standard as the OBD specific PIDs, but can be addressed to any module developed to do

so. Of interest in this research is the distribution of manufacturer PIDs containing information on a vehicle's high-voltage battery. For this work, the diagnostic connector was modified so it could be connected to either the standard DLC port or to the developed battery diagnostic port with additionally provided 12V direct BMS power. The wireless connector and connections are shown below in Figure 76.



Figure 76: Wireless diagnostic adapter integration with developed battery diagnostic port

Once the diagnostic protocols have been developed for a specific vehicle, a wide range of existing software tools and apps can be used to access and display the requested diagnostic information. In the case of this work, an app called “Torque Pro” was chosen for the ability to provide customizable display of data, data logging capability, as well as allowing for inclusion of custom PIDs. To test out the capability of this system, the list of diagnostic PIDs for the 2012 Chevrolet Volt was developed and uploaded to the application. Figure 77 shows an example screen from the app working with the PIDs developed for this project. As can be seen in the figure, the app provides individual voltages as well as module temperatures, terminal voltage, and isolation resistance (screenshot was taken while the vehicle was not operating, thus resistance, current, and voltage all display zero values).



Figure 77: Prototype wireless diagnostics using an off-the-shelf app and wireless connector (Chevrolet Volt data shown)

Simple Isolation Resistance Tracking and Notification (alarm)

Another useful tool that was developed over the course of this work is a simple offline, battery-powered isolation resistance measurement tool. Although ultimately integrated into the handheld unit, this prototype illustrates the feasibility of a simple tool that could be placed in a vehicle to track isolation during an evaluation period. While the current tool simply used an on-board LCD screen and audible alarm to notify the user of an isolation failure, this methodology could easily be extended to provide wireless alerts and tracking that would be useful for many evaluation and “wait-and-hold” type scenarios. Similar to the isolation monitoring of the main discharge and assessment tool, this prototype also uses a Bender isolation monitoring system. In addition to this core piece, batteries, fuses, and test leads have been added. Shown below the tool is self-contained in its own box and can run off its own battery power. Aside from the isolation monitoring system, the tool is made very simply and cheaply.



Figure 78: Offline isolation monitoring prototype tool

Figure 79 shows the prototype tool installed in a vehicle at the MSD. This installation is evaluating half the pack and has a probe connected on the MSD connector and a clip to vehicle ground on the other side for evaluation of isolation.



Figure 79: Tool installation in a BEV to evaluate isolation of half pack via removed MSD

While basic, this tool would provide insight into a pack's isolation resistance without requiring any internal battery access aside from the MSD connections. A simple and effective tool to evaluate battery isolation, would aid a range of stakeholders since isolation deterioration that could lead to a thermal event can typically be identified prior to the actual thermal event, allowing greater scrutiny or mitigation measures to be applied to avoid a large thermal event.

Project Conclusions and Recommendations

This work provides a wide variety of research, analysis, discussion, and development work related to understanding, assessing, and mitigating the hazards associated with stranded battery energy. Specifically, this work was broken into four major sections:

- **Battery System Architecture and Stranded Energy Background Research**

Within this section the concepts of stranded energy were introduced and discussed within the context of a vehicle's high-voltage distribution system. The term stranded energy itself is somewhat of a misnomer, because in a sense, the real difficulty is how to assess (and possibly mitigate) stability and safety issues for a battery pack with little or no prior information. Several factors such as loss of 12V power and the frequent lack of easily accessible battery terminals drive some of the more practical development aspects of a stranded energy discharge and assessment tool. Currently several OEMs offer some sort of high-voltage battery discharge tool, but these tools vary widely in their complexity and often require a significant amount of OEM input during development. Several highlighted battery thermal incidents were also discussed and one of the major observations from these incidents is that many vehicle battery issues begin outside of the cells themselves. This suggests assessing the battery system as a whole is important to help understand the stability and safety of a pack under assessment. Furthermore, the concept of tracking values over time to observe changes indicating a decreased state of stability or safety seems a reasonable addition to any developed tool.

- **Battery Failure and Thermal Runaway Background and Supporting Research**

This section provides an overview of existing research regarding the impacts of battery SOC relative to thermal event severity and onset. While a wide variety of research sources suggest there is a clear correlation between elevated SOC levels and incident severity, there are fewer research reports that clearly discuss what SOC levels are acceptable for "safer" storage and transport. Ultimately, through a mix of outside research and work funded through this project an SOC threshold of 30 percent and below is suggested to ameliorate the severity of a thermal event should one occur.

- **Battery Diagnostics and Stability Assessment Techniques**

A wide range of possible battery diagnostics is presented in this section as means to identify deteriorating (or already unacceptable) battery stability and safety. The preferred metrics used for this assessment rely heavily on the use of existing individual voltage sensors within a pack. These sensors are queried and read using a vehicle's diagnostics protocol that is already functioning as needed for most vehicles evaluated during this work. This work strongly suggests having vehicle diagnostic messaging protocols support the broadcasting of all individual cells as well as suggesting the additional step of standardizing a set of battery voltage specific diagnostic communications protocols. Supplemental offline measurement of pack voltage, current, and isolation resistance are also recommended due to their utility for situations where the BMS sensing may not be operational. Moreover, isolation resistance tracking is suggested as a means for tracking the long term stability of a battery during storage following an accident. Last, this section discusses the use of "SOC" for stranded energy assessment and suggests that a manufacturer specified voltage tolerance would be sufficient for determining a battery's SOC. If a voltage limit is unavailable, tracking the relative trends of terminal voltage during a discharge and identifying roll-off could also be used to determine that the SOC has been decreased to a "safer" level from the thermal event perspective.

- **Prototype Stranded Energy Tool-set Development**

This section discusses the development process and decisions made to create a stranded energy assessment and discharge tool set. Multiple options are discussed and the section provides details for each of the system's core components. Screenshots of the tool in operation are also provided to provide the reader with a better understanding of how the tool conveys information to a user. Ultimately, the developed tool provides a range of functionality and connection options to provide insight across the range of possible battery and related system damage. While this tool is prototype in nature, it is hoped that this information and the thoughts used to develop the tool and protocols will promote a discussion regarding how to assess stranded energy and what to do if pack stability and safety is found to be below a desired level.

References

1. Hyundai Sonata Shop Manual, www.hyundaitechinfo.com/
2. Toyota Shop Manual (Prius PHV), <https://techinfo.toyota.com/>
3. 2011 Chevrolet Volt Emergency Response Guide, www.evsaftytraining.org/~media/Electric%20Vehicle/Files/PDFs/VoltRespondersGuide.pdf
4. Midtronics GRX-5100 EV/HEV Battery Service Tool, www.midtronics.com/shop/grx-5100
5. Capacitor (i-ELOOP) Disposal Manual, www2.mazda.com/en/csr/recycle/capa/pdf/ca_m3_useng.pdf
6. Smith, B. (2012, January 20). *Chevrolet Volt battery incident overview report* (Report No. DOT HS 811 573). Washington, DC: National Highway Traffic Safety Administration. Available at www.nhtsa.gov/staticfiles/nvs/pdf/Final_Reports.pdf
7. Spotnitz, R., & J. Franklin. (2003). Abuse behavior of high-power, lithium-ion cells. *Journal of Power Sources*, 113(1): 81-100.
8. Roth, E. P., Crafts, C. C., Doughty, D. H., & McBreen, J. (2004, March). *Advanced technology development program for Lithium-ion batteries: Thermal abuse performance of 18650 Li-ion cells*. (Report No. SAND2004-0584). Albuquerque, NM: Sandia National Laboratories.
9. Doughty, D., & Roth, E. P. (2012). A general discussion of Li ion battery safety. *Electrochemical Society Interface* 21(2): 37-44.
10. Mikolajczak, C. J., & Moore, C. D. (2002). The aircraft cargo hold environment: the implications of a fire on lithium-ion battery shipments. *17th Annual Battery Conference on Applications and Advances*.
11. Doughty, D. H., & Crafts, C. C. (2006). *Electrical energy storage system abuse test manual for electric and hybrid electric vehicle applications*. Livermore, CA: Sandia National Laboratory.
12. Doughty, D. H. (2010). *SAE J2464 EV & HEV Rechargeable Energy Storage System (RESS) Safety and Abuse Testing Procedure*. (Paper No. No. 2010-01-1077). Warrendale, PA: SAE International.
13. Webster, H. (*Lithium Battery Update The Effect of State of Charge On Flammability and Propagation of Thermal Runaway*, H Webster, www.fire.tc.faa.gov/pdf/systems/May12Meeting/Webster-0512-Effect_of_State_of_Charge.pdf
14. *Report of the Second International Multidisciplinary Lithium Battery Transport Coordination Meeting, Multidisciplinary Lithium Battery Transport Coordination Meetings, 9 to 11 September 2014 (Cologne, Germany)*, www.icao.int/safety/DangerousGoods/Second%20International%20Multidisciplinary%20Lithium%20Bat/ICAO.LB.COORDINATION.2ndMeeting.Report.pdf
15. Roth, E. P. Thermal Abuse Performance of MOLI, Panasonic and Sanyo 18650 Li-Ion Cells. *SANDIA REPORT* (2004), SAND2004-6721
16. Wang, Q., Jinhua, S., & Chunhua, C. (2007). Thermal stability of delithiated LiMn₂O₄ with electrolyte for lithium-ion batteries. *Journal of The Electrochemical Society* 154, no. 4: A263-A267.
17. NEW CAR ASSESSMENT PROGRAM (NCAP) Side Impact Pole Test: General Motors LLC 2011 Chevrolet Volt 5-Dr Hatchback NHTSA No.: MB0125, Report Number: SPNCAP-MGA-2011-081, MGA Research Corporation, Final Report Date: June 7, 2011
18. *Numerical and Experimental Investigation of Internal Short Circuits in a Li-ion Cell*, M. Keyser et al, NREL 2011 DOE Annual Merit Review Presentation, NREL/PR-5400-50917
19. Abraham, D. P., et al., *Diagnostic examination of thermally abused high-power lithium-ion cells*. *Journal of Power Sources*, 2006. **161**(1): p. 648-657.
20. Kim, G.-H., Pesaran, A., & Spotnitz, R. (2007). *A three-dimensional thermal abuse model for lithium-ion cells*. *Journal of Power Sources*. **170**(2): p. 476-489.
21. Roth, E. P., *Abuse response of 18650 Li-Ion cells with different cathodes using EC:EMC/LiPF₆ and EC:PC:DMC/LiPF₆ electrolytes*. Battery Safety and Abuse Tolerance at the 212th ECS Meeting, 2008: p. 19-4141.

22. Roth, E. P., et al., *Advanced technology development program for lithium-ion batteries: thermal abuse performance of 18650 Li-ion cells. SAND2004-0584*, 2004, Sandia National Laboratories: Albuquerque, NM.
23. Doughty, D. H., et al., *Lithium battery thermal models*. *Journal of Power Sources*, 2002. **110**(2): p. 357-363.
24. Yang, H., G. V. Zhuang, & P. N. Ross Jr, *Thermal stability of LiPF₆ salt and Li-ion battery electrolytes containing LiPF₆*. *Journal of Power Sources*, 2006. **161**(1): p. 573-579.
25. Roth, E. P., *Final report to NASA JSC: thermal abuse performance of MOLI, Panasonic and Sanyo 18650 Li-ion Cells SAND2004-6721*, 2005, Sandia National Laboratories: Albuquerque, NM.
26. Xing, Y., Ma, E. W. M., Tsui, K. L., & Pecht, M.. Battery management systems in electric and hybrid vehicles. *Energies* 4, no. 11 (2011): 1840-1857.
27. Chen, J., Buhrmester, C., & Dahn, J. R. Chemical overcharge and overdischarge protection for lithium-ion batteries. *Electrochemical and Solid-State Letters* 8, no. 1 (2005): A59-A62.
28. Maleki, H., & Howard, J. N. Effects of overdischarge on performance and thermal stability of a Li-ion cell. *Journal of power sources* 160, no. 2 (2006): 1395-1402.
29. Arora, P., White, R. E., & Doyle, M. Capacity fade mechanisms and side reactions in lithium-ion batteries. *Journal of the Electrochemical Society* 145, no. 10 (1998): 3647-3667.
30. Pattipati, B., Pattipati, K., Christopherson, J. P., Namburu, S. M., Prokhorov, D. V. & Liu, Q. *Automotive battery management systems*. IEEE, 2008.
31. Moore, S. W., & Schneider P. J. (2001). *A review of cell equalization methods for lithium ion and lithium polymer battery systems*. No. 2001-01-0959. SAE Technical Paper. Warrendale, PA: SAE International.
32. Plett, G. L. Extended Kalman filtering for battery management systems of LiPB-based HEV battery packs: Part 1. Background. *Journal of Power sources* 134, no. 2 (2004): 252-261.
33. Santhanagopalan, S., & White, R. E. Online estimation of the state of charge of a lithium ion cell. *Journal of power sources* 161, no. 2 (2006): 1346-1355.
34. Pop, V., Bergveld, H. J., Notten, P. H. L., & Regtien, P. P. L. State-of-the-art of battery state-of-charge determination. *Measurement Science and Technology* 16, no. 12 (2005): R93.
35. Laboratory Test Procedure for FMVSS 305, Electric Powered Vehicles: Electrolyte Spillage and Electric Shock Protection, U.S. Department of Transportation, TP-305-01.
36. Mikolajczak, C., Harmon, J., White, K., Horn, Q., Wu, M., & Shah, K. Detecting lithium-ion cell internal faults in real time. *Power Electronics Technology* (2010).
37. Darcy, E., Smith, K., & Park, C. A. R. *Advanced Mitigating Measures for the Cell Internal Short Risk*. National Renewable Energy Laboratory, 2010.
38. 608.3 Thermal Runaway, Chapter 6 Building Services and System, 2015 International Fire Code, http://codes.iccsafe.org/app/book/toc/2015/I-Codes/2015_IFC_HTML/index.html
39. *Around the Clock Protection From Battery Thermal Runaway*, Canara, http://canara.com/docs/Canara_DS_AvoidThermalRunaway.pdf
40. *How Cellwatch Works*, CELLWATCH, www.cellwatch.com/products/cellwatch/how-cellwatch-works/
41. Deveau, E. Technical Note: Understanding Thermal Runaway, Alber, www.alber.com/Docs/TN-11001Thermal%20Runaway%20Detection%20Tech%20Note.pdf
42. Feder, D. O., & Hlavac, M. J. Analysis and interpretation of conductance measurements used to assess the state-of-health of valve regulated lead acid batteries. In *Telecommunications Energy Conference, 1994. INTELEC'94., 16th International*, pp. 282-291. IEEE, 1994.
43. Hlavac, M. J., & Feder D.. VRLA battery monitoring using conductance technology. In *Telecommunications Energy Conference, 1995. INTELEC'95., 17th International*, pp. 284-291. IEEE, 1995.
44. Karden, E., Buller, S. & De Doncker, R. W. A method for measurement and interpretation of impedance spectra for industrial batteries. *Journal of Power sources* 85, no. 1 (2000): 72-78.

45. Aurbach, D., Gamolsky, K., Markovsky, B., Salitra, G., Gofer, Y., Heider, U., ... Schmidt, M. The study of surface phenomena related to electrochemical lithium intercalation into Li_xMO_y host materials (M= Ni, Mn). *Journal of The Electrochemical Society* 147, no. 4 (2000): 1322-1331.
46. Hjelm, A.-K., & Lindbergh, G. Experimental and theoretical analysis of LiMn_2O_4 cathodes for use in rechargeable lithium batteries by electrochemical impedance spectroscopy (EIS). *Electrochimica Acta* 47, no. 11 (2002): 1747-1759.
47. Liu, L., & Zhu, M. Modeling of SEI Layer Growth and Electrochemical Impedance Spectroscopy Response using a Thermal-Electrochemical Model of Li-ion Batteries. *ECS Transactions* 61, no. 27 (2014): 43-61.
48. Belov, D., & Yang, M.-H. Failure mechanism of Li-ion battery at overcharge conditions. *Journal of Solid State Electrochemistry* 12, no. 7-8 (2008): 885-894.
49. Howey, D., Mitcheson, P. D., Yufit, V., Offer, G., J., & Brandon, N. P. Online Measurement of Battery Impedance Using Motor Controller Excitation. *Vehicular Technology, IEEE Transactions on* 63, no. 6 (2014): 2557-2566.
50. Garcia, H. E., Mohanty, A., Christophersen, J. P., & Lin, W.. On-line State-of-Health and Remaining-Useful-Life Assessment of Batteries using Rapid Impedance Spectrum Measurements. In *45th Power Sources Conference Proceedings*. 2012.
51. Christophersen, J. P., Morrison, J. L., Motloch, C. G., & Morrison, W. H. *Long-Term Validation of Rapid Impedance Spectrum Measurements as a Battery State-of-Health Assessment Technique*. No. 2013-01-1524. SAE Technical Paper, 2013. Warrendale, PA: SAE International.
52. Christophersen, J. P., Morrison, J. L. & Morrison, W. H. *Universal auto-calibration for a rapid battery impedance spectrum measurement device*. No. INL/CON-13-30523. Idaho National Laboratory (INL), 2014.
53. Hill, D., Gully, B., Agarwal, A., Nourai, A., Thrun, L., Swartz, S., ... Moore, B. Detection of off gassing from Li-ion batteries. In *Energytech, 2013 IEEE*, pp. 1-7. IEEE, 2013.
54. Wenger, M., Waller, R., Lorentz, V. R. H., Marz, M., & Herold, M. Investigation of gas sensing in large lithium-ion battery systems for early fault detection and safety improvement. In *Industrial Electronics Society, IECON 2014-40th Annual Conference of the IEEE*, pp. 5654-5659. IEEE, 2014.
55. Cattin, V., Perichon, P., Dahmani, J., Schwartzmann, B., & Heiries, V. Detection of electric arcs in large batteries. In *Electric Vehicle Symposium and Exhibition (EVS27), 2013 World*, pp. 1-9. IEEE, 2013.
56. Lee, S., Kim, J., Lee, J., & Cho, B. H. State-of-charge and capacity estimation of lithium-ion battery using a new open-circuit voltage versus state-of-charge. *Journal of power sources* 185, no. 2 (2008): 1367-1373.
57. Toepfer, C. SAE Electric Vehicle Conductive Charge Coupler, SAE J1772. *Society of Automotive Engineers* (2009).
58. BK Precision Sales Page for the 8522 Load Bank. (2014, November 22). Retrieved November 22, 2014, from www.bkprecision.com/products/dc-electronic-loads/8522-2400-w-500-v-programmable-dc-electronic-load.html
59. U.S. Environmental Protection Agency. (n.d.). U.S. Environmental Protection Agency Website - OBD-II. Retrieved from www.epa.gov/obd/index.htm

DOT HS 812 789
February 2020



U.S. Department
of Transportation
**National Highway
Traffic Safety
Administration**

